



THE REACTION OF AQUOAMINE RUTHENIUM(II)  
SPECIES WITH NITROUS OXIDE AND AZIDE ION

by

TREVOR RONALD NORMAN B.Sc. (Hons)

A thesis presented for the degree of  
Doctor of Philosophy

Department of Physical and Inorganic Chemistry  
University of Adelaide

January 1974

CONTENTS	Page
SUMMARY	
STATEMENT	
ACKNOWLEDGEMENTS	
ABBREVIATIONS	
CHAPTER 1 - BONDING IN SOME $\pi$ -ACCEPTOR RUTHENIUM(II) AMMINE	
COMPLEXES	1
1.1 Introduction	1
1.2 Bonding of $\pi$ -Acceptor Ligands to Ruthenium(II)	
Ammines	2
1.3 Outline of Research	5
REFERENCES	8
CHAPTER 2 - REACTION OF AQUO PENTAAMMINE RUTHENIUM(II) ION	
WITH AZIDE ION	10
2.1 Introduction	10
2.2 Properties of the Azide Ion	14
2.3 Reaction of Aquo Pentaammine Ruthenium(II) Ion with	
Azide Ion	16
2.4 Stoichiometry of the Reaction Between Aquo	
Pentaammine Ruthenium(II) Ion and Azide Ion	23
2.5 Kinetics and Mechanism of the Reaction Between	
$[\text{RuA}_5(\text{OH}_2)]^{2+}$ and Azide Ion	27

CONTENTS	Page
2.6 Attempted Isolation of Azido Pentaammine Ruthenium(II) Salts, $[\text{RuA}_5\text{N}_3]\text{X}$ , ( $\text{X} = \text{Br}^-$ , $\text{I}^-$ , $\text{BF}_4^-$ , $\text{PF}_6^-$ )	34
2.7 Summary	39
REFERENCES	56
CHAPTER 3 - STRUCTURE AND REACTIVITY OF DINITROGEN OXIDE	
PENTAAMMINE RUTHENIUM(II) SALTS	60
3.1 Introduction	60
3.2 Crystal Structure of $[\text{RuA}_5\text{N}_2\text{O}]\text{X}_2$ , ( $\text{X} = \text{Br}^-$ , $\text{I}^-$ , $\text{BF}_4^-$ and $\text{PF}_6^-$ )	60
3.3 Linkage Isomerism in Dinitrogen Oxide Complexes	64
3.4 Thermal Decomposition of $[\text{RuA}_5\text{N}_2\text{O}]\text{X}_2$	79
3.5 Summary	84
REFERENCES	95
CHAPTER 4 - THE REACTION OF NITROUS OXIDE WITH DIAQUO	
TETRAAMMINE RUTHENIUM(II) SPECIES	98
4.1 Introduction	98
4.2 The Reaction of $\text{cis}-[\text{Ru}(\text{en})_2(\text{OH}_2)_2]^{2+}$ with Nitrous Oxide	98
4.3 Isolation and Characterisation of Aquo Dinitrogen Oxide Tetraammine Ruthenium(II) Complexes	103
4.4 Summary	121
REFERENCES	133

CONTENTS	Page
CHAPTER 5 - REACTION OF BENZOYLHYDRAZINE AND CHLORO-	
PENTAAMMINE RUTHENIUM(III) CHLORIDE	136
5.1 Introduction	136
5.2 The Reaction of Chloropentaammine Ruthenium(III) with N-benzoylhydrazine	137
5.3 Infrared Spectra of the Complexes	138
5.4 Electronic Absorption Spectrum	139
5.5 Decomposition of $[RuA_5BH]Br_3$	140
5.6 Summary	142
REFERENCES	146
CHAPTER 6 - EXPERIMENTAL	148
6.1 Preparation of Compounds	148
6.2 Analyses	152
6.3 Production of Ruthenium(II) Solutions	152
6.4 Preparation of Nitrous Oxide Complexes	156
6.5 Preparation of Azido Pentaammine Ruthenium(II) Complexes	158
6.6 Preparation of Benzoylhydrazine Complexes	159
6.7 Spectral Measurements	160
6.8 Powder Photographs	161
6.9 Manometric Measurements	162
6.10 Balances	163

CONTENTS	Page
6.11 Gases	163
6.12 Characterisation of the Tetraammine Nitrous Oxide Complexes	164
6.13 The Reaction Between $[\text{RuA}_5(\text{OH}_2)]^{2+}$ and Azide	166
6.14 Thermal Decomposition of $[\text{RuA}_5\text{N}_2\text{O}]\text{X}_2$ ( $\text{X} = \text{BF}_4, \text{PF}_6$ )	172
6.15 pH and Millivolt Measurements	173
6.16 Computer Calculations	173
6.17 Magnetic Measurements	174
REFERENCES	170

## SUMMARY

Monomer dinitrogen complex,  $[\text{Ru}(\text{NH}_3)_5\text{N}_2]^{2+}$ , and dimer dinitrogen complex  $[\{\text{Ru}(\text{NH}_3)_5\}_2\text{N}_2]^{4+}$  are formed when  $[\text{Ru}(\text{NH}_3)_5\text{OH}_2]^{2+}$  reacts with azide ion in the presence of an external reducing agent. At constant pH the reaction exhibited second order kinetics with a rate constant of  $14.9 \times 10^{-2} \text{ M}^{-1} \text{ sec}^{-1}$  at  $25^\circ\text{C}$ . Values of  $\Delta H^\ddagger$  and  $\Delta S^\ddagger$  at  $25^\circ\text{C}$  were  $74.9 \text{ kJ mole}^{-1}$  and  $-33.5 \text{ J K}^{-1} \text{ mole}^{-1}$  respectively. The mechanism of the reaction proceeded through an azido complex intermediate, which was isolated and its infrared spectrum examined. The stoichiometry of the reaction was determined by quantitative estimation of the dinitrogen complexes, using ultraviolet spectroscopy, and of ammonium ion released, using Kjeldahl determination. In the absence of an external reducing agent the dinitrogen complexes were also formed. The product ratios and any gases released as byproducts were determined.

The structure of the series of salts  $[\text{Ru}(\text{NH}_3)_5\text{N}_2\text{O}]\text{X}_2$ , ( $\text{X} = \text{Br}^-$ ,  $\text{I}^-$ ,  $\text{BF}_4^-$  and  $\text{PF}_6^-$ ) was determined by using the X-ray powder diffraction technique. They are isostructural with the corresponding monomer dinitrogen complexes, with a linear ruthenium to nitrous oxide linkage. Thermal decomposition of  $[\text{Ru}(\text{NH}_3)_5\text{N}_2\text{O}](\text{BF}_4)_2 \cdot \text{H}_2\text{O}$  leads to the formation of ruthenium red and monomer dinitrogen complex in the mole ratio of 1:2. The amount and composition of the gas released was determined manometrically and mass spectroscopically. The implications are discussed in terms of the solid state mechanism of decomposition.

Evidence for the presence of linkage isomers in the complex  $[\text{Ru}(\text{NH}_3)_5\text{N}_2\text{O}](\text{PF}_6)_2 \cdot \text{H}_2\text{O}$  is discussed.

Attempts were made to isolate dinitrogen oxide complexes using the ions  $\text{cis-}[\text{Ru}(\text{en})_2(\text{OH}_2)_2]^{2+}$  and  $\text{cis-}[\text{Ru}(\text{NH}_3)_4(\text{OH}_2)_2]^{2+}$ . In the case of the tetraammine, two complexes formulated as  $\text{cis-}[\text{Ru}(\text{NH}_3)_4(\text{OH}_2)\text{N}_2\text{O}](\text{BF}_4)_2 \cdot 2\text{H}_2\text{O}$  and  $\text{cis-}[\text{Ru}(\text{NH}_3)_4(\text{OH}_2)\text{N}_2\text{O}](\text{PF}_6)_2 \cdot \text{H}_2\text{O}$ , were isolated and characterised. Evidence for the presence of a nitrous oxide species in solution was found with  $[\text{Ru}(\text{en})_2(\text{OH}_2)_2]^{2+}$  but no solids could be isolated. The infrared spectra of the tetraammine complexes showed evidence of coordinated nitrous oxide. The rate of decomposition of  $[\text{Ru}(\text{NH}_3)_4(\text{OH}_2)\text{N}_2\text{O}]^{2+}$  measured in 0.1M hydrochloric acid was  $1.66 \times 10^{-2} \text{ sec}^{-1}$  at  $25^\circ\text{C}$  and  $\Delta H^\ddagger$  was determined as  $76.7 \text{ kJ mole}^{-1}$  and  $\Delta S^\ddagger$  was  $-21.8 \text{ J K}^{-1} \text{ mole}^{-1}$ . The powder pattern of the hexafluorophosphate salt revealed a face centred cubic structure with a linear ruthenium to nitrous oxide linkage.

The reaction of chloropentaammine ruthenium(III) chloride with N-benzoylhydrazine in aqueous solution produced the monomer dinitrogen complex. A series of benzoylhydrazine complexes,  $[\text{Ru}(\text{NH}_3)_5\text{BH}]\text{X}_3$  ( $\text{X} = \text{Br}^-, \text{I}^-, \text{BF}_4^-, \text{PF}_6^-$ ) were isolated in which benzoylhydrazine acts as a monodentate ligand. The rate of decomposition of the bromide salt to monomer dinitrogen complex was measured in acid as  $5.23 \times 10^{-5} \text{ sec}^{-1}$  at  $26^\circ\text{C}$ .

#### STATEMENT

This thesis contains no material which has been accepted for the award of any other degree or diploma in any University and to the best of my knowledge and belief, this thesis contains no material previously published or written by another person, except when due reference is made in the text of the thesis.

TREVOR NORMAN



#### ACKNOWLEDGEMENTS

I wish to sincerely thank my supervisor, Dr. A.A. Diamantis, for his encouragement, guidance and help throughout the course of the work. I also thank Professors D.O. Jordan and D.R. Stranks for granting me the facilities to carry out the work. My thanks are due to Drs. M.R. Snow and K.R. Butler for their assistance with the crystallographic aspects of the project and to Dr. G.J. Sparrow for his assistance throughout the course of this work. I thank other members of staff and my fellow research students who have helped during the course of the work. I also thank Mrs. D. Hewish who typed the manuscript.

## ABBREVIATIONS

The following list of abbreviations has been used in this thesis:

monomer	$[\text{RuA}_5\text{N}_2]^{2+}$	
dimer	$[\text{A}_5\text{RuN}_2\text{RuA}_5]^{4+}$	
A	ammonia,	$\text{NH}_3$
en	ethylenediamine,	$\text{NH}_2\text{CH}_2\text{CH}_2\text{NH}_2$
trien	triethylenetetraamine,	$\text{NH}_2\text{CH}_2\text{CH}_2\text{NHCH}_2\text{CH}_2\text{NHCH}_2\text{CH}_2\text{NH}_2$
py	pyridine	
Me	methyl	
OAc	acetate,	$\text{CH}_3\text{C} \begin{array}{l} \text{// } \text{O} \\ \text{\textbackslash } \text{O} \end{array} -$
Ph	phenyl	
Tu	thiourea,	$\text{NH}_2\text{C}(\text{S})\cdot\text{NH}_2$

In reference to infrared spectra:

s	strong	sh	shoulder
m	medium	br	broad
w	weak	a	region covered by the anion



## CHAPTER 1

BONDING IN SOME  $\pi$ -ACCEPTOR RUTHENIUM(II) AMMINE COMPLEXES

## 1.1 Introduction

It has long been postulated that a metal dinitrogen complex is probably involved in the initial step of biological nitrogen fixation.<sup>1</sup> This idea was reinforced when it was demonstrated that both iron and molybdenum are essential in the enzymic fixation.<sup>2</sup> Many unsuccessful attempts were made to prepare dinitrogen complexes of both metals. Success was achieved in 1965 when  $[\text{RuA}_5\text{N}_2]\text{X}_2$  was prepared.<sup>3</sup>

The discovery of the first dinitrogen complex gave impetus to the study of ruthenium chemistry. Further it promoted attempts to find transition metal complexes which could act as models of enzymic nitrogen fixation. The system chosen was the pentaammine ruthenium(II) aquo. It was subsequently demonstrated that the ion  $[\text{RuA}_5\text{N}_2]^{2+}$  could be formed in solution by the reaction of  $[\text{RuA}_5\text{OH}_2]^{2+}$  and dinitrogen gas,<sup>4</sup> or even dinitrogen from the air.<sup>5</sup> The aquo complex is also known to react with carbon monoxide,<sup>6</sup> nitrous oxide<sup>7</sup> and hydrogen cyanide<sup>8</sup> all of which are substrates of the enzyme. Thus the aquo complex resembles the active site of the enzyme in that it is reactive towards the same substrates as nitrogenase. However, all attempts to reduce the coordinated nitrogen have been unsuccessful as coordinated dinitrogen has a high bond order and consequently its reduction has a high activation

energy.

### 1.2 Bonding of $\pi$ -Acceptor Ligands to Ruthenium(II) Ammines

Several complexes of the type  $[\text{RuA}_5\text{L}]^{2+}$  where  $\text{L} = \text{N}_2$ ,<sup>3</sup>  $\text{N}_2\text{O}$ ,<sup>7</sup>  $\text{CO}$ ,<sup>6</sup>  $\text{HCN}$ ,<sup>8</sup> pyridine<sup>9</sup> and pyrazine<sup>9</sup> are well known. In each case the ligand has empty  $\pi$  orbitals able to accept charge from the metal by back donation. For the dinitrogen complex Chatt<sup>1</sup> has given a description of the bonding.

The energy levels of the nitrogen molecule are given in Table 4.7 (p. 129). A simple description of the bonding involves  $\sigma$  donation of electrons from the nitrogen ligand to the metal and  $\pi$  back-bonding from the metal to ligand. Consideration of Table 4.7 shows that the  $3\sigma_g$  orbital of the dinitrogen is of the correct symmetry to donate electrons to the metal and the  $1\pi_g$  orbital of the ligand can accept charge from the metal  $t_{2g}$  orbitals. This is represented schematically in figure 1.1.

Evidence for back-bonding has been obtained from the infrared spectra of the dinitrogen complexes. Loss of charge into the  $\pi$  bond increases the positive character of the metal and so the ammonia vibrations are affected. Thus it is found that the infrared bands of the coordinated ammonia resemble those of a ruthenium(III) complex rather than ruthenium(II).<sup>3</sup>

Studies of the charge distribution of some nitrogen complexes has been made using Electron Spectroscopy (E.S.C.A.).<sup>10</sup> For

$[\text{RuA}_5\text{N}_2]\text{X}_2$  and  $[\text{OsA}_5\text{N}_2]\text{X}_2$  the N 1s electron spectra from the dinitrogen ligand overlap with the peak observed for the ammonia nitrogen. Thus no information regarding charge separation on the two nitrogen atoms in the ligand could be gained. However, the charge on the metal was determined. The binding energies of the Ru  $3p_{3/2}$  and Ru  $3d_{5/2}$  electron levels for the dinitrogen complexes were close to those found for  $\text{RuCl}_3$  and  $\text{RuO}_2$ . The reason for the high positive charge on the metal was attributed to the  $d\pi\text{-}p\pi^*$  back donation from metal to ligand assisted by the presence of the highly electronegative halide ions.

In other systems coordination of stronger  $\pi$ -acceptor ligands to a metal ion already coordinated to dinitrogen increases the  $\nu_{\text{N-N}}$  stretching frequency and decreases the  $\text{M-N}_2$  bond strength.<sup>11</sup> This is further evidence for back-bonding in the complexes. Also the metal ions which form the dinitrogen complexes are predominantly  $d^6$  and  $d^8$  spin-paired configurations, systems which are good  $\pi$ -donors.<sup>11</sup>

A comparison between metal carbonyls and the corresponding dinitrogen complex has been made for several systems.<sup>6,12,13</sup> In all cases it was concluded that carbon monoxide is a better  $\sigma$ -donor and  $\pi$ -acceptor ligand than nitrogen. The  $5\sigma$  donor orbital of carbon monoxide is 1.6 eV higher in energy than the  $3\sigma_g$  donor orbital of nitrogen, while the  $2\pi$  acceptor orbital of carbon monoxide is 1.0 eV higher than the  $1\pi_g$  orbital of nitrogen (see Table 4.7). It is expected on this basis, that carbon monoxide would be the better

$\sigma$ -donor and nitrogen the better  $\pi$ -acceptor of the two molecules. However, it has been calculated<sup>14</sup> that the  $2\pi$  orbital of carbon monoxide is 68% carbon 2p and 32% oxygen 2p and is thus directed toward the metal. The nitrogen  $1\pi_g$  orbital is disposed symmetrically between the two nitrogen atoms. Thus the overlap of the metal  $t_{2g}$  orbitals with the  $\pi$  antibonding orbitals of the ligand is more effective for carbon monoxide than for nitrogen.<sup>6</sup>

A similar explanation has been advanced to explain the bonding in  $[\text{RuA}_5\text{L}]\text{X}_2$  ( $\text{L} = \text{N}_2\text{O}$ ,<sup>15</sup>  $\text{py}$ ,<sup>9</sup>  $\text{Ph-C}\equiv\text{N}$ ,<sup>16</sup>  $\text{CH}_3\text{-C}\equiv\text{N}$ ,<sup>16</sup>  $\text{py-C}\equiv\text{N}$ <sup>17</sup>) complexes, i.e.  $\sigma$ -donation and back-bonding into the  $\pi$ -antibonding orbitals of the ligand. Such a diversity of ligands suggests that other ligands with similar molecular orbital energies would form stable complexes with ruthenium(II) ammines. Ligands such as azide, cyanate and thiocyanate may form stable complexes. In Table 1.1 the energy levels of the molecular orbitals for these ions are listed. Their common feature is a filled  $\sigma$  orbital with an energy of  $\sim -9$  eV and an empty  $\pi$  antibonding orbital with an energy of  $\sim -4$  eV. These values are much higher than those of the corresponding donor-acceptor set of nitrogen and carbon monoxide, so that the electrons are more readily available for  $\sigma$ -donation. The extent of overlap of the metal  $t_{2g}$  orbitals with the  $\pi$ -antibonding orbitals will depend on the shape of the orbital and the linearity or non-linearity of the metal-ligand bond. For the azide and S-bonded thiocyanate the bond will probably be bent so reducing the amount of overlap on back-bonding.

### 1.3 Outline of Research

In order to complete the analogy of the aquo site of  $[\text{RuA}_5\text{H}_2\text{O}]^{2+}$  with nitrogenase, the reaction with azide ion was studied. Azide ion competes with dinitrogen gas for the active site of nitrogenase,<sup>2</sup> and the products of azide reduction are ammonia and nitrogen gas. The reaction of  $[\text{RuA}_5\text{H}_2\text{O}]^{2+}$  with azide ion produced  $[\text{RuA}_5\text{N}_2]^{2+}$  and ammonia ( $\text{NH}_4^+$  in acidic solution) with small amounts of dimer dinitrogen complex,  $[\text{A}_5\text{RuN}_2\text{RuA}_5]^{4+}$  in the presence of a reducing agent. The stoichiometry and kinetics of the reaction were studied with a view to elucidating the mechanism of the reaction. A series of complexes  $[\text{RuA}_5\text{N}_3]\text{X}$ , ( $\text{X} = \text{Br}^-$ ,  $\text{I}^-$ ,  $\text{BF}_4^-$  and  $\text{PF}_6^-$ ) in which azide ion was coordinated to the metal were isolated and their infrared spectra studied. Thus, the reaction of aquopentaammine ruthenium(II) with azide ion is similar to its reaction with the isoelectronic nitrous oxide.

In view of the similarity of azide and nitrous oxide some investigations of the pentaammine nitrous oxide complexes were carried out. In particular the possibility of the presence of linkage isomers in the salt  $[\text{RuA}_5\text{N}_2\text{O}](\text{PF}_6)_2 \cdot \text{H}_2\text{O}$  was indicated by its infrared spectrum,<sup>15b</sup> and this was studied using infrared spectroscopy.

Structural investigations using the X-ray powder photography method were performed on the salts  $[\text{RuA}_5\text{N}_2\text{O}]\text{X}_2$ , ( $\text{X} = \text{I}^-$ ,  $\text{BF}_4^-$  and  $\text{PF}_6^-$ ). Like the bromide salt,<sup>15b</sup> they were face centred cubic with a substantially linear metal to nitrous oxide linkage.

The complexes  $[\text{RuA}_4(\text{OH}_2)\text{N}_2]\text{X}_2$  ( $\text{X} = \text{Cl}^-$ ,  $\text{Br}^-$ ,  $\text{I}^-$ ) are known.<sup>11</sup> Starting from  $\text{cis-}[\text{RuA}_4\text{Cl}_2]^+$ , the diaquo ion was produced and subjected to pressure of nitrous oxide in the presence of a precipitating agent, in the expectation of producing salts of the composition  $[\text{RuA}_4(\text{OH}_2)\text{N}_2\text{O}]\text{X}_2$ . The characterisation, properties and reactions of the solids isolated are discussed in Chapter 4.

Finally the reaction of benzoylhydrazine with chloropentammine ruthenium(III) chloride is described in Chapter 5 along with the properties of the benzoylhydrazine complexes isolated.



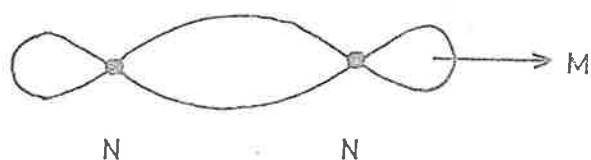
TABLE 1.1

*Molecular Orbital Energy Levels of Some Ions.*<sup>18</sup>

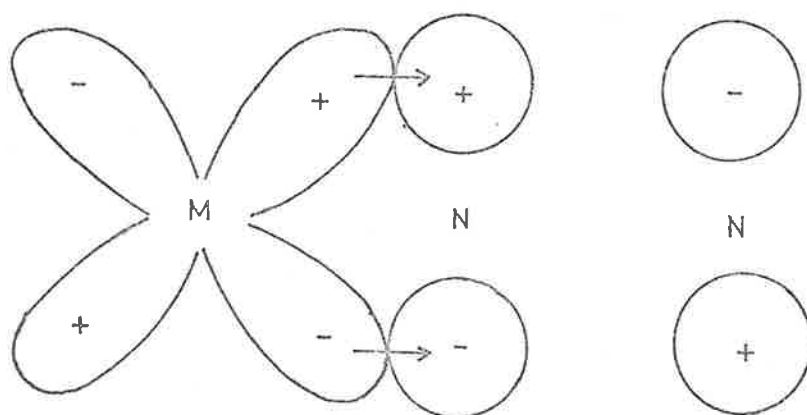
$\text{N}_3^-$		$\text{NCS}^-$		$\text{NCO}^-$	
Orbital	Energy eV	Orbital	Energy eV	Orbital	Energy eV
$2\pi_u$	-4.43	$3\pi$	-4.24	$3\pi$	-4.24
$1\pi_g$	-7.77	$2\pi$	-7.87	$2\pi$	-8.59
$3\sigma_u$	-9.53	$7\sigma$	-8.59	$3\sigma$	-9.21
$1\pi_u$	-12.41	$1\pi$	-10.38	$1\pi$	-11.33
$4\sigma_g$	-12.62	$6\sigma$	-11.79	$6\sigma$	-12.23

FIGURE 1.1 FORMATION OF METAL DINITROGEN BONDS

(A) METAL NITROGEN  $\sigma$  BOND



(B) METAL NITROGEN  $\pi$  BOND



## CHAPTER 1

## REFERENCES

1. J. Chatt, Proc. Roy. Soc. B., 1969, 172, 327.
  2. R.H. Burris, Proc. Roy. Soc. B., 1969, 172, 339.
  3. A.D. Allen, F. Bottomley, R.O. Harris, V.P. Reinslau and C.V. Senoff, J. Amer. Chem. Soc., 1967, 89, 5595.
  4. D.E. Harrison and H. Taube, J. Amer. Chem. Soc., 1967, 89, 5706.
  5. A.D. Allen and F. Bottomley, Can. J. Chem., 1968, 46, 469.
  6. C.H. Campbell, A.R. Dias, M.L.H. Green, T. Saito and M.G. Swanwick, J. Organometal. Chem., 1968, 14, 349.
  7. A.A. Diamantis and G.J. Sparrow, Chem. Comm., 1969, 469;  
J.N. Armor and H. Taube, J. Amer. Chem. Soc., 1969, 91, 6874.
  8. P.C. Ford, Chem. Comm., 1971, 7.
  9. P.C. Ford, D.F. Rudd, R. Gaunder and H. Taube, J. Amer. Chem. Soc., 1968, 90, 1187.
  10. B. Folkesson, Acta Chem. Scand., 1973, 27, 287.
  11. J.E. Fergusson and J.L. Love, Rev. Pure and Appl. Chem. (Aust.), 1970, 20, 33, and references therein.
  12. D.J. Darensbourg, Inorg. Chem., 1971, 10, 2399.
  13. G.M. Bancroft, M.J. Mays and B.E. Prater, Chem. Comm., 1969, 585.
  14. J. Pople and G. Segal, J. Chem. Phys., 1965, 43, 5136.
  15. (a) A.A. Diamantis and G.J. Sparrow, J. Chem. Soc. (Dalton),  
in the press.  
(b) G.J. Sparrow, Ph.D. Thesis, Univ. of Adel., March, 1972.
-

16. R.E. Clarke and P.C. Ford, *Inorg. Chem.*, 1970, 9, 227.
17. R.E. Clarke and P.C. Ford, *Inorg. Chem.*, 1970, 9, 495.
18. J.W. Rabalias, J.M. McDonald, V. Scherr and S.P. McGlynn,  
*Chem. Rev.*, 1971, 71, 73.

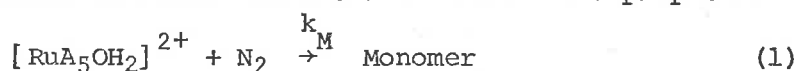
## CHAPTER 2

## REACTION OF AQUO PENTAAMMINE RUTHENIUM(II) ION WITH AZIDE ION

## 2.1 Introduction

The aquo pentaammine ruthenium(II) ion  $[\text{RuA}_5(\text{OH}_2)]^{2+}$  has been shown<sup>1</sup> to interact with dinitrogen gas to form Allen and Senoff's<sup>2</sup> ion  $[\text{RuA}_5\text{N}_2]^{2+}$  and binuclear ion  $[\text{A}_5\text{RuN}_2\text{RuA}_5]^{4+}$ . The monomeric complex  $[\text{RuA}_5\text{N}_2](\text{BF}_4)_2$  is characterised by a single strong nitrogen-nitrogen stretch at  $2144 \text{ cm}^{-1}$  in its infrared spectrum<sup>2</sup> and an absorption at  $221 \text{ nm}$  ( $\epsilon = 1.8 \times 10^4 \text{ M}^{-1} \text{ cm}^{-1}$ ) in its ultraviolet spectrum.<sup>3</sup> The dimeric complex  $[\text{A}_5\text{RuN}_2\text{RuA}_5](\text{BF}_4)_4$  has only a broad weak band  $2060 \text{ cm}^{-1}$  in its infrared spectrum, but its Raman spectrum exhibits a strong absorption around  $2100 \text{ cm}^{-1}$  due to the nitrogen-nitrogen stretching vibration.<sup>4</sup> The ion has a strong absorption at  $262 \text{ nm}$  ( $\epsilon = 4.8 \times 10^4 \text{ M}^{-1} \text{ cm}^{-1}$ ) in its ultraviolet spectrum.<sup>3</sup>

Page et al.<sup>6</sup> have studied the kinetics of the reaction of dinitrogen with  $[\text{RuA}_5(\text{OH}_2)]^{2+}$  in potassium sulphate-sulphuric acid medium. From the results obtained the mechanism below was proposed.



$$\text{So } d[\text{Monomer}]/dt = k_M'[\text{RuA}_5(\text{OH}_2)^{2+}][\text{N}_2] - k_D[\text{RuA}_5(\text{OH}_2)^{2+}][\text{Monomer}] \quad (3)$$

$$\text{and } d[\text{Dimer}]/dt = k_D[\text{RuA}_5(\text{OH}_2)^{2+}][\text{Monomer}] \quad (4)$$

For a solution saturated with dinitrogen at one atmosphere

$$d[\text{Monomer}]/dt = k_M'[\text{RuA}_5(\text{OH}_2)^{2+}] - k_D[\text{RuA}_5(\text{OH}_2)^{2+}][\text{Monomer}] \quad (5)$$

where

$$k_M' = k_M[\text{N}_2].$$

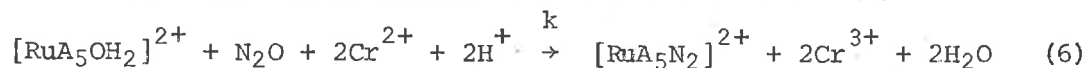
## 11.

Reaction (1) was studied at low initial concentrations of aquo ( $< 2 \times 10^{-4}$  M) with dimer formation only becoming noticeable at four hours. The formation of the dimer (reaction (2)) was studied separately by addition of solid monomer to a solution of the aquo ion. At initial concentrations of  $1 \times 10^{-3}$ – $3 \times 10^{-3}$  M aquo, the formation of both species could be followed together.

Second order rate constants for reactions (1) and (2) at 25°C, pH 3.3 and an ionic strength ( $\mu$ ) of 0.30M are  $k_M = 8.0 \times 10^{-2} \text{ M}^{-1} \text{ sec}^{-1}$  and  $k_D = 3.6 \times 10^{-2} \text{ M}^{-1} \text{ sec}^{-1}$ . The value of  $k_M$  ( $7.3 \times 10^{-2} \text{ M}^{-1} \text{ sec}^{-1}$  at 25°C,  $\mu = 0.10\text{M}$ ) determined by Armor and Taube<sup>5</sup> is in good agreement with that of Page. However, the marked effect of ionic strength on the rate of dimer formation,  $k_D$ , does not allow a comparison to be made.

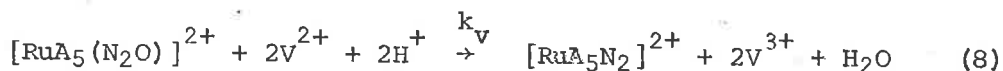
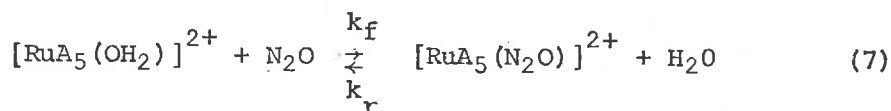
It has also been shown that the monomer and dimer dinitrogen complexes are formed when  $[\text{RuA}_5\text{Cl}]^{2+}$  is reduced in an atmosphere of nitrous oxide.<sup>7</sup> A nitrous oxide complex as an intermediate was proposed but no evidence for its presence was found. However, Armor and Taube showed that the presence of an absorption maximum at 238 nm ( $\epsilon = 1.7 \times 10^4 \text{ M}^{-1} \text{ cm}^{-1}$ ), when solutions of  $[\text{RuA}_5\text{OH}_2]^{2+}$  were exposed to dinitrogen oxide, was due to the presence of the  $[\text{RuA}_5\text{N}_2\text{O}]^{2+}$  ion in solution.<sup>8</sup>

By following the appearance of the dinitrogen complexes, Armor and Taube were able to determine<sup>8</sup> the rate of reaction (6).



The rate constant  $k$ , determined was  $10.1 \times 10^{-3} \text{ M}^{-1} \text{ sec}^{-1}$  at  $6.8^\circ\text{C}$ ,  $\mu = 0.023\text{M}$ , and at  $25^\circ\text{C}$  it was  $7.6 \times 10^{-2} \text{ M}^{-1} \text{ sec}^{-1}$ . The rate determining step is the formation of the nitrous oxide complex and it is reduced virtually as rapidly as it is formed.

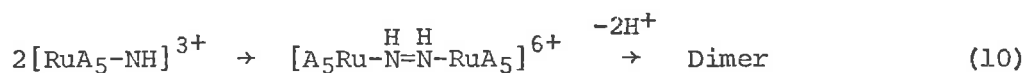
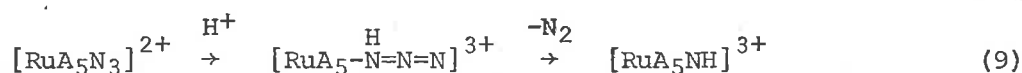
Experiments on the rate of reduction of the nitrous oxide complex by  $\text{Cr}^{2+}$  and  $\text{V}^{2+}$  gave additional information as to the mechanism of the reaction.<sup>9</sup> The rate of reduction by  $\text{Cr}^{2+}$  at  $25^\circ\text{C}$ ,  $\mu = 0.07\text{M}$  was  $8.2 \times 10^2 \text{ M}^{-1} \text{ sec}^{-1}$  and for  $\text{V}^{2+}$  at  $25^\circ\text{C}$  the rate was calculated as  $1.0 \text{ M}^{-1} \text{ sec}^{-1}$ . The mechanism given in equations (7) and (8) accounts for the kinetic data.



Formation of any dimer present can be accounted for by the reaction of the monomer with free aquo complex.

Along with nitrous oxide the isoelectronic azide ion ( $\text{N}_3^-$ ) has been used as a source of coordinated dinitrogen. Like nitrous oxide, azide is a competitive inhibitor of the enzyme nitrogenase, being reduced to ammonia and dinitrogen gas.<sup>10</sup> Formation of  $[\text{RuA}_5\text{N}_2]^{2+}$  occurs when the aquo ion  $[\text{RuA}_5(\text{OH}_2)]^{3+}$  and azide ion interact, the reaction occurring by the intermediate complex  $[\text{RuA}_5\text{N}_3]^{2+}$ . A series of azido amine complexes of ruthenium(III) have been prepared and all decompose in solution to form the corresponding dinitrogen complex with loss of dinitrogen gas.<sup>11</sup>

The mechanism of the reaction has been investigated and is thought to proceed with formation of a coordinated nitrene intermediate. For the azido pentaammine the mechanism is given in equations (9)-(11).



In the presence of acid large amounts (>60% of total ruthenium present) of the dimer are produced; monomer is the main product in the absence of acid.

The reaction of  $[\text{RuA}_5(\text{OH}_2)]^{2+}$  and azide has been shown<sup>12</sup> to form the dinitrogen complex, but no details of the reaction were reported. Another report<sup>13</sup> of this reaction found no evidence for the formation of the dinitrogen complex, only release of dinitrogen and formation of  $\text{Ru}(\text{NH}_3)_6^{3+}$ . An investigation of the kinetics and stoichiometry of the reaction was undertaken, after the first report but before the second, and also show that the dinitrogen complex is formed.

Interest in the reaction of the aquo species with azide ion stems from the proposition that the ion can be considered as a model species for the enzyme nitrogenase. It has now been demonstrated that the ion can bind dinitrogen gas (either from the air<sup>15</sup> or pure gas<sup>1,5</sup>), dinitrogen oxide,<sup>7,8,9</sup> carbon monoxide<sup>14</sup> and now azide. These compounds are known to interact with the enzyme. The only unsolved problem is that of



facile reduction of coordinated dinitrogen to ammonia with regeneration of the reactive complex.

## 2.2 Properties of the Azide Ion

Spectroscopic<sup>16</sup> and crystallographic<sup>17</sup> studies have established that azide is a symmetric, linear ion with a N-N distance of 1.15 Å.

In acidic solution azide ion is readily protonated to form hydrazoic acid. Estimates<sup>18,19,20</sup> of the dissociation constant of hydrazoic acid at 25°C range from  $1.91 \times 10^{-5}$  -  $2.56 \times 10^{-5}$ . Pure hydrazoic acid can be obtained from aqueous solutions as a colourless liquid, boiling point 37°C. By continuous bubbling with a gas (e.g. dinitrogen, argon), hydrazoic acid can be purged from solutions with pH values at which a significant amount of the acid is in an undissociated form.<sup>21</sup>

The effect of pH on the ultraviolet spectrum of the azide ion was determined in the same sulphuric acid-potassium sulphate medium used for the kinetic investigation of the reaction between  $[\text{RuA}_5(\text{OH}_2)]^{2+}$  and azide ion. From pH 1 to 4 a single absorption was observed at 260 nm whose molar absorptivity remained constant. At pH 6.9 the peak was not evident but is shifted to wavelengths beyond the range of the spectrophotometer. The changes in the spectrum are consistent with the absorption at 260 nm being due to the undissociated acid. Over the concentration range  $6 \times 10^{-4}$  M to  $3 \times 10^{-2}$  M for each of the pH's examined the peak obeyed Beer's law. The molar absorptivities at 221 nm

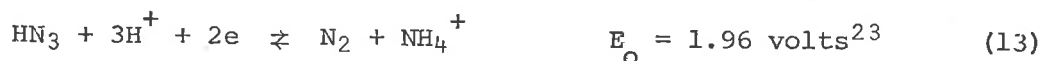
and 262 nm (these are the absorption maxima of the dinitrogen complexes) were also calculated and are shown in Table 2.1.

The  $E_o$  value for the half-equation



reveals that hydrazoic acid is a strong reducing agent.<sup>23</sup> Solutions of azide ion in acid are readily oxidised to dinitrogen gas by Ce(IV),<sup>24</sup>  $[Co(H_2O)_6]^{3+}$ <sup>25</sup> and Mn(III)<sup>26</sup> 1.5 mole of gas being liberated for each mole of metal ion. The metals thus undergo a one-electron reduction in the reaction.

On the other hand metals which are reducing agents, such as Cr(II),<sup>27</sup> V(II),<sup>27</sup> Ti(III),<sup>28</sup> Co(II)<sup>29</sup> and Ni(I)<sup>29</sup> show different behaviour. For example, both Cr(II) and V(II) reduced the azide ion to dinitrogen gas and ammonia, recovered as ammonium ion or present bound to the metal as  $[Cr(H_2O)_5NH_3]^{3+}$ . The half-equation for azide reduction is:



This stoichiometry was obeyed for both reductions. Neither Cr(II) nor V(II) were used as reducing agents for the reaction between  $[RuA_5(OH_2)]^{2+}$  and azide ion in acidic medium, because of the reduction of azide by these reagents, and because the ammonia produced may compete with the azide ion for the pentaammine aquo.

Photochemical decomposition of the azide ion has been studied.<sup>30,31</sup> Irradiation of solutions of azide ion can lead to the formation of dinitrogen gas, hydroxylamine, hydrazine and ammonia, depending on the

pH of the medium. The mechanism of these reactions usually proceeds by the formation of the imide radical ( $\text{NH}^\bullet$ ). Acid decomposition of certain azido-metal complexes, e.g.  $[\text{IrA}_5\text{N}_3]^{2+}$  is thought to involve the imide radical.<sup>32</sup>

Azide forms an insoluble precipitate with silver ions<sup>33</sup> ( $K_{\text{sp}} = 2.63 \times 10^{-8}$ ). The analysis of sodium azide using standard silver nitrate was based on this reaction (see section 6.1.6). Ferric ion forms a red solution of  $[\text{Fe}(\text{H}_2\text{O})_5\text{N}_3]^{2+}$  with azide ion and this test was used to determine the presence of the ion in solution.<sup>34</sup>

### 2.3 Reaction of Aquo Pentaammine Ruthenium(II) Ion with Azide Ion

Aquo pentaammine ruthenium(II) ion,  $[\text{RuA}_5(\text{OH}_2)]^{2+}$ , was generated from the chloro pentaammine ruthenium(III) ion,  $[\text{RuA}_5\text{Cl}]^{2+}$ , by reduction with zinc amalgam, amalgamated zinc, hydrogen on platinum black or electrolytic means in an atmosphere of argon. Low oxidation metal ions (e.g.  $\text{Cr}^{2+}$ ,  $\text{V}^{2+}$ ) were not used for the reasons discussed in section 2.2. The reaction was initiated when sodium azide was added, samples were withdrawn under argon, and their ultraviolet spectra examined. The products of the reaction were the monomer,  $[\text{RuA}_5\text{N}_2]^{2+}$ , and dimer,  $[\text{A}_5\text{RuN}_2\text{RuA}_5]^{4+}$ , dinitrogen complexes which were identified from their ultraviolet spectra and the monomer from the infrared spectrum of the precipitated tetrafluoroborate salt as well.

The parameter chosen to indicate the extent of reaction is the "% Conversion", where

$$\% \text{ Conversion} = \frac{[\text{Monomer}] + 2[\text{Dimer}]}{[\text{RuA}_5\text{Cl}_3]_i} \times 100$$

$$\text{i.e. } \% \text{ Conversion} = \% \text{ Monomer} + 2 \% \text{ Dimer}$$

and

$$\% \text{ Monomer} = \frac{[\text{Monomer}]}{[\text{RuA}_5\text{Cl}_3]_i} \times 100$$

$$\% \text{ Dimer} = \frac{[\text{Dimer}]}{[\text{RuA}_5\text{Cl}_3]_i} \times 100$$

Hence the % Conversion represents the amount of ruthenium present as the dinitrogen complexes. Alternatively, the "% Fixed nitrogen" can be used to represent the extent of reaction

$$\% \text{ Fixed N}_2 = \% \text{ Monomer} + \% \text{ Dimer}$$

and it is therefore an expression of the amount of dinitrogen bound to ruthenium. Table 2.2 gives the values of the molar absorptivities of the dinitrogen complexes used to calculate their concentration in solution and hence the "% Conversion". The concentrations of the monomer (M) and dimer (D) at different times were calculated from the set of simultaneous equations:

$$A^{221} = \epsilon_M^{221} \cdot l \cdot C_M + \epsilon_D^{221} \cdot l \cdot C_D$$

$$A^{262} = \epsilon_M^{262} \cdot l \cdot C_M + \epsilon_D^{262} \cdot l \cdot C_D$$

The molar absorptivities of  $[\text{RuA}_5(\text{OH}_2)]^{2+}$  at 221 nm and 262 nm are given in Table 2.2 and the values are much smaller (10-30 times) than the dinitrogen complexes and so were ignored in the calculations.

Previously it was shown that under argon the monomer complex loses dinitrogen to form the aquo ion.<sup>5</sup> Free aquo ion is known to react with

monomer to produce the dimer.<sup>1,5</sup> Hence after standing under argon for prolonged periods, a solution of monomer changes to the dimer with loss of nitrogen. As such behaviour could interfere with the study of the reaction products, the rate of formation of the dimer from the monomer under the conditions of the kinetic experiments was investigated.

A solution of monomer ( $3.52 \times 10^{-3}$  M) and dimer ( $1.88 \times 10^{-4}$  M) in 0.10M sulphuric acid was allowed to stand under argon in the presence of zinc amalgam. Another solution of the same monomer and dimer concentrations was allowed to stand for the same time (21 hours) without a reducing agent being present. The monomer and dimer concentrations were determined from the ultraviolet spectra. Both flasks showed an increase in the dimer concentration as expected. The results are listed in Table 2.3 below. The flask without a reducing agent has a lower value of D because of oxidation of some of the free  $[\text{RuA}_5\text{OH}_2]^{2+}$ .

TABLE 2.3

*Decomposition of  $[\text{RuA}_5\text{N}_2]^{2+}$  Under Argon*

Reducing Agent	M	D	Time (hrs)	k sec <sup>-1</sup>
Absent	$3.01 \times 10^{-3}$ M	$2.77 \times 10^{-4}$ M	20.5	$2.12 \times 10^{-6}$
Present	$2.93 \times 10^{-3}$ M	$4.75 \times 10^{-4}$ M	21.0	$2.50 \times 10^{-6}$

The values of the rate constant for decomposition of monomer in

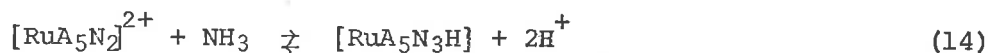
column 5 of Table 2.3, were calculated from the first order expression<sup>35</sup>

$$\ln \frac{a}{a-x} = kt.$$

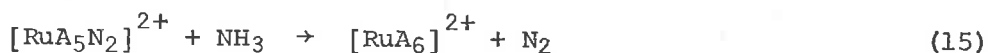
Armor and Taube<sup>6</sup> also calculated this decomposition rate using isonicotinamide to complex the  $[\text{RuA}_5(\text{OH}_2)]^{2+}$  as it was formed. The value of  $2.03 \times 10^{-6} \text{ sec}^{-1}$  was obtained by measuring the rate of formation of  $[\text{RuA}_5(\text{isoamide})]^{2+}$ . The values are in good agreement, and show that any dimer arising from the reactions described below cannot arise from decomposition of the monomer. Characteristically the runs described below were carried out over one-two hours while decomposition of monomer only occurs to a significant extent over very much longer time intervals.

The reaction of  $[\text{RuA}_5(\text{OH}_2)]^{2+}$  and azide ion was investigated in the presence of the reducing agents given above at various concentrations of  $[\text{RuA}_5(\text{OH}_2)]^{2+}$  ( $\sim 10^{-2} \text{ M}$ ) and of azide ion ( $1 \times 10^{-2}$ – $10 \times 10^{-2} \text{ M}$ ). The reaction was generally carried out using 0.1M sulphuric acid as solvent in an atmosphere of argon. In the presence of zinc amalgam greater than 90% conversion occurred within one hour, while in two or three hours 100% conversion could be achieved. The slow conversion of the last 10% may be due to neutralisation of the acid by its reaction with ammonia, the other product of the reaction (see section 2.4), and its reaction with the amalgam to produce hydrogen, thereby lowering the hydrogen ion concentration. Volatilisation of hydrazoic acid from solution may also contribute to the slow conversion, or an equilibrium

may be established. The first reason seems to offer the most likely explanation. For the equilibrium situation the reverse reaction, viz.



is unlikely because the reaction of nitrogen and ammonia is unfavourable<sup>23</sup> ( $E^\circ$  -1.96 volts). The reaction



takes place only in concentrated aqueous ammonia.<sup>2</sup> Consequently the equilibrium situation does not offer a likely explanation for the slow conversion. When amalgamated zinc was used as the reducing agent the conversion was particularly slow, 100% conversion was achieved with reaction times in excess of six hours. Neutralisation of the acid present probably accounts for the slow conversion as the reaction is very pH sensitive (see section 2.5). Similarly with hydrogen on platinum black, 100% conversion was not achieved. In this case, the hydrazoic acid, formed in solution when azide is added, is volatized. It is carried out of solution by the continuous bubbling with hydrogen. This was checked by passing the exhaust gases through a solution of ferric ammonium sulphate, which turned instantly red as the azide was added. This method of studying the reactions was abandoned. For some runs electrolytic reduction of  $[\text{RuA}_5\text{Cl}_3]$  at a potential of -0.6 V vs. SCE was used to generate the aquo complex. The potential was maintained when azide was added and the reaction monitored as before. This method tended to give 100% conversion to the dinitrogen complexes in 2-3 hours.

The results of each of these runs are listed in Table 2.4.

In several runs the external reducing agent was removed before the addition of sodium azide. Basolo<sup>13</sup> investigated the reaction under similar conditions, however the products of the reaction were the monomer dinitrogen complex and a species with an absorption maximum at 298 nm (probably  $\text{RuA}_5\text{SO}_4^+$ , lit.<sup>51</sup>  $\lambda$ : 308-310 nm), as well as a small amount (<5% of the total ruthenium) of the dimer dinitrogen complex. Basolo<sup>13</sup> observed the formation of  $[\text{RuA}_6]^{3+}$ ,  $[\text{RuA}_5(\text{OH}_2)]^{3+}$  and dinitrogen gas.

To check this discrepancy several runs were performed on a vacuum line with attached manometer and any gases evolved were monitored. The results of these runs are listed in Table 2.5. No gas was evolved during the course of the reaction. At the end of each reaction the amount of dinitrogen complex formed was checked by examination of the ultraviolet spectrum. Sodium tetrafluoroborate was added to one of these runs and the products isolated. The infrared spectrum showed a single sharp peak at  $2145\text{ cm}^{-1}$  due to  $\nu_{\text{N-N}}$  of coordinated dinitrogen.

The reaction in the absence of a reducing agent produces the same products as that with the reducing agent as well as a ruthenium(III) species. For these runs the only potential reducing agent was  $[\text{RuA}_5\text{OH}_2]^{2+}$  itself. If two mole of it are considered to be oxidised for each mole of azide ion which is reduced (i.e. for each mole of  $\text{N}_2$  fixed) then



$$\% \text{ Ru(III) formed} = 2 \times (\% \text{ Fixed N}_2)$$

$$= 2 \times (\% \text{ Monomer} + \% \text{ Dimer})$$

$$\text{and } \% \text{ Total Ru} = \% \text{ Ru(III) formed} + \% \text{ Monomer} + 2 \% \text{ Dimer}$$

$$= 3 \% \text{ Monomer} + 4 \% \text{ Dimer.}$$

The results of runs in which an external reducing agent was absent, are listed in Table 2.6. The % Total Ru was calculated as described above and tend to 100% indicating that two mole of  $[\text{RuA}_5\text{OH}_2]^{2+}$  are required for each mole of azide ion reduced. These reactions are essentially complete in 15-30 mins., i.e. about one-third of time taken for the reaction when a reducing agent is present. The reaction is therefore faster under these conditions.

These reactions showed a marked dependence on pH (as did the reactions with reducing agent present (see section 2.5)) of the medium. At high pH's (pH  $\approx$  1, 0.1M  $\text{H}_2\text{SO}_4$  solvent) the reaction was very rapid, being 100% complete in 15-30 mins. When sodium acetate-acetic acid buffer solution was used (pH  $\approx$  4) the reaction was not complete in 3-4 hours. At the low pH an orange colour was imparted to the solution with an absorption at 430 nm ( $\epsilon \approx 300 \text{ M}^{-1} \text{ cm}^{-1}$ ) in acetate or water. This absorption probably corresponds to the formation of  $[\text{RuA}_5\text{N}_3]^+$ . Red solids were isolated from solution (see section 2.6).

The marked dependence of the reaction on pH probably reflects the relative abilities of  $\text{HN}_3$  and  $\text{N}_3^-$  to enter the first coordination sphere of the  $[\text{RuA}_5]^{2+}$  moiety. As the  $\text{pK}_a$  of  $\text{HN}_3$  is 4.77, then reactions at this pH and above are essentially reactions of  $\text{N}_3^-$ . Thus the

reaction in acetate is slower because  $\text{HN}_3$  enters the coordination sphere faster than  $\text{N}_3^-$ . A more detailed investigation of this phenomenon was carried out using electrolytic reduction (see section 2.5).

These preliminary investigations provided a background to study the reaction in more detail. In addition to the pH study, the effect of temperature, initial  $[\text{RuA}_5\text{OH}_2]^{2+}$  and  $\text{N}_3^-$  concentrations and the stoichiometry of the reaction were studied in some depth.

#### 2.4 Stoichiometry of the Reaction Between Aquo Pentaammine

##### *Ruthenium(II) Ion and Azide Ion*

The preliminary investigations of the reaction described above revealed that monomer and dimer dinitrogen pentaammine ruthenium complexes were formed. In addition to these products it is possible that a further product arising from the reduction of azide ion is present. Azide ion, like dinitrogen gas, is a substrate of the enzyme nitrogenase and when it is reduced by the enzyme dinitrogen gas and ammonia are formed.<sup>10</sup> When azide ion is reduced by either chromium(II) or vanadium(II), the products are dinitrogen gas and ammonia, present as free ammonium ion or bound to the metal.<sup>27</sup> The stoichiometry of the reaction requires two mole of the reductant for each mole of azide reduced. In view of this information a likely product of the reaction is ammonia. Flash photolysis<sup>30</sup> of azide also produces dinitrogen gas and ammonia by a mechanism involving the  $\text{NH}$  radical. Photochemical

decomposition<sup>31</sup> of aqueous hydrazoic acid produces dinitrogen gas, hydroxylamine, ammonia and hydrazine. Consequently these products may also be present in the reaction mixture.

Qualitative tests identified ammonia as the other product of the reaction and it was determined quantitatively using the Kjeldahl determination<sup>36</sup> (see section 6.13.2) and the results are given in Table 2.7. From the table of values presented it is clear that a 1:1 relationship exists between the initial concentration of  $\text{RuA}_5\text{Cl}_3$  (and therefore  $[\text{RuA}_5(\text{OH}_2)]^{2+}$ ) and the concentration of free ammonium ion in solution at the completion of the reaction. No studies were made of ammonium ion concentrations at intermediary stages of the reaction, however, it can be assumed that the 1:1 ratio will still hold. It was established in section 2.3 that at 1:1 relationship between  $\text{RuA}_5\text{Cl}_3$  and dinitrogen complexes produced exists, i.e. 100% of the ruthenium present can be accounted for as dinitrogen complexes after some period. Thus, based on these facts, it can be stated that the equations



are representative of the reactions occurring in the presence of a reducing agent, e.g.  $\text{Zn}(\text{Hg})$  or  $\text{Pt}(\text{H}_2)$ .

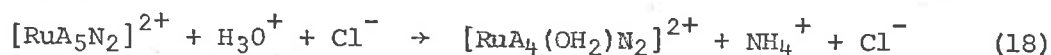
During the investigations of the stoichiometry of the reaction of  $[\text{RuA}_5(\text{OH}_2)]^{2+}$  and azide ion, the stability of the aquo complex and the monomer to ammonia loss were investigated to eliminate the possibility

that ammonia determined arose by dissociation from these complexes. It was found that both complexes are sensitive to the presence of halide ions, in particular chloride.

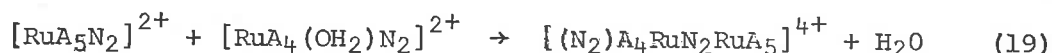
Ammonia loss from  $[\text{RuA}_5(\text{OH}_2)]^{2+}$  was checked by reducing  $[\text{RuA}_5\text{Cl}]^{2+}$  in the presence of chloride ion (0.02-0.03M). The results listed in Table 6.5 (p. 179) show an ammonia loss of one mole per mole of  $[\text{RuA}_5(\text{OH}_2)]^{2+}$  present. By carrying out the reduction under nitrous oxide the dinitrogen complex was isolated by precipitation with lithium chloride. It had a single band at  $2080 \pm 5 \text{ cm}^{-1}$  (lit.<sup>37</sup> for  $[\text{RuA}_4(\text{OH}_2)\text{N}_2]\text{Cl}_2$ ;  $2088 \text{ cm}^{-1}$ ) in its infrared spectrum. A similar solution in which chloride was absent gave only  $[\text{RuA}_5\text{N}_2]^{2+}$  (characterised by the infrared spectrum of the precipitated  $\text{BF}_4^-$  salt:  $\nu_{\text{N-N}}$  found  $2145 \pm 5 \text{ cm}^{-1}$ ; lit.<sup>2</sup>  $2144 \text{ cm}^{-1}$ ). Thus ammonia loss from  $[\text{RuA}_5(\text{OH}_2)]^{2+}$  is chloride catalysed.

To check ammonia loss in the absence of chloride, a solution of  $[\text{RuA}_5\text{N}_2](\text{BF}_4)_2$  in 0.1M sulphuric acid was stirred in the presence of zinc amalgam under nitrogen for 1-2 hours. Argon was not used because dinitrogen loss from this complex is significant over long periods. Ammonia loss from the complex was one mole per mole of complex present. The effect of 0.2M potassium chloride used to elute the ammonium ion from the column, was to catalyse ammonia loss from the dinitrogen complex during the prolonged contact of the dinitrogen complex and the chloride ion. As a check, a solution of monomer was prepared by reducing  $[\text{RuA}_5\text{Cl}]^{2+}$  under nitrous oxide gas. Dinitrogen gas then replaced the

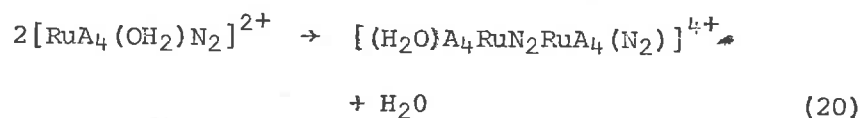
nitrous oxide and potassium chloride to make the solution 1M was added. Examination of the ultraviolet spectrum showed a shift in the wavelength of maximum absorption from 221 nm to 262 nm within half an hour. Loss of ammonia, followed by dimerisation was invoked to explain the observation and the equations given below show possible species present in the reaction mixture.



either



or



Both dimers in the equations would be expected to have similar absorption maxima and molar absorptivities as the other dinitrogen dimers isolated<sup>3,38</sup> e.g.,  $[\text{A}_5\text{RuN}_2\text{RuA}_5]^{4+}$  ( $\lambda_{\text{max}}$  262 nm  $\epsilon = 4.8 \times 10^4 \text{ M}^{-1} \text{ cm}^{-1}$ ),  $[\text{A}_5\text{OsN}_2\text{RuA}_4(\text{OH}_2)]^{4+}$  ( $\lambda_{\text{max}}$  257 nm  $\epsilon = 5.1 \times 10^4 \text{ M}^{-1} \text{ cm}^{-1}$ ) and the two species cannot be distinguished by the position of their ultraviolet absorption maxima. The loss of ammonia also occurs with  $[\text{RuA}_5\text{CO}]^{2+}$  in hydrohalic acid<sup>37</sup> to give  $\text{trans-}[\text{RuA}_4(\text{OH}_2)\text{CO}]^{2+}$ . The stereochemistry of the aquo species was not determined for the dinitrogen ammonia loss, but it is probably trans. The  $\pi$ -acceptor ability of the dinitrogen ligand is similar to that of carbon monoxide.<sup>12</sup> Thus, electron density is effectively withdrawn from the metal ammonia bond trans to the

dinitrogen ligand, thereby labilising the trans ammonia relative to those cis. The products from this reaction mixture were precipitated with saturated potassium chloride and the infrared spectrum recorded. Two bands were noted: one strong band at  $2085\text{ cm}^{-1}$  and a shoulder at  $2100\text{ cm}^{-1}$ . These two bands correspond to the tetraammine (lit.<sup>37</sup>  $\nu_{\text{N-N}}$   $2088\text{ cm}^{-1}$ ) and the pentaammine (lit.<sup>2</sup>  $\nu_{\text{N-N}}$   $2105\text{ cm}^{-1}$ ). Thus  $[\text{RuA}_5\text{N}_2]^{2+}$  is susceptible to ammonia loss in the presence of high chloride ion concentrations.

Both the aquo complex and the monomer are susceptible to loss of ammonia from the first coordination sphere and appropriate corrections were applied to the amount of ammonia determined as described in section 6.13.2.

## 2.5 Kinetics and Mechanism of the Reaction Between $[\text{RuA}_5(\text{OH}_2)]^{2+}$ and Azide Ion

### 2.5(i) Kinetics

The kinetic behaviour was investigated by monitoring the appearance of the monomer and dimer dinitrogen complexes in the ultraviolet region. Variation of the rate with azide ion concentration was readily determined as a wider concentration range is available experimentally than with aquo pentaammine ruthenium(II), which is limited by its solubility. Further, very low concentrations ( $<10^{-3}\text{ M}$ ) of  $[\text{RuA}_5\text{OH}_2]^{2+}$  were undesirable experimentally because of the possibility of oxidation by traces of oxygen in the system. Because the system is heterogeneous a sampling technique was used to follow the reaction. The zinc amalgam used as

the reducing agent consumed acid during the course of the reaction with a consequent slowing of the rate as the reaction proceeded. As no large excess of either reagent could be used the rate constants were calculated from the initial rates. Although the accuracy of the rates so obtained is not very great they are of sufficient accuracy to determine the order with respect to the various reactants.

The effect of azide ion is most readily seen in runs for which the metal concentration is constant. The relationship

$$-d[\text{RuA}_5\text{OH}_2]^{2+}/dt = k[\text{RuA}_5\text{OH}_2]^{2+m}[\text{N}_3^-]^n = k_{\text{obs}}[\text{N}_3^-]^n$$

represents the rate expression at constant aquo pentaammine ruthenium(II) concentration. Under the initial conditions the rate of loss of the aquo complex is equal to the rate of appearance of the monomer, as the formation of the dimer is a slower reaction. Not only the initial slope but a plot of % Monomer at a given time versus azide concentration is a straight line passing through the origin (see figure 2.1), and hence the reaction is first order with respect to azide ion. Table 2.8 lists the values obtained for these runs at  $1.40 \times 10^{-3}$  M  $[\text{RuA}_5\text{OH}_2]^{2+}$  and  $1.81-10.70 \times 10^{-3}$  M azide ion and figure 2.2 shows them graphically.

The order of the reaction with respect to metal ion concentration was studied in cases where the azide ion was in moderate excess. Plots of  $\log(C_o - C_t)$  against time were not linear, where  $C_o$  is the initial aquo concentration and  $C_t$  is the aquo concentration at time  $t$ . Plots of  $(C_{\text{AZ}} - C_o)^{-1} \{ \log C_o(C_{\text{AZ}} - x) - \log C_{\text{AZ}}(C_o - x) \}$  versus time (where  $C_o$  is the initial concentration of the aquo pentaammine,  $C_{\text{AZ}}$  is the

concentration of the azide ion and  $x$  is the extent of the reaction and is equal to  $\% \text{ Monomer} \times C_0$ ) were linear over the first fifteen minutes of reaction, but showed increasing deviations at longer times. Thus the reaction initially showed overall second order kinetics, i.e. was first order with respect to the metal and first order with respect to azide ion. Values of the rate constant were determined from the linear portion of the second order plots as  $10.3 \times 10^{-2} \pm 0.9 \times 10^{-2} \text{ M}^{-1} \text{ sec}^{-1}$  (average of five determinations;  $C_0$  covered the range  $1.40 \times 10^{-3} \text{ M}$  to  $1.06 \times 10^{-2} \text{ M}$  and  $C_{AZ}$  covered the range  $1.81 \times 10^{-3} \text{ M}$  to  $1.31 \times 10^{-2} \text{ M}$ ). The validity of the second order expression was independently checked by determining the initial rate of the reaction ( $d(\text{Monomer})/dt$ ) and plotting this against the product  $C_0 \times C_{AZ}$ , which should be a straight line of slope  $k$  passing through the origin if the reaction is second order. The results are given in Table 2.9 and plotted in figure 2.3 and the plot is linear with a slope of  $9.3 \pm 1.0 \times 10^{-2} \text{ M}^{-1} \text{ sec}^{-1}$ . The values show only a small scatter about the line of "best fit". Thus the reaction is first order in both reactants, at least for the first fifteen minutes, where the diminution of acid concentration by the zinc amalgam is not very great.

The dependence of the rate on the strength of the zinc amalgam was investigated using three different dilutions of a strong amalgam. From the results listed in Table 2.10 the  $\% \text{ Monomer}$  formed after 10 mins. and 20 mins. is the same, within experimental error, regardless of the strength of the amalgam. No variation of the rate constant was



observed with amalgam strength (see Table 2.10). Clearly the reduction step is not rate determining under these conditions. The rate of reaction was also shown to be independent of the nature of the reducing agent. Thus, for the same azide and aquo pentaammine concentrations, the rate constants obtained with zinc amalgam and electrolytic reduction were the same within experimental error ( $10.3 \times 10^{-2} \text{ M}^{-1} \text{ sec}^{-1}$  cf  $10.0 \times 10^{-2} \text{ M}^{-1} \text{ sec}^{-1}$ ).

The effect of temperature on the reaction using zinc amalgam as a reducing agent was investigated and the activation energy for the reaction determined and the results are given in Tables 2.11 and 2.12. A plot of the logarithm of the rate constant against the reciprocal of the absolute temperature was a straight line and from it a value of  $74.9 \pm 7.6 \text{ kJ mole}^{-1}$  at  $25^\circ\text{C}$  was calculated for  $\Delta H^\ddagger$  and  $-33.5 \pm 6.2 \text{ J K}^{-1} \text{ mole}^{-1}$  for  $\Delta S^\ddagger$ .

The observed second order rate constants for the substitution of  $[\text{RuA}_5(\text{OH}_2)]^{2+}$  by several nucleophiles along with  $\Delta H^\ddagger$  and  $\Delta S^\ddagger$  for each of the processes are given in Table 2.13. The values obtained for the azide reaction closely resemble the others. The reaction of aquo pentaammine ruthenium(II) with azide is similar to the heterogeneous reaction with nitrous oxide.<sup>7</sup>

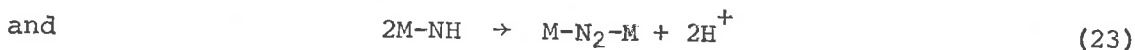
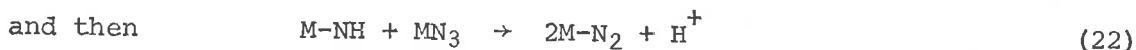
The second order kinetics observed for the substitution reactions of  $[\text{RuA}_5(\text{OH}_2)]^{2+}$  can arise from either an associative ( $\text{SN}_2$ ) or a dissociative ( $\text{SN}_1$ ) pathway. No distinction between the two can be made on a kinetic basis alone, but it has been suggested that a

dissociative reaction pathway is operative.<sup>39</sup> As the substitution rates and activation parameters for a wide variety of nucleophiles are all the same within an order of magnitude, the limiting  $SN_2$  pathway was regarded as unlikely. The insensitivity of the rate to the stability of the ruthenium(II)-ligand bond which is being formed also supports an  $SN_1$  mechanism. Tobe<sup>40</sup> has shown that dissociative pathways occurring by trigonal-bipyramidal intermediates give positive  $\Delta S^\ddagger$  values while negative  $\Delta S^\ddagger$  values are observed with square-pyramidal intermediates. Thus the reactions, including the azide substitution, probably occur by a dissociative pathway with a square-pyramidal intermediate.

Variation of the rate with pH was studied using electrolytic reduction, as the concentration of hydrogen ion is not as variable as with zinc amalgam and the results are given in Tables 2.14 and 2.15 and plotted in figure 2.4. The range of pH's studied was from 1 to 4 at a constant ionic strength of 0.33M in sulphuric acid-potassium sulphate medium. In the range 1-2.1 the rate is almost independent of pH but above 2.1 the rate decreases rapidly until at 4.0 it is very slow.

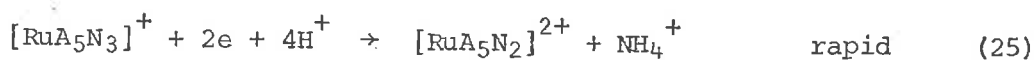
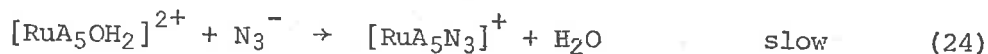
#### 2.5(ii) Mechanism

Basolo<sup>11,13</sup> has suggested that the reaction of azide with aquo pentaammine ruthenium(II) and the decomposition of azide coordinated to ruthenium(III) proceed according to the equations:



Clearly, in the present instance, the mechanism is different because no nitrogen gas is evolved (see Table 2.5) and the formation of dimer is small and can be accounted for by the reaction of the monomer with free aquo. In the acid decomposition of  $[\text{RuA}_5\text{N}_3](\text{N}_3)_2$ , thiourea was used by Kane-Maguire to demonstrate the presence of the nitrene intermediate.<sup>11</sup> The presence of thiourea in the ruthenium(II)-azide system was inconclusive as thiourea substituted the aquo ligand to form a complex, presumably  $[\text{RuA}_5\text{Tu}]^{2+}$ , with a shoulder at 244 nm ( $\epsilon = 7.5 \times 10^3 \text{ M}^{-1} \text{ cm}^{-1}$ ) on an intense absorption.

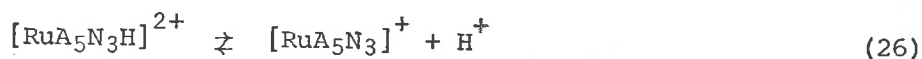
It is clear from the results that the rate determining step is the substitution of azide or hydrazoic acid on the aquo complex to form an azido complex, which is rapidly reduced to give the monomer dinitrogen complex and ammonia.



The ability of the azide ion to act as a ligand is well known. Basolo<sup>13</sup> has proposed an initial attack of hydrazoic acid on the aquo pentaammine, but a different subsequent reaction. The reaction of chromium(II) and vanadium(II) with azide in acid proceeded by substitution of hydrazoic acid on the metal.<sup>27</sup> The rate constants for the chromium and vanadium reactions were independent of hydrogen ion concentration from 0.16M to

1.0M, but the reaction was not investigated at higher pH's.

If the reaction is with hydrazoic acid the product is likely to change rapidly to the azido complex at the pH's investigated:



Although such complexes as  $[\text{CoA}_5\text{N}_3\text{H}](\text{ClO}_4)_3$  are known,<sup>41</sup> the  $\text{pK}_a$  of the complexes  $[\text{MA}_5\text{N}_3\text{H}]^{3+}$  ( $\text{M} = \text{Co}, \text{Rh}, \text{Ir}$  and  $\text{Cr}$ ) have been measured<sup>32,42</sup> as -2 to -3, and so they are completely dissociated in all but strong acids.

Not only the kinetics but the enthalpy of activation for the reaction are in agreement with other substitution reactions of aquo pentaammine ruthenium(II), so providing support for the mechanism as presented above.

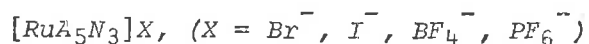
The effect of acid concentration on the reaction presents some puzzling features. The relative rates of reactions (24) and (25) changed because at  $\text{pH} > 3$  the colour of the azido intermediate (see section 2.6) persisted for ten to fifteen minutes. The formation of the azido complex was no longer the rate determining step but the decomposition was rate determining.

The changes in the value of  $k_{\text{obs}}$  at pH 1 to 4 parallels the changes in the hydrazoic acid concentration ( $\text{pK}_a \text{ HN}_3$  4.8 at  $20^\circ\text{C}$ <sup>20</sup>), and this would appear to favour the participation of hydrazoic acid in the rate determining step. However, because of the rapid ionisation of an intermediate hydrazoic acid complex and the obvious dependence of the reduction on hydrogen ion concentration, this may be coincidental.

Feltham<sup>43</sup> has proposed a mechanism similar to the one above for the decomposition of trans-azidochlorobis[o-phenylene bis(dimethyl arsine)] ruthenium(II), trans-[RuN<sub>3</sub>Cl(das)<sub>2</sub>], in acid solution. The products of the decomposition are the corresponding dinitrogen complex trans-[RuN<sub>2</sub>Cl(das)<sub>2</sub>] and a product identified as trans-[RuCl(NH<sub>3</sub>)(das)<sub>2</sub>] or trans-[RuCl(NH<sub>2</sub>OH)(das)<sub>2</sub>]. The mechanism proceeds by the protonation of either the terminal or coordinated nitrogen of the azide group which decomposes into dinitrogen and the imido radical.

These factors combined with the evidence from the experiments with no reducing agent present, pH variation and the kinetics present a reasonable argument in favour of the mechanism of the reaction as presented here. The final evidence of the mechanism came with the moderately successful attempts, which are described in section 2.6, to isolate the azido intermediate.

#### 2.6 Attempted Isolation of Azido Pentaammine Ruthenium(II) Salts,



Preparation of the azido complexes, [RuA<sub>5</sub>N<sub>3</sub>]X was accomplished in neutral solution at 0°C by rapid precipitation of the salts with a saturated solution of the appropriate anion. Red solids were isolated from the orange solution and handled in a nitrogen glove bag. On standing the colour of the complexes rapidly faded to a pale yellow.

The characterisation of the compounds was based mainly on the infrared spectra which are listed in Table 2.16 along with the band

assignments. For comparison, the bromide and iodide salts of the corresponding ruthenium(III) compound,  $[\text{RuA}_5\text{N}_3]\text{X}_2$  were prepared and their infrared spectra are also included. The assignment of bands was made difficult by the presence of two compounds in the solids isolated - the azido and the dinitrogen complex.

The azide ion is linear<sup>17</sup> and has the point group  $D_{\infty h}$  and therefore has two infrared active fundamental vibrations,  $\Sigma_u^+$  and the doubly degenerate  $\Pi_u$ . Extensive studies<sup>44</sup> of the infrared spectrum have identified the fundamental vibrations of  $\text{N}_3^-$  as  $\nu_3$  (antisymmetric stretch)  $2037\text{ cm}^{-1}$ ;  $\nu_2$  (bending vibration)  $640\text{ cm}^{-1}$ . The  $\nu_1$  (symmetric stretch) fundamental which is Raman active has been observed at  $1358\text{ cm}^{-1}$ . An intense absorption band which occurs above  $2000\text{ cm}^{-1}$  is characteristic of azide ion coordinated to a transition metal.<sup>45</sup> On coordination to a metal the azide symmetric stretch becomes infrared active and is observed<sup>46</sup> at about  $1300\text{ cm}^{-1}$ . The doubly degenerate bending vibration occurring between  $500$  and  $700\text{ cm}^{-1}$  has been reported for several azido complexes.<sup>46</sup>

For the complexes isolated the asymmetric stretching vibration of the azide ion was readily identified as an absorption at  $2030\text{ cm}^{-1}$ . On standing in the infrared beam the peak disappeared while that of the nitrogen complex, present as an impurity, increased (see figure 2.5). No bands assignable to the symmetric stretching frequency were observed, because the symmetric deformation of the ammonia ligands occur in the same region and their intensity is larger than that of  $\nu_1$ . A weak band

near  $550\text{ cm}^{-1}$  was assigned to the doubly degenerate bending mode of the azide group. For other ruthenium azido complexes trans- $[\text{RuN}_3\text{Cl}(\text{das})_2]$ ,<sup>47</sup> cis- $[\text{Ru}(\text{en})_2(\text{N}_3)(\text{N}_2)]\text{PF}_6$ <sup>11</sup> and cis- $[\text{Ru}(\text{trien})(\text{N}_2)(\text{N}_3)]\text{PF}_6$ <sup>11</sup> the asymmetric stretching frequency of the azide ligand was observed at 2038, 2050 and  $2050\text{ cm}^{-1}$  respectively, but no assignments of the bending vibration were made. The assignments of  $\nu_3$  and  $\nu_2$  made here are supported by the assignments made for other azido complexes.

For the complexes  $[\text{CoA}_6]\text{X}_2$  and  $[\text{CoA}_6]\text{X}_3$ ,  $\text{X} = \text{Cl}^-$ ,  $\text{Br}^-$ ,  $\text{I}^-$ , the  $\rho(\text{NH}_3)$  rocking vibrations and the  $\delta_s(\text{NH}_3)$  vibration are the most affected by changes in the oxidation state of the metal,<sup>45</sup> with shifts of  $\sim 180\text{ cm}^{-1}$  evident for the corresponding anions. Other regions of the spectrum, viz.  $\nu_{\text{N-H}}$  and  $\delta_d(\text{NH}_3)$  undergo only small variations of the frequency of vibration. Similar trends have been found for the chloride salts of ruthenium(II) and ruthenium(III) hexaammine.<sup>48</sup> The  $\delta_s(\text{NH}_3)$  vibration is shifted about  $100\text{ cm}^{-1}$  for  $[\text{RuA}_6]\text{Cl}_2$  compared with  $[\text{RuA}_6]\text{Cl}_3$ , i.e.  $1220\text{ cm}^{-1}$  for Ru(II) to  $1316\text{ cm}^{-1}$  for Ru(III). In the case of  $\rho(\text{NH}_3)$  however the variation is not as pronounced as for the cobalt hexaammines. Thus,  $[\text{RuA}_6]\text{Cl}_3$  has an absorption at  $788\text{ cm}^{-1}$  while  $[\text{RuA}_6]\text{Cl}_2$  has an absorption at  $\sim 770\text{ cm}^{-1}$ . The band positions are very dependent on the nature of the anion used and the degree of back-bonding in the complexes. However, it can be asserted that, providing comparison is made between salts of the same anion, ruthenium(II) and ruthenium(III) compounds can be distinguished from their infrared spectra.

The complexes are assigned as ruthenium(II) from the position of the ammine bands. The position of the ammine bands in  $[\text{RuA}_5\text{N}_2]\text{X}_2$  are more typical of ruthenium(III) amines than ruthenium(II) amines, because of the back-bonding to the dinitrogen ligand.<sup>2</sup> Thus in the infrared spectra recorded for the ruthenium(II) azido complexes two separate  $\delta_s(\text{NH}_3)$  vibrations are observed, one at  $\sim 1300\text{ cm}^{-1}$  (due to the dinitrogen complex) and another at  $\sim 1250\text{ cm}^{-1}$  (due to the azido complex), i.e. at positions similar to that observed for the ruthenium hexaamines. Further, two absorptions are observed in the  $\rho\text{NH}_3$  region in the ruthenium(II) azido spectra, but not in the spectra of the ruthenium(III) azido complexes.

The electronic spectrum of  $[\text{RuA}_5\text{N}_3]^+$  was recorded in water and an acetate buffer (pH  $\sim 4$ ). At these pH's the decomposition rate was slower than in acid but still quite rapid. Several runs were performed in which the absorbance was monitored with time. The first order rate plots were linear over the first thirty minutes of the reaction with a deviation being apparent after that time. The reaction produces both  $[\text{RuA}_5\text{N}_2]^{2+}$  and  $[\text{RuA}_5\text{OH}_2]^{3+}$ . As the reaction proceeds a slower reaction between the aquo pentaammine ruthenium(III) and acetate produces  $[\text{RuA}_5\text{OAc}]^{2+}$  ( $\lambda_{\text{max}} 296\text{ nm}$ ,  $\epsilon = 1.44 \times 10^3\text{ M}^{-1}\text{ cm}^{-1}$ ),<sup>49</sup> and the absorption of this species becomes predominant at longer times. An average of six determinations gave a decomposition rate of  $3.10 \times 10^{-4} \pm 0.40 \times 10^{-4}\text{ sec}^{-1}$  for the azido complex. This can be compared with the rate of decomposition observed<sup>11</sup> for  $[\text{RuA}_5\text{N}_3](\text{N}_3)_2$  of  $1.17 \times 10^{-3}\text{ sec}^{-1}$ . Thus,



the decomposition of azido ruthenium(II) is much slower than the decomposition of the ruthenium(III) azido complex under the same conditions.

Using the calculated rate constant a value of the molar absorptivity of  $[\text{RuA}_5\text{N}_3]^+$  was calculated. Assuming 100% formation of the azido complex from the reactant  $[\text{RuA}_5\text{OH}_2]^{2+}$ , the molar absorptivity at 430 nm ( $\lambda_{\text{max}}$ ) was approximately  $300 \text{ M}^{-1} \text{ cm}^{-1}$ . The absorption maximum of  $[\text{RuA}_5\text{N}_3]^{2+}$  was observed<sup>2</sup> at 463 nm. This shift of 33 nm correlates with the shift found in absorption maxima for other ruthenium(II), (III) azido pairs,<sup>11</sup> e.g.  $\text{cis-}[\text{Ru}(\text{en})_2\text{N}_2\text{N}_3]^+ \lambda_{\text{max}} 460 \text{ nm}$ ,  $\text{cis-}[\text{Ru}(\text{en})_2(\text{N}_3)_2]^+ \lambda_{\text{max}} 484 \text{ nm}$ ;  $\text{cis-}[\text{Ru}(\text{trien})\text{N}_2(\text{N}_3)]^+ \lambda_{\text{max}} 460 \text{ nm}$ ,  $\text{cis-}[\text{Ru}(\text{trien})(\text{N}_3)_2]^+ \lambda_{\text{max}} 500 \text{ nm}$ . The intensity of the absorption suggests that it probably arises due to a d-d transition rather than a charge transfer band. If this is the case then it can be assigned as  $^1\text{A}_{1g} \rightarrow ^1\text{T}_{1g}$  transition as found for other octahedral ruthenium(II) complexes.<sup>50</sup>

No absorptions assignable to the azido complex were observed down to the limit of the range investigated (200 nm). This may be because such absorptions are weak compared with those of the dinitrogen complex, which always appear, or the compound may not have any other absorptions.

In an attempt to characterise the solids an analysis of a freshly prepared sample of  $[\text{RuA}_5\text{N}_3]\text{Br}$ , for bromide ion was performed. The average value obtained (four determinations) was 39.6% and is too high for the ruthenium(II) azide (% Br = 25.9%) and slightly low for the

ruthenium(III) azide (% Br = 41.2%). However, precipitation of  $[\text{RuA}_5\text{N}_2]\text{Br}_2$  (% Br 42.7%), present as an impurity, tends to raise the amount of bromide actually determined. The results could still indicate a ruthenium(II) complex, if the complex precipitated were  $[\text{RuA}_5\text{N}_3\text{H}]\text{Br}_2$  (% Br = 41.1%), such hydrazoic acid complexes are known,<sup>41</sup> but the results obtained are inconclusive.

## 2.7 Summary

The reaction between  $[\text{RuA}_5(\text{OH}_2)]^{2+}$  and azide ion has been shown to form the pentaammine ruthenium dinitrogen complexes. The stoichiometry of the reaction was investigated and for each mole of aquo complex and azide ion present, one mole of dinitrogen complex and one mole of ammonia were formed. Thus,  $[\text{RuA}_5(\text{OH}_2)]^{2+}$  treats azide ion analogously to the enzyme nitrogenase. From kinetic studies it was shown, that the rate of azide substitution on  $[\text{RuA}_5(\text{OH}_2)]^{2+}$  was similar to that observed for other substitution reactions involving nitrogen donor ligands, viz.  $\sim 10 \times 10^{-2} \text{ M}^{-1} \text{ sec}^{-1}$ . Activation parameters were also of the same order, viz.  $\Delta H^\ddagger 74.9 \text{ kJ mole}^{-1}$  and  $\Delta S^\ddagger -33.5 \text{ J K}^{-1} \text{ mole}^{-1}$ . From these measurements a mechanism of the reaction involving the formation of an intermediate azido complex was proposed. The mechanism was reinforced by the isolation of the intermediate.

TABLE 2.1

*Molar Absorptivities<sup>‡</sup> of Sodium Azide at Various pH's*

pH	$\epsilon_{221} \text{ M}^{-1} \text{ cm}^{-1}$	$\epsilon_{260}^{\dagger} \text{ M}^{-1} \text{ cm}^{-1}$	$\epsilon_{262} \text{ M}^{-1} \text{ cm}^{-1}$
1.1	69.0	39.0	39.0
2.2	73.5	39.5	39.5
3.4	120.0	39.5	39.5
4.5	400	*	27.9
6.9	755	*	15.0

<sup>†</sup>  $\lambda_{\text{max}}$ ; lit.<sup>22</sup>  $\epsilon_{260} = 43.8 \text{ M}^{-1} \text{ cm}^{-1}$  in 0.76M  $\text{H}_2\text{SO}_4$ .

\* a maximum was no longer observed at 260 nm.

<sup>‡</sup> Obtained from a Beer's Law plot over the concentration range  
 $6.40 \times 10^{-4} \text{ M}$  -  $2.82 \times 10^{-2} \text{ M}$ .

TABLE 2.2

*Molar Absorptivities of Dinitrogen Complexes\**

Species	$\epsilon_{221 \text{ nm}} \text{ M}^{-1} \text{ cm}^{-1}$	$\epsilon_{262 \text{ nm}} \text{ M}^{-1} \text{ cm}^{-1}$
$[\text{RuA}_5\text{N}_2]^{2+}$	$1.80 \times 10^4 \text{ (a)}$	$0.084 \times 10^4$
$[\text{A}_5\text{RuN}_2\text{RuA}_5]^{4+}$	$0.30 \times 10^4$	$4.8 \times 10^4$
$[\text{RuA}_5\text{OH}_2]^{2+}$	$0.068 \times 10^4$	$0.055 \times 10^4$

\* Taken from reference 6, except (a) which was taken from reference 5.

TABLE 2.4

Reaction of  $[\text{RuA}_5(\text{OH}_2)]^{2+}$  with Azide Using Various Reducing Agents

$[\text{RuA}_5\text{Cl}_3]_i$	$[\text{N}_3^-]$	Time (mins)	% Monomer	% Dimer	% Fixed $\text{N}_2$	% Total Ru
(i) Electrolytic Reduction						
$1.35 \times 10^{-2} \text{ M}$	$4.97 \times 10^{-2} \text{ M}$	4	33.0	1.60	34.6	36.2
		15	43.8	1.26	45.1	46.4
		30	63.9	3.09	66.9	70.0
		55	77.4	6.75	84.1	90.0
(ii) Amalgamated Zinc						
$8.29 \times 10^{-3} \text{ M}$	$3.17 \times 10^{-2} \text{ M}$	60	25.8	10.1	35.9	46.0
		120	37.3	18.3	55.6	73.9
		300	28.6	25.3	53.9	79.2
		360	26.3	33.9	60.2	94.1
(iii) Hydrogen on Platinum Black						
$1.29 \times 10^{-2} \text{ M}$	$4.96 \times 10^{-2} \text{ M}$	4	23.9	0.81	24.7	25.5
		13	22.9	1.24	24.1	25.4
		28	22.8	3.32	26.1	29.4
		43	20.0	5.73	25.7	31.5

TABLE 2.5

Reaction Between  $[\text{RuA}_5(\text{OH}_2)]^{2+}$  and  $\text{N}_3^-$  in the Absence of a Reducing Agent: Monitor of Gas Release

$[\text{RuA}_5\text{Cl}_3]_i$	$[\text{N}_3^-]$	% Conversion <sup>a</sup>	Vol. gas obtained (ml)	Vol. gas calculated <sup>b</sup> (ml)	% Gas
$1.07 \times 10^{-2}$ M	$9.87 \times 10^{-2}$ M	98.40	0.02	0.60	~3%
$1.07 \times 10^{-2}$ M	$7.40 \times 10^{-2}$ M	90.80	0.07	0.60	~9%
$1.07 \times 10^{-2}$ M	$9.87 \times 10^{-3}$ M	95.10	0.00	0.60	0

a. Conversion to dinitrogen complexes and ruthenium(III) oxidation product.

b. Based on the stoichiometry reported by Basolo and Sheridan,<sup>13</sup> i.e. 1 mole of dinitrogen released for each two mole of  $[\text{RuA}_5(\text{OH}_2)]^{2+}$  consumed.

TABLE 2.6

*Reaction of  $[\text{RuA}_5(\text{OH}_2)]^{2+}$  and Azide in the Absence of a Reducing Agent*

$[\text{RuA}_5\text{Cl}_3]$	$[\text{N}_3^-]$	Time (mins)	% Monomer	% Dimer	% Oxidised	% Conversion
$6.18 \times 10^{-3} \text{ M}$	$2.0 \times 10^{-2} \text{ M}$	10	25.6	2.8	56.8	88.0
		30	26.2	2.8	58.0	89.8
$1.46 \times 10^{-2} \text{ M}$	$2.30 \times 10^{-2} \text{ M}$	10	31.2	0.95	64.3	97.4
		30	32.6	1.00	67.2	101.8
$1.29 \times 10^{-2} \text{ M}$	$5.1 \times 10^{-2} \text{ M}$	11	28.6	1.7	60.6	92.6
		30	31.9	1.4	66.6	101.3
$6.75 \times 10^{-3} \text{ M}$	$1.42 \times 10^{-2} \text{ M}$	15	25.0	0.85	51.7	77.6
		40	27.6	0.91	57.0	85.5
		60	29.0	1.12	60.2	90.3
$1.20 \times 10^{-2} \text{ M}$	$4.8 \times 10^{-2} \text{ M}$	10	35.7	0.90	73.2	110.7
		30	35.7	0.90	73.2	110.7

TABLE 2.7

*Stoichiometry of the Reaction Between  $[\text{RuA}_5(\text{OH}_2)]^{2+}$  and Azide Ion*

$[\text{RuA}_5\text{Cl}_3]_i$	Titre Value (ml)	No. mole $\text{NH}_4^+$	Correction (mole) <sup>d</sup>	Molar Concentration	$\text{NH}_4^+$
$1.12 \times 10^{-2}$ M	7.64	$22.16 \times 10^{-5}$	$12.13 \times 10^{-5}$	$1.00 \times 10^{-2}$ M	b
$1.11 \times 10^{-2}$ M	7.50	$21.75 \times 10^{-5}$	$12.03 \times 10^{-5}$	$0.97 \times 10^{-2}$ M	b
$1.13 \times 10^{-2}$ M	10.40	$15.03 \times 10^{-5}$	$4.24 \times 10^{-5}$	$1.08 \times 10^{-2}$ M	a
$2.19 \times 10^{-2}$ M	11.10	$16.04 \times 10^{-5}$	$4.24 \times 10^{-5}$	$2.36 \times 10^{-2}$ M	c
$2.19 \times 10^{-2}$ M	11.70	$16.91 \times 10^{-5}$	$4.24 \times 10^{-5}$	$2.53 \times 10^{-2}$ M	c

<sup>a</sup> 10 ml of solution used;  $1.45 \times 10^{-2}$  M HCl used in titres.

<sup>b</sup> 10 ml of solution used;  $2.9 \times 10^{-2}$  M HCl used in titres.

<sup>c</sup> 5 ml of solution used;  $1.45 \times 10^{-2}$  M HCl used in titres.

<sup>d</sup> Corrected for ammonia arising from other sources, e.g. from the monomer losing ammonia, as described in section 6.13.2.



TABLE 2.8

Reaction of  $[\text{RuA}_5(\text{OH}_2)]^{2+}$  with Azide Ion in the Presence of Zinc Amalgam

Effect of Varying the Initial Azide Ion Concentration

$[\text{RuA}_5\text{Cl}_3]_i$	$[\text{N}_3^-]_i$	Time (mins)	% Monomer	% Dimer	% Fixed $\text{N}_2$	% Total Ru
$1.42 \times 10^{-3} \text{ M}$	$1.81 \times 10^{-3} \text{ M}$	2	4.2 <sub>0</sub>	0.7 <sub>4</sub>	4.9 <sub>3</sub>	5.6 <sub>7</sub>
		15	13.2 <sub>4</sub>	0.9 <sub>0</sub>	14.1 <sub>4</sub>	15.0 <sub>4</sub>
		30	20.7 <sub>8</sub>	1.1 <sub>4</sub>	21.9 <sub>1</sub>	23.0 <sub>5</sub>
		45	23.5 <sub>7</sub>	1.3 <sub>5</sub>	24.9 <sub>2</sub>	26.2 <sub>7</sub>
		60	24.2 <sub>2</sub>	1.7 <sub>0</sub>	25.9 <sub>1</sub>	27.6 <sub>1</sub>
$1.40 \times 10^{-3} \text{ M}$	$4.34 \times 10^{-3} \text{ M}$	2	10.2 <sub>6</sub>	1.0 <sub>7</sub>	11.3 <sub>3</sub>	12.4 <sub>0</sub>
		15	27.1 <sub>1</sub>	1.0 <sub>4</sub>	28.1 <sub>5</sub>	29.1 <sub>9</sub>
		30	36.1 <sub>1</sub>	1.1 <sub>5</sub>	37.2 <sub>6</sub>	38.4 <sub>1</sub>
		45	43.6 <sub>8</sub>	1.5 <sub>2</sub>	45.2 <sub>0</sub>	46.7 <sub>2</sub>
		60	50.6 <sub>8</sub>	1.6 <sub>1</sub>	52.2 <sub>9</sub>	53.9 <sub>0</sub>
$1.49 \times 10^{-3} \text{ M}$	$10.7_0 \times 10^{-3} \text{ M}$	2	17.2 <sub>0</sub>	1.4 <sub>6</sub>	18.6 <sub>6</sub>	20.1 <sub>2</sub>
		15	48.9 <sub>6</sub>	1.4 <sub>9</sub>	50.4 <sub>5</sub>	51.9 <sub>4</sub>
		30	59.2 <sub>5</sub>	1.2 <sub>7</sub>	60.5 <sub>2</sub>	61.7 <sub>9</sub>
		45	65.3 <sub>7</sub>	1.4 <sub>7</sub>	66.8 <sub>4</sub>	68.3 <sub>1</sub>
		60	70.0 <sub>4</sub>	1.4 <sub>8</sub>	71.5 <sub>2</sub>	73.0 <sub>0</sub>

TABLE 2.9

Reaction of  $[\text{RuA}_5\text{OH}_2]^{2+}$  with Azide Ion in the Presence of Zinc Amalgam

Test of the second order kinetics based on initial slopes.

$[\text{RuA}_5\text{Cl}_3] = C_O$	$[\text{N}_3^-] = C_{AZ}$	Initial Slope = $\frac{d[\text{Monomer}]}{dt}$	$C_O \times C_{AZ}$
M	M	$\text{M sec}^{-1}$	$\text{M}^2$
$1.42 \times 10^{-3}$	$1.81 \times 10^{-3}$	$0.28 \times 10^{-6}$	$0.26 \times 10^{-5}$
$1.40 \times 10^{-3}$	$4.34 \times 10^{-3}$	$0.55 \times 10^{-6}$	$0.61 \times 10^{-5}$
$1.49 \times 10^{-3}$	$1.07 \times 10^{-2}$	$1.63 \times 10^{-6}$	$1.59 \times 10^{-5}$
$5.18 \times 10^{-3}$	$7.63 \times 10^{-3}$	$4.48 \times 10^{-6}$	$3.95 \times 10^{-5}$
$5.47 \times 10^{-3}$	$1.08 \times 10^{-2}$	$6.63 \times 10^{-6}$	$5.91 \times 10^{-5}$
$6.34 \times 10^{-3}$	$1.42 \times 10^{-2}$	$8.22 \times 10^{-6}$	$9.00 \times 10^{-5}$
$5.46 \times 10^{-3}$	$2.38 \times 10^{-2}$	$11.33 \times 10^{-6}$	$13.00 \times 10^{-5}$
$1.06 \times 10^{-2}$	$1.31 \times 10^{-2}$	$12.02 \times 10^{-6}$	$13.89 \times 10^{-5}$
$5.33 \times 10^{-3}$	$2.63 \times 10^{-2}$	$14.03 \times 10^{-6}$	$14.02 \times 10^{-5}$
$6.74 \times 10^{-3}$	$2.53 \times 10^{-2}$	$16.85 \times 10^{-6}$	$17.05 \times 10^{-5}$

Average value of  $k = 9.3 \pm 1.0 \times 10^{-2} \text{ M}^{-1} \text{ sec}^{-1}$  determined from the line of best fit.

TABLE 2.10

Effect of Amalgam Strength on the Reaction Between  $[\text{RuA}_5(\text{OH}_2)]^{2+}$  and Azide Ion

$[\text{RuA}_5\text{Cl}_3]_i$	$[\text{N}_3^-]$	Amalgam	Time (mins)	% Monomer	% Dimer	% Total Ru
$1.04 \times 10^{-2} \text{ M}$	$1.88 \times 10^{-2} \text{ M}$	A	10	53.11	1.88	56.86
			25	64.83	5.28	75.38
			40	69.45	9.60	88.65
			80	61.31	13.55	88.41
$9.44 \times 10^{-3} \text{ M}$	$1.78 \times 10^{-2} \text{ M}$	B		$k_{\text{obs}} = 10.2 \times 10^{-2} \text{ M}^{-1} \text{ sec}^{-1}$		
			10	56.22	1.47	59.16
			20	67.74	3.72	75.17
			40	69.86	5.24	80.34
$1.06 \times 10^{-2} \text{ M}$	$1.31 \times 10^{-2} \text{ M}$	C		$k_{\text{obs}} = 11.1 \times 10^{-2} \text{ M}^{-1} \text{ sec}^{-1}$		
			15	51.88	3.87	59.62
			30	53.35	7.82	68.99
			45	51.12	11.64	74.40
			60	42.80	16.96	76.72
				$k_{\text{obs}} = 10.9 \times 10^{-2} \text{ M}^{-1} \text{ sec}^{-1}$		

Amalgam A: as prepared by the method of Vogel (see experimental section).

Amalgam B: 1 in 5 dilution of amalgam A.      Amalgam C: 1 in 5 dilution of amalgam B.

TABLE 2.11

*Effect of Temperature on the Reaction Between  $[\text{RuA}_5(\text{OH}_2)]^{2+}$  and Azide Ion*

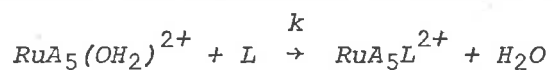
Temp.	$[\text{RuA}_5\text{Cl}_3]_i$	$[\text{N}_3^-]$	Time (mins)	% Monomer	% Dimer	% Fixed $\text{N}_2$	% Total Ru
19.7°C	$2.30 \times 10^{-3} \text{ M}$	$7.20 \times 10^{-3} \text{ M}$	4	13.71	1.06	14.78	15.84
			17	26.14	1.19	27.32	28.51
			31	27.30	1.76	29.05	30.81
			45	28.69	1.81	30.50	32.31
25.0°C	$3.11 \times 10^{-3} \text{ M}$	$6.95 \times 10^{-3} \text{ M}$	2	11.21	1.02	12.23	13.25
			13	14.63	1.40	16.03	17.42
			28	14.48	2.27	16.75	19.0 <sub>3</sub>
			44	13.89	3.07	16.95	20.0 <sub>2</sub>
30.6°C	$3.55 \times 10^{-3} \text{ M}$	$5.38 \times 10^{-3} \text{ M}$	2	13.02	1.14	14.1 <sub>6</sub>	15.3 <sub>0</sub>
			14	18.08	2.43	20.5 <sub>1</sub>	22.9 <sub>4</sub>
			30	15.93	4.37	20.3 <sub>0</sub>	24.6 <sub>7</sub>
			45	14.99	6.37	21.36	27.7 <sub>2</sub>
35.6°C	$3.04 \times 10^{-3} \text{ M}$	$6.77 \times 10^{-3} \text{ M}$	2	17.50	1.44	18.94	20.38
			16	19.08	3.17	22.24	25.41
			33	16.58	7.12	23.70	30.8 <sub>2</sub>
			48	14.22	9.27	23.48	32.74

TABLE 2.12

*Effect of Temperature on the Observed Rate Constant*<sup>†</sup>

Temp. °C	$k_{\text{obs}} \times 10^2 \text{ M}^{-1} \text{ sec}^{-1}$
19.7	$9.02 \pm 1.80$
25.0	$14.9_0 \pm 2.50$
30.6	$24.8_0 \pm 5.62$
35.6	$46.1_4 \pm 9.17$

<sup>†</sup> Average of two determinations.

TABLE 2.13<sup>1</sup>Observed Rate Constants<sup>2</sup> and Activation Parameters for the Reaction:

L	k M <sup>-1</sup> sec <sup>-1</sup>	$\Delta H^\ddagger$	$\Delta S^\ddagger$	Reference
		kJ mole <sup>-1</sup>	J K <sup>-1</sup> mole <sup>-1</sup>	
Pyridine	0.091	64.0	-54.4	39 (a)
Acetonitrile	0.260	67.8	-29.3	39 (a)
Benzonitrile	0.268	66.1	-33.5	39 (a)
N <sub>2</sub> O	0.072	73.6	-46	8
N <sub>2</sub>	0.073	76.6	-8.4	5
N <sub>2</sub>	0.080	89.5	+33.5	6 (b)
RuA <sub>5</sub> N <sub>2</sub> <sup>2+</sup>	0.036	80.8	-4.2	6 (b)
Pyrazine	0.056	73.2	-23.9	39 (b)
3-Picoline	0.091	70.7	-28.0	39 (b)
N <sub>3</sub> <sup>-</sup> (HN <sub>3</sub> )	0.149	74.9	-33.5	This work
iso-Nicotinamide	0.105	-	-	39 (b)
Imidazole	0.200	69.0	-27.2	39 (b)

<sup>1</sup> Taken, in part, from ref. 39(a).<sup>2</sup> In aqueous solution at 25°C.

TABLE 2.14

Effect of pH on the Reaction Between  $\text{RuA}_5(\text{OH}_2)^{2+}$  and  $\text{N}_3^-$ 

pH	$[\text{RuA}_5\text{Cl}_3]_i$	$[\text{N}_3^-]_i$	Time (mins)	% Monomer	% Dimer	% Fixed $\text{N}_2$	% Total Ru
1.5	$1.22 \times 10^{-2} \text{ M}$	$4.97 \times 10^{-2} \text{ M}$	2	26.1 <sub>4</sub>	0.8 <sub>5</sub>	26.9 <sub>9</sub>	27.8 <sub>4</sub>
			4	31.0 <sub>5</sub>	0.6 <sub>8</sub>	31.7 <sub>3</sub>	32.4 <sub>1</sub>
			6	34.0 <sub>9</sub>	0.6 <sub>3</sub>	34.7 <sub>1</sub>	35.3 <sub>4</sub>
			12	44.9 <sub>8</sub>	0.9 <sub>4</sub>	45.9 <sub>2</sub>	46.8 <sub>6</sub>
			28	56.4 <sub>2</sub>	1.4 <sub>3</sub>	57.8 <sub>5</sub>	59.2 <sub>8</sub>
			42	65.9 <sub>2</sub>	2.4 <sub>7</sub>	68.3 <sub>9</sub>	70.8 <sub>6</sub>
2.1	$1.31 \times 10^{-2} \text{ M}$	$5.02 \times 10^{-2} \text{ M}$	2	25.9 <sub>3</sub>	1.00	26.9 <sub>3</sub>	27.9 <sub>3</sub>
			4	28.9 <sub>9</sub>	0.71	29.7 <sub>0</sub>	30.4 <sub>1</sub>
			6	33.1 <sub>9</sub>	0.7 <sub>0</sub>	33.8 <sub>9</sub>	34.6 <sub>0</sub>
			13	42.8 <sub>6</sub>	1.6 <sub>5</sub>	44.5 <sub>1</sub>	46.1 <sub>6</sub>
			29	51.4 <sub>0</sub>	1.6 <sub>6</sub>	53.0 <sub>6</sub>	54.7 <sub>2</sub>
			44	62.5 <sub>0</sub>	3.3 <sub>7</sub>	66.8 <sub>7</sub>	70.2 <sub>4</sub>
2.5	$1.22 \times 10^{-2} \text{ M}$	$5.01 \times 10^{-2} \text{ M}$	2	25.13	0.82	25.95	26.77
			4	27.61	0.51	28.11	28.62
			6	28.72	0.40	29.13	29.53
			12	36.88	0.66	37.54	38.20
			28	43.35	1.04	44.39	45.42
			42	46.68	1.96	48.63	50.59 (contd.)

TABLE 2.14 (contd.)

pH	$[\text{RuA}_5\text{Cl}_3]_i$	$[\text{N}_3^-]_i$	Time (mins)	% Monomer	% Dimer	% Fixed $\text{N}_2$	% Total Ru
3.2	$1.29 \times 10^{-2} \text{ M}$	$5.05 \times 10^{-2} \text{ M}$	2	20.74	1.38	22.12	23.51
			4	23.12	1.08	24.20	25.28
			6	25.45	1.04	26.49	27.53
			14	33.40	1.66	35.07	36.73
			28	45.75	2.31	48.07	50.38
			43	55.07	4.57	59.64	64.21



TABLE 2.15

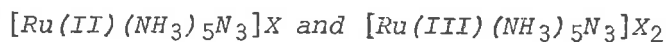
*Effect of pH on the Observed Rate Constant*

pH	Reaction Medium	$k_{\text{obs}} \times 10^2 \text{ M}^{-1} \text{ sec}^{-1}$
1.2	0.1M $\text{H}_2\text{SO}_4$ -0.01M $\text{K}_2\text{SO}_4$	7.15
1.5	" " *	6.83
2.1	0.01M $\text{H}_2\text{SO}_4$ -0.10M $\text{K}_2\text{SO}_4$	5.31
2.1	" "	5.46
2.5	" " *	3.07
2.7	" " *	2.43
3.2	0.001M $\text{H}_2\text{SO}_4$ -0.109M $\text{K}_2\text{SO}_4$	2.01
4.0	" " *	1.48

\* Adjusted to the required pH with dilute pot. hydroxide.

 $\mu = 0.33\text{M}$  $T = 18.0^\circ\text{C}$

TABLE 2.16

*Infrared Spectra of Azido Pentaammine Ruthenium Salts,*All frequencies recorded as  $cm^{-1}$ .

Assignment	X = Br	Br <sub>2</sub>	I	I <sub>2</sub>	BF <sub>4</sub>	PF <sub>6</sub>
$\nu_{N-H}$	3200 br	3200 br	3200 br	3150 br	3360 s 3290 s	3310 s 3260 sh
$\nu_{N-N}$	2115 s	2115 s	2130 s	2130 s	2145 s	2170 s
$\nu_3 N_3$	2015 w	2030 w	2020 w	2050 w	2040 w	2050 w
$\delta NH_3$ asym	1600	1600	1600	1600	1630	1630
$\delta NH_3$ sym N <sub>2</sub>	1285	1300	1298	1315	1300	1300
$\delta NH_3$ sym N <sub>3</sub>	1228	n.o.	1242	n.o.	1270	1260 sh
$\nu_3 BF_4^-$ , $PF_6^-$	-	-	-	-	1050 br	850 br
$\rho NH_3$ of N <sub>2</sub>	760	790	770	775	770 sh <sup>a</sup>	750 sh <sup>a</sup>
$\rho NH_3$ of N <sub>3</sub>	720	-	720	-	730	720
$\nu_4 BF_4^-$ , $PF_6^-$					530	560
$\nu_2 N_3$	n.o.	565	570	565	n.o.	n.o.
$\delta_{M-N_2}$	505	505	n.o.	n.o.	500	480

n.o.: not observed; br: broad; w: weak; s: strong;

sh: shoulder; a: area covered by the anion.

FIGURE 2.1 PLOT OF % MONOMER AT A GIVEN

TIME VERSUS AZIDE ION CONCENTRATION

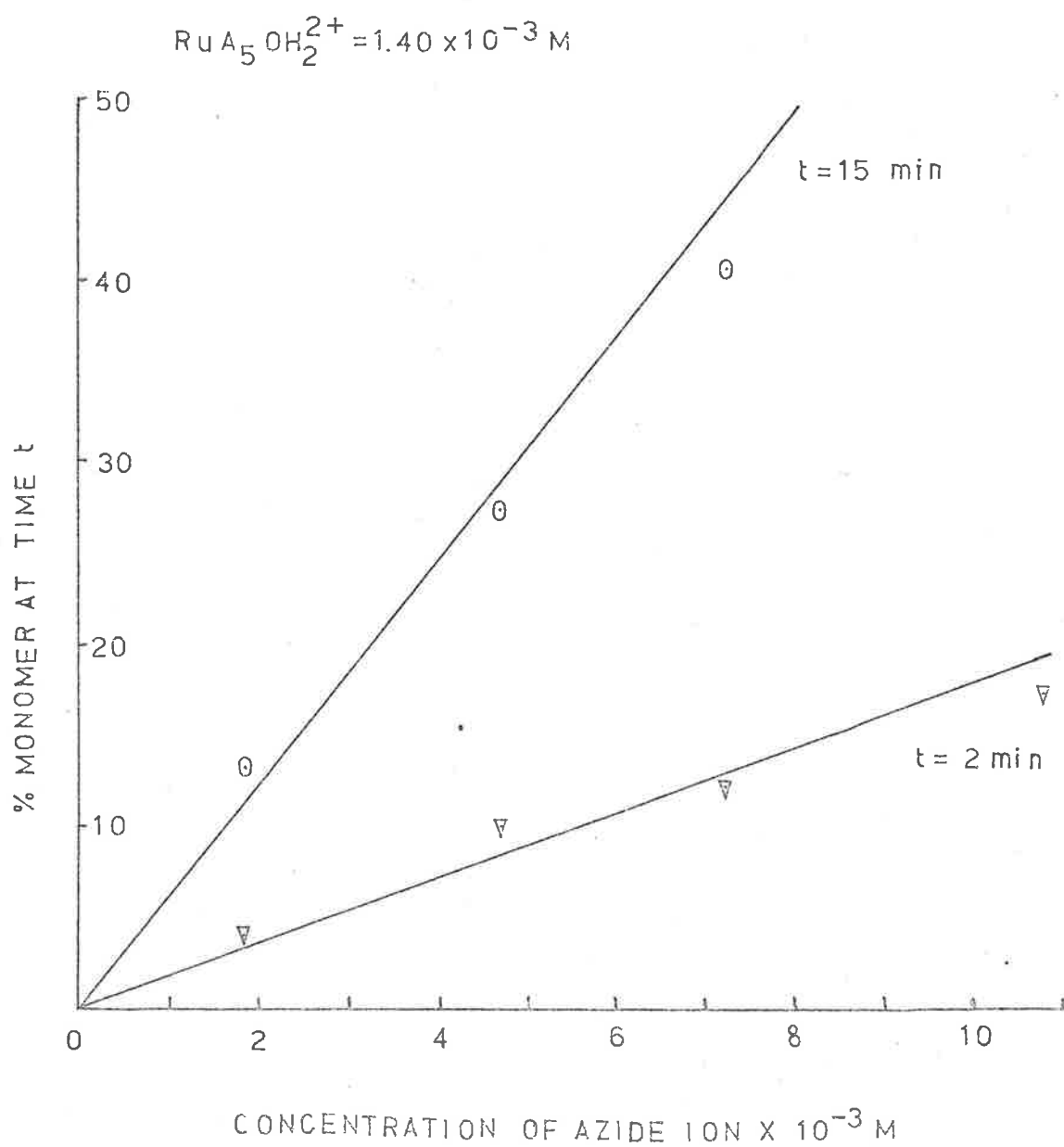


FIGURE 2.2 EFFECT OF THE INITIAL AZIDE  
CONCENTRATION ON THE REACTION BETWEEN  
 $\text{RuA}_5\text{OH}_2^{2+}$  AND AZIDE

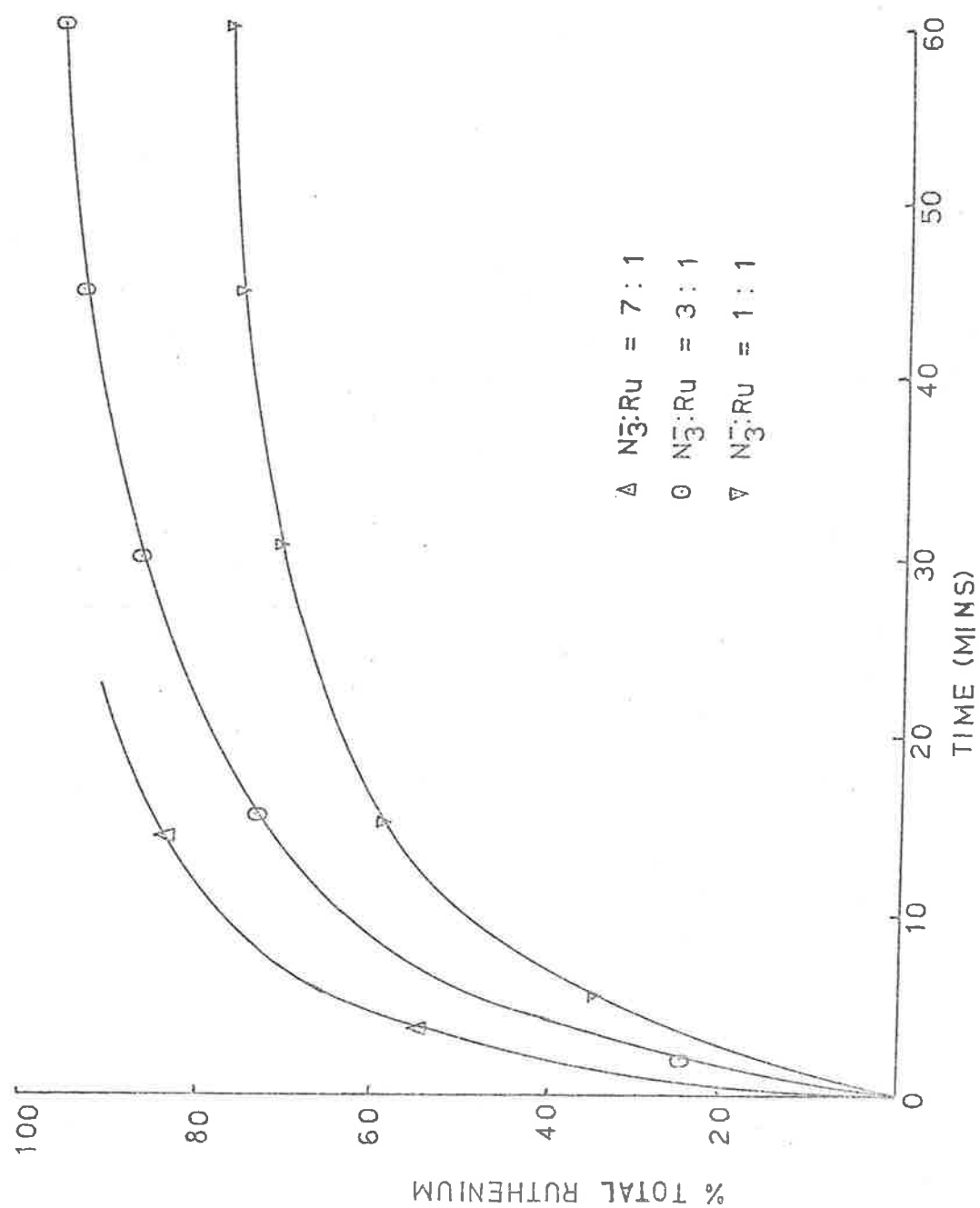


FIGURE 2.3 TEST OF SECOND ORDER

KINETICS FOR THE REACTION OF

$\text{RuA}_5\text{OH}_2^{2+}$  WITH AZIDE ION

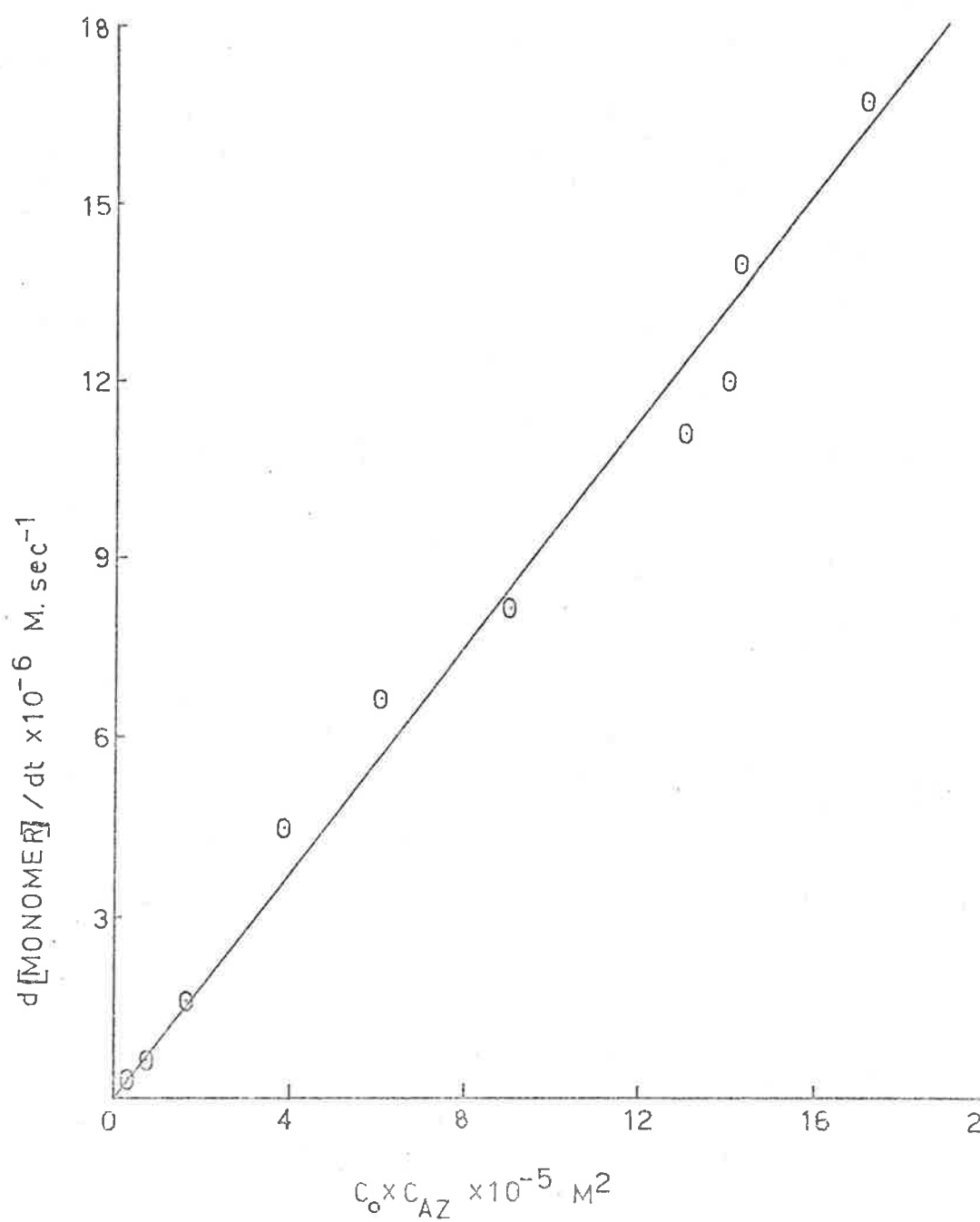


FIGURE 2.4 EFFECT OF pH ON THE REACTION BETWEEN

$\text{RuA}_5\text{OH}_2^{2+}$  AND AZIDE

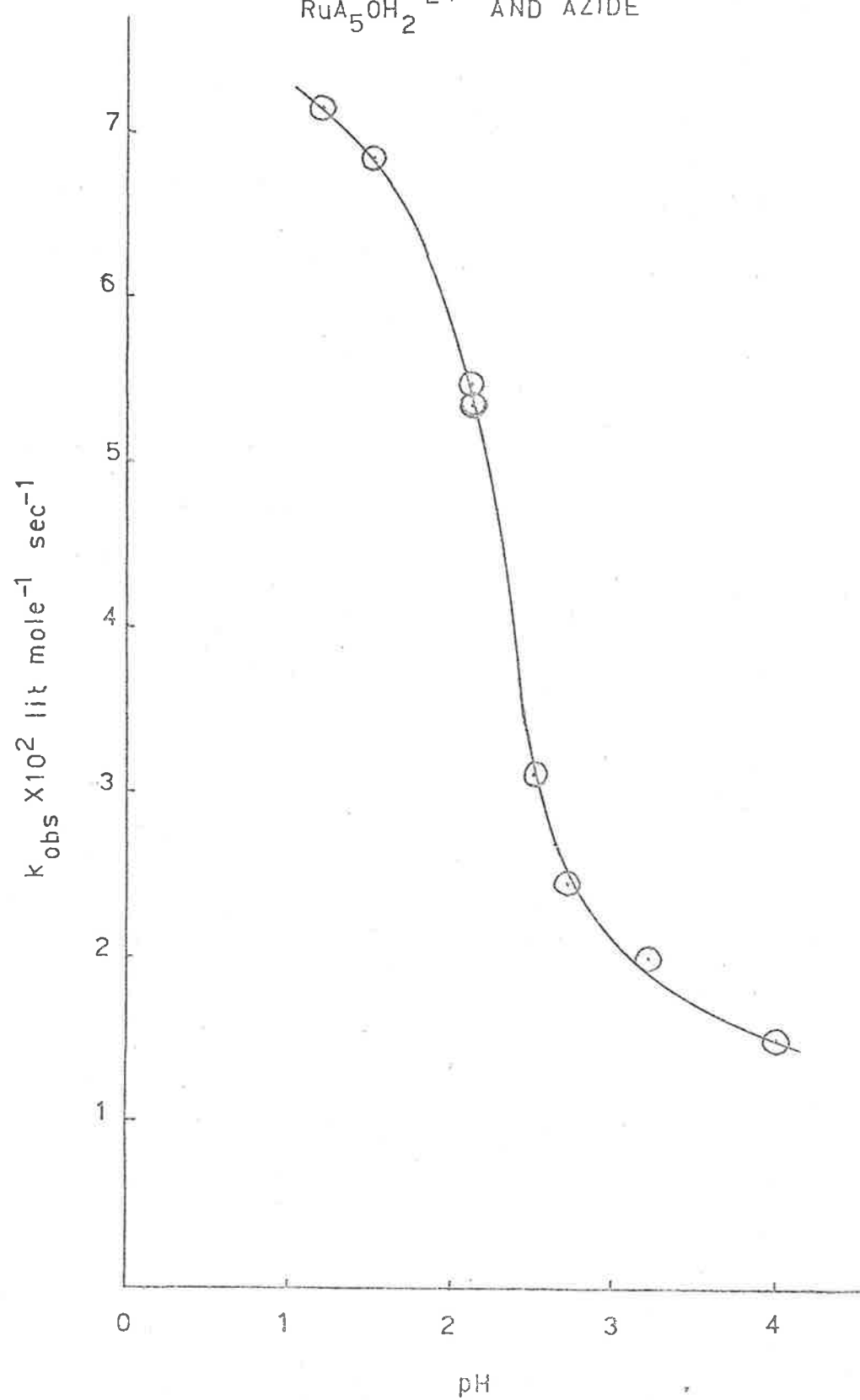
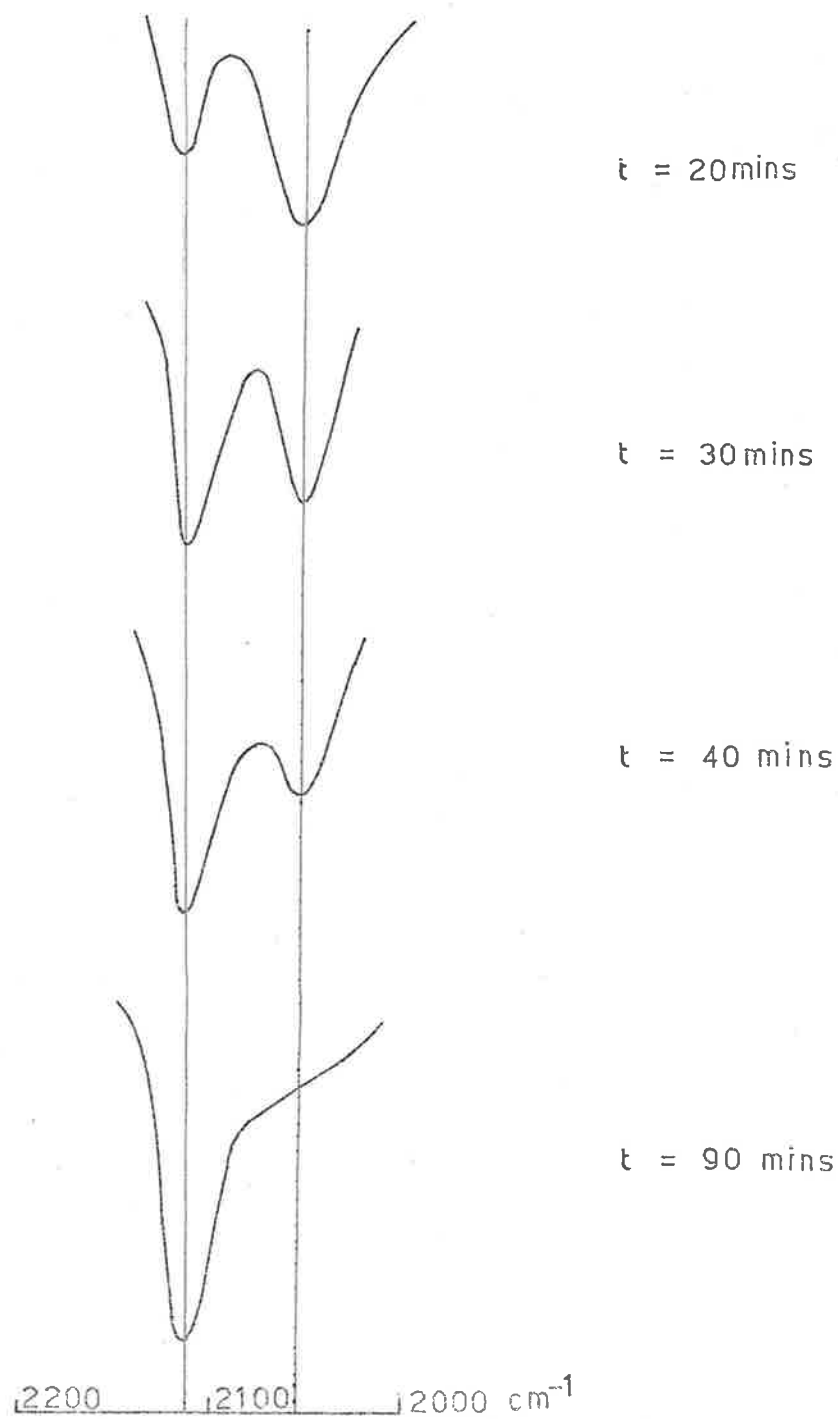


FIGURE 2.5 DECOMPOSITION OF  $\text{RuA}_5\text{N}_3\text{Br}$  IN THE  
INFRA-RED BEAM



## CHAPTER 2

## REFERENCES

1. D.E. Harrison, E. Weissberger and H. Taube, *Science*, 1968, 159, 320.
2. A.D. Allen, F. Bottomley, R.O. Harris, V.P. Reinslau and C.V. Senoff, *J. Amer. Chem. Soc.*, 1967, 89, 5595.
3. D.E. Harrison and H. Taube, *J. Amer. Chem. Soc.*, 1967, 89, 5706.
4. J. Chatt, A. Nikolsky, R. Richards and J. Sanders, *Chem. Comm.*, 1969, 154.
5. J.N. Armor and H. Taube, *J. Amer. Chem. Soc.*, 1970, 92, 6170.
6. (a) I.J. Itzkovitch and J.A. Page, *Can. J. Chem.*, 1968, 46, 2743.  
(b) C.M. Elson, I.J. Itzkovitch and J.A. Page, *Can. J. Chem.*, 1970, 48, 1639.
7. A.A. Diamantis and G.J. Sparrow, *Chem. Comm.*, 1969, 469.
8. J.N. Armor and H. Taube, *J. Amer. Chem. Soc.*, 1969, 91, 6874.
9. J.N. Armor and H. Taube, *J. Amer. Chem. Soc.*, 1971, 93, 6476.
10. R.H. Burris, *Proc. Roy. Soc. B.*, 1969, 172, 339.
11. L.A.P. Kane-Maguire, P.S. Sheridan, F. Basolo and R.G. Pearson, *J. Amer. Chem. Soc.*, 1970, 92, 5865.
12. J. Chatt, *Pure and Applied Chem.*, 1970, 24, 425.
13. P.S. Sheridan and F. Basolo, *Inorg. Chem.*, 1972, 11, 2721.
14. C. Campbell, A. Dias, M.L.H. Green, T. Saito and M.G. Swanwick, *J. Organometal. Chem.*, 1968, 14, 349.
15. A.D. Allen and F. Bottomley, *Can. J. Chem.*, 1968, 49, 469.



16. A. Delay, C. Duval and J. Lecomte, *Compt. Rend.*, 1944, 219, 329.
  17. L.K. Frevel, *J. Amer. Chem. Soc.*, 1936, 58, 779.
  18. H.T.S. Britton and R.A. Robinson, *Trans. Faraday Soc.*, 1932, 28, 531.
  19. W.S. Hughes, *J. Chem. Soc.*, 1928, 491.
  20. N. Yui, *Bull. Inst. Phys. Chem. Res. (Tokyo)*, 1941, 20, 390;  
*Chem. Abs.* 36, 1230.
  21. H. Figour, *Bull. Soc. Chim.*, 1947, 1096.
  22. J.C. Templeton and E.L. King, *J. Amer. Chem. Soc.*, 1971, 93, 7160.
  23. W.M. Latimer, "The Oxidation States of the Elements and Their Potentials in Aqueous Solution", Second Edition, Prentice-Hall Inc., Englewood Cliff, N.J., 1952.
  24. C.F. Wells and M. Husain, *J. Chem. Soc. A.*, 1969, 2891.
  25. R.K. Murmann, J.C. Sullivan and R.C. Thompson, *Inorg. Chem.*, 1970, 9, 1590.
  26. M.A. Suwyn and R.E. Hamm, *Inorg. Chem.*, 1967, 6, 2150.
  27. R.G. Linck, *Inorg. Chem.*, 1972, 11, 61.
  28. R.S.P. Coutts and J.R. Surtees, *Aust. J. Chem.*, 1966, 19, 387.
  29. W.C. Kasko, C. Sutton and E. Serros, *Chem. Comm.*, 1970, 100.
  30. B.A. Thrush, *Proc. Roy. Soc.*, 1956, 235A, 143.
  31. K. Gleu, *Ber.*, 1928, 61B, 702.
  32. B.C. Lane, J.W. McDonald, F. Basolo and R.G. Pearson, *J. Amer. Chem. Soc.*, 1972, 94, 3786.
  33. Chemical Society Special Publication No. 7, "Stability Constants", 1958, compiled by J. Bjerrum, G. Schwarzenbach and L.G. Sillen.
-

34. I. Ricca, *Gazz. Chim. Ital.*, 1945, 75, 71.
35. A.A. Frost and R.G. Pearson, "Kinetics and Mechanism", Second Edition, Wiley and Sons, 1961, p. 14.
36. A.I. Vogel, "Textbook of Quantitative Inorganic Analysis", Third Edition, Longmans Green and Co. Ltd., 1962, p. 256.
37. A.D. Allen, T. Elaidis, R.O. Harris and P. Reinslau, *Can. J. Chem.*, 1969, 47, 1605.
38. C.M. Elson, J. Gulens and J.A. Page, *Can. J. Chem.*, 1971, 49, 207.
39. (a) R.J. Allen and P.C. Ford, *Inorg. Chem.*, 1972, 11, 679.  
(b) R.E. Shepherd and H. Taube, *Inorg. Chem.*, 1973, 12, 1392.
40. M.L. Tobe, *Inorg. Chem.*, 1968, 7, 1260.
41. F. Monacelli, G. Mattagno, D. Gattegno and M. Maltese, *Inorg. Chem.*, 1970, 9, 686.
42. P.J. Staples, *J. Chem. Soc. (A)*, 1971, 2213.
43. P.G. Douglas and R.D. Feltham, *J. Amer. Chem. Soc.*, 1972, 94, 5254.
44. T. Theophanides and G.C. Turrell, *Spectrochim. Acta, Part A*, 1967, 23, 1927.
45. K. Nakamoto, "Infrared Spectra of Inorganic and Coordination Compounds", John Wiley and Sons, 1963, (a) p. 176, (b) p. 149.
46. W. Beck, W.P. Fehlhammer, P. Pollman, E. Schierev and K. Feldl, *Chem. Ber.*, 1967, 100, 2335.
47. P.G. Douglas, R.D. Feltham and H.G. Metzger, *J. Amer. Chem. Soc.*, 1971, 93, 84.

48. A.D. Allen and C.V. Senoff, *Can. J. Chem.*, 1967, 45, 1337.
49. S.W. Lin and A.F. Schreiner, *Inorg. Chim. Acta*, 1971, 5, 290.
50. J.A. Stanko and T.W. Starinshak, *Inorg. Chem.*, 1969, 8, 2156.
51. J.A. Broomhead, F. Basolo and R.G. Pearson, *Inorg. Chem.*, 1964, 3, 826.

## CHAPTER 3

## STRUCTURE AND REACTIVITY OF DINITROGEN OXIDE PENTAAMMINE RUTHENIUM(II)

## SALTS

## 3.1 Introduction

Complexes of the composition,  $[\text{RuA}_5\text{N}_2\text{O}]\text{X}_2$  ( $\text{X} = \text{Br}^-$ ,  $\text{I}^-$ ,  $\text{BF}_4^-$  and  $\text{PF}_6^-$ ) were isolated by exposing solutions of  $[\text{RuA}_5\text{OH}_2]^{2+}$  to high pressures of nitrous oxide in the presence of the anion.<sup>1</sup> The complexes were characterised by elemental analysis, infrared spectra and their reactions in solution to form known ruthenium species. The present study has extended the investigation of the structure of the compounds to include the iodide, tetrafluoroborate and hexafluorophosphate salts. In addition, the thermal decomposition of the compounds has been studied in detail. Possible linkage isomerism in  $[\text{RuA}_5\text{N}_2\text{O}](\text{PF}_6)_2$  has also been investigated.

3.2 Crystal Structure of  $[\text{RuA}_5\text{N}_2\text{O}]\text{X}_2$ , ( $\text{X} = \text{Br}^-$ ,  $\text{I}^-$ ,  $\text{BF}_4^-$  and  $\text{PF}_6^-$ )

The series of complexes  $[\text{RuA}_5\text{N}_2]\text{X}_2$  ( $\text{X} = \text{Cl}^-$ ,  $\text{Br}^-$ ,  $\text{I}^-$ ,  $\text{BF}_4^-$  and  $\text{PF}_6^-$ )<sup>2</sup> and the isostructural species  $[\text{CoA}_5\text{NCS}]\text{Cl}_2$ <sup>3</sup> crystallise in the cubic space group  $\text{Fm}\bar{3}\text{m}$ . The cations are statistically disordered with the metal at the origin of the unit cell. The ligands lie on the cell edge such that each site averages 5/6 of an ammonia group and 1/6 of a dinitrogen or a thiocyanate group. Sparrow<sup>1</sup> suggested that the nitrous oxide complexes may have similar structures. However, in this case single crystal X-ray

analysis was not possible. The nitrous oxide complexes were precipitated from solution as microcrystalline solids. Slow crystallisation was impossible because of

- (a) rapid solvolysis under low pressure of nitrous oxide (1 atmosphere), and
- (b) disproportionation of the complexes in solution.

Therefore, X-ray powder patterns of the freshly prepared salts were examined to establish the lattice types.

In the case of the bromide salt, crystals showed complete extinction through  $360^\circ$  under a polarising microscope with crossed polars, characteristic of a cubic space group. For each of the salts, all of the lines observed on the powder patterns could be indexed in the face centred cubic system. The cell constants, obtained by extrapolation of a plot of  $a$  versus  $\sin^2\theta$  to  $\theta = 90^\circ$ , are compared with those of the corresponding dinitrogen complexes in Table 3.1. The cell constants for the two series of compounds are closely parallel and infrared spectra, run at the same time as the powder patterns, showed no significant contamination of the nitrous oxide species by the dinitrogen complex. An infrared spectrum of the tetrafluoroborate salt, run before and after exposure to X-rays for two hours, showed no formation of the dinitrogen species. For the bromide salt the relative observed intensities were corrected for Lorentz and polarisation effects and converted to the structure factors<sup>1</sup> in Table 3.2. Structure factors

were calculated<sup>4</sup> with the atomic parameters of Table 3.3 appropriate to the space group Fm3m. A linear Ru-N(1)-N(2)-O model was assumed (the Ru-O-N(2)-N(1) model is indistinguishable in this case) with the bond distances Ru-NH<sub>3</sub> and Ru-N(1) set equal to that found in [RuA<sub>5</sub>N<sub>2</sub>]Cl<sub>2</sub>.<sup>2</sup> Bond distances for the coordinated nitrous oxide were taken equal to the values for the free gas.<sup>5</sup> This assumption is valid when the changes in bond length for free and coordinated dinitrogen are considered. A change of .2% occurs on coordination viz. for dinitrogen gas<sup>6</sup> the bond length is 1.10 Å and in [RuA<sub>5</sub>N<sub>2</sub>]Cl<sub>2</sub><sup>2</sup> the bond length is 1.12 Å. Similar small changes would be anticipated for free and coordinated nitrous oxide. The isotropic temperature factors were estimated at reasonable values and only an overall scale factor was refined. The observed and calculated structure factors given in Table 3.2 show reasonable agreement and yield an R factor  $(\sum |F_o| - \sum |F_c|) / \sum |F_o|$  of 0.28. This is a value low enough to confirm the structure type as only powder data were used and the atomic model was not refined.

The adoption by the nitrous oxide complexes of the Fm3m space group does not by itself prove that the Ru-N-N-O or Ru-O-N-N linkage is rigorously linear. Linearity was established by refinement with single crystal X-ray data in the cases of the dinitrogen and isothiocyanate complexes. A slight bending of the linkage is possible resulting in further disorder, but it will be limited by packing contacts. In particular the extreme oxygen (or nitrogen)

atom of the nitrous oxide away from ruthenium at the origin will be surrounded by ammonia groups attached to other (face centred) ruthenium atoms. Assuming a limiting contact  $\text{N} \cdots \cdots \text{NH}_3$  or  $\text{O} \cdots \cdots \text{NH}_3$  of  $2.8 \text{ \AA}$  and the model of Table 3.3, the minimum linkage angle is about  $173^\circ$  (see figure 3.1). A disorder due to a slight bending of this kind only involves the movement of approximately two electrons in the X-ray model and would not be sensible to the data. Likewise the choice of an oxygen or nitrogen bonded model, differing because of the existing disorder by fractional electrons, cannot be made by the X-ray data. An infrared study with nitrogen-15 labelled nitrous oxide has been made and it strongly favours ruthenium to oxygen bonding.<sup>1</sup>

Bottomley and Crawford<sup>7</sup> prepared the nitrous oxide complex by the reaction of hydroxylamine and nitrosyl pentaammine ruthenium(II). A powder pattern of the bromide salt showed it to be face centred cubic with  $a = 10.32 \text{ \AA}$ . This result is in good agreement with the value observed above ( $a = 10.16 \text{ \AA}$ ). Intensities of the powder lines from the nitrous oxide complex and the dinitrogen complex were similar. On this basis they concluded that a linear  $\text{RuNNO}$  group was favoured relative to a bent  $\text{RuONN}$ . Attachment of the nitrous oxide via the nitrogen atom is in conflict with Sparrow's evidence<sup>1</sup> for coordination through the oxygen atom. On the other hand, attachment through the oxygen atom is in conflict with the known angular coordination of the isoelectronic azide<sup>8</sup> and

S-linked thiocyanate<sup>3</sup> species. However, the linearity of the ruthenium to nitrous oxide linkage, whatever the donor atom, does not appear to be in question.

### 3.3 Linkage Isomerism in Dinitrogen Oxide Complexes

An investigation of the infrared spectra of the complexes  $[\text{RuA}_5\text{N}_2\text{O}]\text{X}_2$  ( $\text{X} = \text{Br}^-$ ,  $\text{I}^-$ ,  $\text{BF}_4^-$  and  $\text{PF}_6^-$ ), showed that each compound had characteristic absorption bands attributable to the coordinated nitrous oxide.<sup>1</sup> Table 3.4 lists these vibrations for each complex along with the band assignment. Of particular interest are the  $\nu_3$  vibrations of the hexafluorophosphate. In contrast to the other three salts, which have a single  $\nu_3$  vibration, the  $\text{PF}_6^-$  has two, which occur at  $2280\text{ cm}^{-1}$  and  $2222\text{ cm}^{-1}$ . Both absorptions have been unambiguously assigned to the presence of nitrous oxide in the compound, as they both undergo a frequency shift when nitrogen-15 labelled nitrous oxide is used in the preparation.<sup>1</sup>

An explanation advanced by Sparrow<sup>1</sup> for the presence of the two peaks is that they arise because of the presence of two linkage isomers. Because of the linearity of the ruthenium to nitrous oxide linkage, the possibility of O- and N-bonded isomers is feasible. Several alternative explanations are plausible ways of explaining the phenomenon. Taube<sup>9</sup> reported infrared and analytical evidence for the isolation of a dimeric complex of composition  $[\text{A}_5\text{RuONNRuA}_5]\text{X}_4$  ( $\text{X} = \text{Br}^-$  or  $\text{BF}_4^-$ ), from a mixture of  $[\text{RuA}_5\text{OH}_2]^{2+}$



and nitrous oxide (1-5 atmospheres pressure). These compounds have a  $\nu_3$  absorption of  $\text{N}_2\text{O}$  at  $2110\text{ cm}^{-1}$  ( $\text{Br}^-$  salt) and  $2105\text{ cm}^{-1}$  ( $\text{BF}_4^-$  salt). Thus a mixture of monomer and dimer complexes in the solid state could explain the observation. Trapping a small amount of nitrous oxide in the lattice of the precipitated complex (i.e. formation of a clathrate) is also a reasonable alternative explanation. The anion used to precipitate the complex may also be important. Hydrolysis of  $\text{PF}_6^-$  is known to occur very readily in basic solution<sup>10</sup> leading to the formation of  $\text{F}^-$  and  $\text{PO}_4^{3-}$ . Either of these two anions may be responsible for precipitating a second complex giving rise to the second peak. Loss of ammonia from  $[\text{RuA}_5\text{OH}_2]^{2+}$  during reduction could lead to the formation and subsequent precipitation of a tetraammine nitrous oxide species. Another alternative is that the peaks arise due to a vibrational anomaly e.g. Fermi resonance or a lattice interaction. An attempt was made to resolve the question with the above possibilities in mind.

### 3.3(i) Occurrence and Relative Abundance of Isomers

For convenience, the two peaks in the infrared spectrum of the  $\text{PF}_6^-$  salt are labelled  $\alpha$  for  $2280\text{ cm}^{-1}$  and  $\beta$  for  $2222\text{ cm}^{-1}$ . Attempts were made to vary the intensity ratio of the two peaks by varying both the pressure of nitrous oxide and the concentration of  $[\text{RuA}_5\text{OH}_2]^{2+}$  used in the preparations.

Based on experience with the formation of the dinitrogen complexes, high concentrations of aquo complex and low gas pressures would favour the formation of the dimeric complex. Low concentrations of the aquo complex and high gas pressures would favour formation of monomeric species. Thus, if the  $\alpha$  peak corresponds to a monomer and the  $\beta$  peak to a dimer, then the ratio of  $\alpha:\beta$  intensity will vary depending on the concentrations of the various reactants used in the preparations. It is most likely that the  $\alpha$  peak corresponds to the monomer species rather than a dimer. From the  $\nu_3$  vibrations in Table 3.4, the  $\alpha$  peak occurs at a higher wavenumber than the  $\nu_3$  of  $\text{BF}_4^-$  as would be predicted, by analogy with the effect of the anion on  $\nu_{\text{N-N}}$  of the dinitrogen complexes, whereas the  $\beta$  peak occurs at a wavenumber lower than that of the  $\nu_3$  of the  $\text{Br}^-$  salt.

Table 3.5 lists the conditions used in the preparation of the nitrous oxide complex along with the results obtained for the  $\alpha:\beta$  ratio. A nujol mull was used for each infrared spectrum recorded; potassium bromide discs were not used, because formation of the bromide salt occurred on discing. The concentration of the mull from one experiment to the next was not reproducible. Further, the absorption maxima were weak in all but a few cases, hence the determination of areas was subject to large error (20-30%).

Despite the inherent inaccuracies in the method of determination, two generalisations can be made. Firstly, for the same concentration

of the aquo complex, low pressures of nitrous oxide favour  $\alpha:\beta$  ratios of one or less. Secondly, for the same pressure of nitrous oxide, high concentrations of the aquo complex favour formation of the  $\alpha$  species over the  $\beta$  species, i.e.  $\alpha:\beta$  ratio greater than one. Thus the dimer hypothesis is not supported by the experiments. If it were then both generalisations above would be incorrect. Low pressures of nitrous oxide and high ruthenium concentrations would favour  $\alpha:\beta$  ratios very much less than one. The equilibrium constant for the formation of the monomeric species is small ( $\sim 8$  at  $25^\circ\text{C}$ )<sup>11</sup> and even under the most favourable conditions for preparation there will be a large amount of free aquo, thus causing formation of any dimeric species. Under the most favourable conditions for dimer formation, high concentrations of ruthenium and low pressures of nitrous oxide, some  $\alpha$  (monomer) species was always formed (see Table 3.5, the runs at 1 atmos. and 0.5 atmos.). In no run did the  $\alpha:\beta$  ratio approach zero, i.e. the conditions for complete  $\beta$  formation were never achieved. This does not of itself prove that a dimer is not formed, but does indicate that it is unlikely that the  $\beta$  peak arises due to dimer formation.

### 3.3(ii) Analytical Evidence

Analytical results are consistent with a linkage isomerism and exclude the possibility of a bridged complex or a complex of a different kind (e.g. a tetraammine or a phosphate salt).

Under argon in a non-coordinating solvent, e.g. 0.1M methane sulphonic acid, the nitrous oxide complexes are quantitatively converted to the aquo complex ( $\lambda_{\text{max}} = 268 \text{ nm}$   $\epsilon \approx 500 \text{ M}^{-1} \text{ cm}^{-1}$ ).<sup>1</sup> From measurements made on the conversion of the hexafluorophosphate salt to the aquo complex, it should be possible to distinguish between an isomer, a dimer or other nitrous oxide containing coordination or ionic species.

Table 3.6(a) lists the results obtained when the solids were decomposed in 0.1M methane sulphonic acid solution under argon, then subjected to high pressures (70-110 atmospheres) of dinitrogen gas. Under these conditions the monomeric dinitrogen complex would form to the exclusion of the dimer. There is a 1:1 correspondence between the amount of monomer dinitrogen complex obtained by treating the  $\alpha\beta$  solid and the amount of monomer obtained by treating the  $\alpha$  solid corresponding to the  $\alpha\beta$  solid. Further there is a simple 1:1 correspondence of the aquo content of both solids, i.e. both give rise to the same absorptivity at 268 nm when dissolved in methane sulphonic acid under argon (Table 3.6(b)).

This direct correspondence supports the isomer theory, as the interconversion of  $\beta$  to  $\alpha$  would not change the aquo content. On the other hand a dimer should give rise to more aquo (and therefore monomer dinitrogen complex) than would be expected from the monomer nitrous oxide complex. From the weight of each solid used, it was possible to calculate the amount of aquo expected, based on the

formula  $[\text{RuA}_5\text{N}_2\text{O}](\text{PF}_6)_2 \cdot \text{H}_2\text{O}$ , and compare that value with the experimentally determined one. In all instances both values were identical within experimental error. Thus an isomer fits the observations, as a dimer would be expected to give more aquo than was calculated.

Addition of the nitrous oxide complex to 1M HCl in air gave almost quantitative conversion to  $[\text{RuA}_5\text{Cl}]^{2+}$ . Sparrow<sup>1</sup> measured the molar absorptivity of the single absorption maximum observed at 327 nm as  $1.82 \times 10^3 \text{ M}^{-1} \text{ cm}^{-1}$  (lit.<sup>23</sup> for  $[\text{RuA}_5\text{Cl}]^{2+}$   $1.93 \times 10^3 \text{ M}^{-1} \text{ cm}^{-1}$ ). No evidence for the presence of cis- or trans- $[\text{RuA}_4\text{Cl}_2]^+$  was found from the absorption spectrum. The three species have sufficiently different spectra to allow such a distinction to be made.<sup>23</sup> Further, the infrared spectrum of cis- $[\text{RuA}_4(\text{H}_2\text{O})\text{N}_2\text{O}](\text{PF}_6)_2$  also contains two peaks one at  $2284 \text{ cm}^{-1}$  and the other at  $2224 \text{ cm}^{-1}$ , i.e. at values quite different to that of the pentaammine (see section 4.3). Thus the second peak does not arise due to the presence of a tetraammine species.

### 3.3(iii) Thermal Stability

In studying the infrared spectrum of  $[\text{RuA}_5\text{N}_2\text{O}](\text{PF}_6)_2$ , it was noted that after four to five hours in the spectrometer beam the  $\beta$  peak disappeared more rapidly than the  $\alpha$  peak. The band at  $1222 \text{ cm}^{-1}$ , assigned to  $\nu_1$  of coordinated nitrous oxide (see Table 3.4), also began to disappear. A new band at  $2170 \text{ cm}^{-1}$  began to appear. This

new band was identical to the  $\nu_{\text{N-N}}$  of  $[\text{RuA}_5\text{N}_2](\text{PF}_6)_2$ . These observations led to attempts to find conditions under which the disappearance of the  $\beta$  peak could be accelerated, while the  $\alpha$  peak remained unaltered and without significant formation of the dinitrogen complex.

The effect of temperature on the solid nitrous oxide complex was examined by using a vacuum line with attached manometer (see section 6.9) and an oil bath to maintain the temperature. At  $120\text{--}140^\circ\text{C}$  the solid was decomposed to the dinitrogen monomer and "ruthenium red" with nitrogen, nitrous oxide and water as the gaseous products (see section 3.4). This behaviour is consistent with that observed for the decomposition of the tetrafluoroborate salt.<sup>1,12</sup> After two to three hours heating at  $60\text{--}80^\circ\text{C}$  in vacuo, the infrared spectrum of the complex revealed the loss of the  $\beta$  peak, no apparent change in the  $\alpha$  peak, no formation of the dinitrogen complex and no change in the  $\nu_1$  peak at  $1222\text{ cm}^{-1}$ . The only obvious change in the spectrum was the loss of the  $\beta$  peak. The peak at  $555\text{ cm}^{-1}$  (assigned to  $\nu_4$  of  $\text{PF}_6^-$ ) was used to standardise each spectrum. The ratio of the area of both  $\nu_3$  peaks and the  $\nu_1$  peak to the area of the peak at  $555\text{ cm}^{-1}$  was measured before and after low temperature thermal decomposition. In this manner any differences arising due to different mull strengths could be eliminated and a comparison of peaks could be made. The ratios remained constant, except for that of the  $\beta$  peak, which became zero after decomposition and in particular the  $\alpha$  peak did not increase its

intensity, within the limitations of the measurements, suggesting that the  $\beta$  peak may arise due to a highly absorbing nitrous oxide impurity.

Evolution of any gaseous products which occurred with the loss of the  $\beta$  peak was monitored manometrically and the gases identified from their mass spectrum. Table 3.7 lists the results of the manometric measurements made. The volumes of gases evolved were corrected to S.T.P. and compared with the amount of gas expected for the loss of one mole of nitrous oxide at S.T.P., per mole of complex present. In all cases, the amount of gas evolved was less than twenty percent of the calculated value for one mole. Further, approximately one-third of the gas evolved was condensable in liquid nitrogen. Thus, the gases nitrous oxide, water or nitrogen may have been released from the complex. The released gases, condensable as well as non-condensable in liquid nitrogen, were examined mass spectrometrically. It was found that nitrogen and water vapour were present in the samples. The absence of any peaks at mass 44 ( $\text{N}_2\text{O}^+$ ) and mass 30 ( $\text{NO}^+$  arising from the cracking of  $\text{N}_2\text{O}^+$ ) showed the absence of any significant amounts of nitrous oxide in the samples, where decomposition was carried out at 60-65°C. The water probably arises from dehydration of the complex, as analysis showed that one mole of lattice water was present in the complex.<sup>1</sup> Dinitrogen present may arise from the decomposition of small amounts of  $[\text{RuA}_5\text{N}_2](\text{PF}_6)_2$ , which was sometimes present as an impurity. Small amounts of air (peaks were observed at mass 16 ( $\text{O}^+$ ) and 32 ( $\text{O}_2^+$ ))

as well as 40 ( $\text{Ar}^+$ ) trapped in the apparatus accounts for 60-70% of the dinitrogen peak observed.

From a consideration of the spatial arrangement of the nitrous oxide complexes (see figure 3.1) the unit cell has a central void surrounded by a cube, created by the bromide ions at 0.25, of body diagonal of approximately  $8 \text{ \AA}$ . The largest void is possible with the largest anion, i.e. hexafluorophosphate. Conditions for the preparation of the complexes required exposure to high pressures of nitrous oxide (20-40 atmospheres) for half an hour. Thus it might be possible to form a clathrate system of nitrous oxide and the nitrous oxide complex. The clathrates of  $\beta$ -quinol with oxygen, nitric oxide, argon and krypton are well known.<sup>19</sup> It is a feature of these compounds that the trapped gas can be released on heating or dissolving the crystals in water.<sup>20</sup> The absence of nitrous oxide in the gases expelled on heating the hexafluorophosphate complex to  $60-65^\circ\text{C}$ , suggests the  $\beta$  peak is not due to clathrate formation. Restoration of the  $\beta$  peak should occur when the solid containing only  $\alpha\text{-}[\text{RuA}_5\text{N}_2\text{O}](\text{PF}_6)_2$  is exposed to nitrous oxide pressure, if the complex is a clathrate. This was not the case when the  $\alpha$  solid was exposed to 25 atmospheres of nitrous oxide for half an hour at room temperature, or when it was exposed to 20 atmospheres of nitrous oxide at  $60-80^\circ\text{C}$  for one hour. Prolonged exposure (4-5 hours) of the  $\alpha\beta$  solid to high vacuum did not affect the relative intensities of the two peaks in the infrared spectrum. These results are not consistent with the



behaviour of other clathrate systems. They are consistent with the formation of an isomer. The change of the  $\beta$  solid to the  $\alpha$  is similar to the behaviour observed for other thermally initiated linkage isomerisations. Thiocyanate to isothiocyanate isomerisation in cobalt pentaammine occurs<sup>15</sup> after one day at 80°C. Also nitrito (O-bonded) complexes of  $[M(NH_3)_5NO_2]^{n+}$  (where M = Co(III), Rh(III), Ir(III) and Pt(IV)) undergo isomerisation to the more stable nitro (N-bonded) forms on heating.<sup>21</sup>

The X-ray powder patterns of the  $\alpha\beta$  and  $\alpha$  containing solid were obtained using  $CuK\alpha$  radiation. This study cannot distinguish between N- and O-bonded isomers, because the scattering factors of the two atoms are similar. Further, the powder method gives only an overall picture of the structure type, without actually locating specific atoms on specific sites in the lattice. However, the method will differentiate between two different structure types. The N- and O-bonded isomers would be expected to crystallise with different space groups. Previously it was shown (section 3.2) that the O-bonded nitrous oxide complexes crystallise in the space group  $Fm3m$ . By analogy with the isoelectronic azide ion<sup>8</sup> and with S-bonded thiocyanate ion,<sup>3</sup> non-linear coordination to the metal would be anticipated for the O-bonded isomer. Hence, the symmetry of the crystal would be destroyed giving rise to a new space group. Likewise a dimeric complex or one in which the nitrous oxide has "sideways on" bonding to the metal, would also give rise to a new space group.

Both the  $\alpha\beta$  and the  $\alpha$  solids gave powder patterns for which all of the lines obtained could be indexed for a face centred cubic structure. Plots of  $a$  versus  $\sin^2\theta$  were extrapolated to  $\theta = 90^\circ$  and values of  $a_0$  obtained. Within the limitations of the experiment the values of  $a_0$  were indistinguishable ( $\alpha\beta$  solid:  $a_0 = 11.85 \text{ \AA}$  and  $\alpha$  solid:  $a_0 = 11.92 \text{ \AA}$ ). This result excludes the possibility of a dimer or a complex which has "sideways on" bonding. Seemingly it also excludes the possibility of an isomer. However, it may be that packing contacts of the face centred ammonia groups around the nitrous oxide force it to adopt a linear or nearly linear attachment to the metal.

### 3.3(iv) Spectroscopic Evidence

If the  $\alpha$  and  $\beta$  peaks arise due to formation of linkage isomers, then each  $\nu_3$  vibration should have associated with it a  $\nu_1$  vibration. For thiocyanate, cyanate, selenocyanate and nitrite ions many examples of linkage isomers are known.<sup>13</sup> For complexes of each of the above ligands, there are three vibrations associated with the ligand and the frequency of each vibration depends on the mode of attachment. Thus for cobalt, rhodium and iridium thiocyanato pentaammine complexes, the  $\nu_1$ ,  $\nu_2$  and  $\nu_3$  vibrations of the thiocyanate ligand are different for the -N and -S bonded linkage isomers as shown in Table 3.8. Such behaviour has been observed for all thiocyanate complexes prepared, where both isomers are known.<sup>14</sup> Similar behaviour is observed for

the other ligands given above. Hence, linkage isomers of nitrous oxide would be expected to show the same behaviour.

The behaviour of nitrous oxide adsorbed on the surface of alkali halide<sup>16</sup> and  $\alpha$ -chromia<sup>17,18</sup> has suggested N- and O-ended attachment to the surface. On  $\alpha$ -chromia both modes of attachment were present together and infrared spectra were used to assign the different attachment modes. Thus for one mode bands at 2230 and 1237  $\text{cm}^{-1}$  and for the other mode bands at 2305 and 1339  $\text{cm}^{-1}$  have been assigned as oxygen and nitrogen attachment respectively.<sup>17</sup> Thus the shifts in wavenumber relative to the free gas, are:  $\Delta\nu_3$  (N-bonded) = +81  $\text{cm}^{-1}$ ;  $\Delta\nu_1$  (N-bonded) = +53  $\text{cm}^{-1}$ ;  $\Delta\nu_3$  (O-bonded) = +14  $\text{cm}^{-1}$ ;  $\Delta\nu_1$  (O-bonded) = -49  $\text{cm}^{-1}$ . For the hexafluorophosphate nitrous oxide complex  $\Delta\nu_3(\alpha) = +56 \text{ cm}^{-1}$ ,  $\Delta\nu_1(\alpha) = -64 \text{ cm}^{-1}$ ,  $\Delta\nu_3(\beta) = -2 \text{ cm}^{-1}$  while the shift in  $\nu_1$  is unknown, assuming the  $\beta$  peak has a  $\nu_1$  vibration associated with it. Thus, the shifts in the  $\alpha$  peak are consistent with O-bonded nitrous oxide as was shown previously.<sup>1</sup> The shift observed for the  $\beta$  peak is opposite to that for N-bonded nitrous oxide, but only slightly removed from that of the free gas. Consequently, if a  $\nu_1$  vibration were associated with the  $\beta$  peak it would be expected to occur near 1286  $\text{cm}^{-1}$  (the  $\nu_1$  frequency of the free gas<sup>28</sup>) or, for a N-bonded isomer, at a somewhat higher wavenumber, e.g. ~1300  $\text{cm}^{-1}$ . Both of these wavenumbers occur in regions obscured by  $\delta\text{NH}_3$  symmetric vibrations. Thus on the basis of the infrared spectra the presence of an O-bonded isomer has been confirmed and the presence of the  $\beta$  peak

is consistent with the presence of a N-bonded isomer.

Borod'ko observed splitting of the N=N vibrations in  $[\text{OsA}_5\text{N}_2]\text{X}_2$  due to a resonance interaction of non-translationally equivalent molecules in the unit cell<sup>24</sup> as shown in the X-ray structure.<sup>30</sup> This does not appear to offer an explanation of the two peaks observed in the infrared spectrum of  $[\text{RuA}_5\text{N}_2\text{O}](\text{PF}_6)_2$  as the powder pattern indicates a structure identical to that of the dinitrogen complex which shows only a single peak. In an attempt to find other structures, in which the two peak phenomenon may be exhibited, other anions were used to precipitate the nitrous oxide complex. Using tetraphenylboron as the anion two peaks were observed in the solid obtained, one at  $2260\text{ cm}^{-1}$ , assigned to  $\nu_3$  of coordinated nitrous oxide, and the other at  $2150\text{ cm}^{-1}$ , assigned to  $\nu_{\text{N-N}}$  of coordinated dinitrogen. When the complex anion tris-oxalatoaluminate,  $[\text{Al}(\text{ox})_3]^{3-}$  was used, a precipitate with a single  $\nu_{\text{N-N}}$  vibration at  $2130\text{ cm}^{-1}$  was observed. No bands attributable to the  $\nu_3$  vibration of nitrous oxide were observed.

Attempts to recrystallise ammonium hexafluorophosphate proved to be unsuccessful, the compound rapidly hydrolysing to phosphate and fluoride ions.<sup>10</sup> The hydrolysis passes through several intermediate steps producing fluoro-oxyanions of phosphorus. Another anion present was the hexafluorosilicate ion arising from attack of fluoride on the glass reaction vessel. The  $\text{F}^-$ ,  $\text{PO}_4^{3-}$  and  $\text{SiF}_6^{2-}$  were used in attempts to precipitate the nitrous oxide complex. Phosphate gave no precipitate

even though it was in vast excess. Fluoride gave a precipitate of  $[\text{RuA}_4(\text{H}_2\text{O})\text{N}_2]\text{F}_2$  ( $\nu_{\text{N-N}} 2075 \pm 5 \text{ cm}^{-1}$ ) on addition of ethanol. Hexafluorosilicate proved an efficient precipitant of the aquopentammine ion. The failure of any of these anions to precipitate complexes with an absorption maximum near  $2200 \text{ cm}^{-1}$  supports the analytical evidence that none of the species  $[\text{RuA}_5\text{N}_2\text{O}]\text{F}_2$ ,  $[\text{RuA}_5\text{N}_2\text{O}]_3[\text{PO}_4]_2$  or  $[\text{RuA}_5\text{N}_2\text{O}][\text{SiF}_6]$  is responsible for the appearance of the  $\beta$  peak in the infrared spectrum of  $[\text{RuA}_5\text{N}_2\text{O}](\text{PF}_6)_2$ . Further, the concentrations of the anion used were far in excess of those likely to be present under the conditions of preparation of the  $\text{PF}_6$  salt. Hence it is most unlikely that these species will be present.

The hexafluorophosphate salt was synthesised by the method of Bottomley and Crawford<sup>7</sup> and it was found that  $\alpha$  and  $\beta$  peaks ( $\alpha > \beta$ ) were produced. This rules out the dimer explanation and favours that of isomer formation. The Bottomley mechanism can accommodate the formation of both isomers by appropriate rearrangement of the intermediate  $\text{RuN}(\text{O})\text{NHOH}$ . It cannot accommodate dimer formation. A very weak band was present at  $1160 \text{ cm}^{-1}$  and this may be the  $\nu_1$  associated with the  $\beta$  peak. The intensity of this peak is in line with that observed in the free gas, viz.  $\nu_3 > \nu_1$  but opposite to that observed for coordinated nitrous oxide.

An overtone or combination band in an infrared spectrum can often be abnormally intense. This occurs when the energy of, say, a

combination level coincides with the fundamental level of a different vibration. A resonance phenomenon, known generally as Fermi resonance, can then arise.<sup>29</sup> For example, the active C-H stretching fundamental of benzene almost coincides with a combination of two other fundamentals at  $1485\text{ cm}^{-1}$  and  $1585\text{ cm}^{-1}$ . The combination level occurs at  $3070\text{ cm}^{-1}$ , neglecting anharmonicity. One of the symmetry species of the new level is the same as that for the C-H fundamental. The result is a resonance occurs and two bands, of nearly equal intensity, occur at  $3099$  and  $3045\text{ cm}^{-1}$ .

For the nitrous oxide complex, a combination of the weak  $\delta\text{OH}_2$  band at  $1700\text{ cm}^{-1}$  and the  $\nu_4$  of  $\text{PF}_6^-$  at  $555\text{ cm}^{-1}$  would occur at  $2255\text{ cm}^{-1}$ . This is very close to  $2251\text{ cm}^{-1}$ , the midpoint of the  $\alpha$  and  $\beta$  bands. Thus, a Fermi resonance between the  $\nu_3$  fundamental of the nitrous oxide complex and the combination, might explain the appearance of the  $\beta$  peak. This explanation may not be very likely, because not all the water is lost during the thermal treatment which leads to the disappearance of the  $\beta$  peak. The presence of some water was detected by the  $\nu_{\text{O-H}}$  and the presence of a shoulder at  $1700\text{ cm}^{-1}$ .

In other systems evidence for the presence of linkage isomers has been obtained from electronic spectra.<sup>13,14,21</sup> Thus, for nitrito and nitro linkage isomers, the  $-\text{ONO}$  and the  $-\text{NO}_2$  groups occur at different positions in the spectrochemical series and the two isomers have different absorption maxima.<sup>21</sup> A similar situation occurs with  $-\text{SCN}$  and  $-\text{NCS}$ , cyanate and other ambidentate ligands.<sup>21</sup> For N- and O-bonded

nitrous oxide a similar situation would be expected to apply with the two isomers exhibiting different absorption maxima. The spectrum of the complex recorded in 0.1M methane sulphonic acid had a single absorption maximum at 240 nm (lit.<sup>1</sup> 238-240 nm for the tetrafluoroborate salt). The absence of any difference in the spectrum of the hexafluorophosphate salt compared with the spectrum of the tetrafluoroborate is not conclusive because the peak may not be observable under the conditions of the experiment, or because of the possibility of isomerism in solution.

### 3.3(v) Conclusion

From the results obtained, it appears that the two peaks in the infrared spectrum of  $[\text{RuA}_5\text{N}_2\text{O}](\text{PF}_6)_2$  arise due to the presence of linkage isomers of the nitrous oxide. No evidence for dimer or clathrate formation could be found. A tetraammine nitrous oxide complex does not appear to be responsible for the second absorption as the hexafluorophosphate salt  $[\text{RuA}_4(\text{OH}_2)\text{N}_2\text{O}](\text{PF}_6)_2 \cdot \text{H}_2\text{O}$  has two  $\nu_3$  absorptions at different maxima (see section 4.3). The  $\beta$  band was unambiguously assigned to a nitrous oxide species,<sup>1</sup> so that non-nitrous oxide containing impurities can be eliminated, but a small amount of a highly absorbing nitrous oxide containing impurity cannot.

### 3.4 Thermal Decomposition of $[\text{RuA}_5\text{N}_2\text{O}]\text{X}_2$

Heating the solid tetrafluoroborate nitrous oxide complex at 135°

in high vacuum gave a solid residue which contained monomer dinitrogen complex and ruthenium red.<sup>1,12</sup> The products were identified by their ultraviolet<sup>22</sup> and visible spectra<sup>25</sup> respectively. Gaseous products from the decomposition were nitrogen, nitrous oxide and water. This reaction was not fully investigated and the present study has investigated the yields of the various products, with a view to elucidating the stoichiometry of the reaction.

In the presence of a reducing agent, the reaction between  $[\text{RuA}_5\text{OH}_2]^{2+}$  and nitrous oxide in solution, gives the monomer dinitrogen complex.<sup>1</sup> In the absence of a reducing agent the monomer and a ruthenium(III) product are formed.<sup>1</sup> It was found that two mole of  $[\text{RuA}_5\text{OH}_2]^{2+}$  were required for each mole of nitrous oxide complex reduced. In other studies<sup>26</sup> where chromium(II) or vanadium(II) were used as reducing agents, the amount of chromium(III) or vanadium(III) formed was always twice as much as the amount of monomer formed. It is conceivable that the solid state decomposition may also proceed by this mechanism.

An indication of the mechanism can be obtained by measurement of the amount of monomer dinitrogen complex and ruthenium red after thermal decomposition. Further, the nature and composition of the gases evolved may also be useful in deciding the mechanism. The results of such experiments are listed in Tables 3.9(a) and 3.9(b). No study was made of the bromide and iodide salts, as the yields of these complexes were very low and difficult to obtain pure. Ruthenium red was



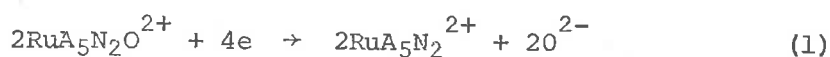
estimated from its absorption at 532 nm and the monomer from its absorption at 221 nm, after it had been separated from the ruthenium red by ion exchange chromatography. Any other ruthenium compounds produced in the reaction may not be detectable because of their low absorbances at the concentrations used.

For the tetrafluoroborate salt, the ratio of monomer to ruthenium red is 2:1. The second run listed shows a value of ~2.8:1, but the infrared spectrum of the complex used showed that monomer was present initially. Thus the ratio is higher than the other two runs. For the  $\text{PF}_6^-$  salt the ratio is much larger than 2:1 and the runs are inconsistent with each other. The explanation for this may lie with the curious two peak phenomenon discussed in section 3.3, although this seems unlikely, because the interconversion of  $\alpha\beta$  to  $\alpha$  solid would occur as the material warmed to 135°C and then the  $\alpha$  solid should follow the same pattern as the tetrafluoroborate salt.

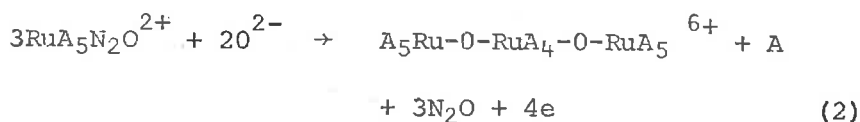
Not all of the ruthenium initially present could be accounted for as ruthenium red and monomer but up to 60% could be accounted for as such in some runs. The rest of the ruthenium may be present as ruthenium(III) species or undecomposed solid, which is oxidised subsequently when the monomer and ruthenium red are estimated.

From the data in Table 3.9(a) the observed stoichiometry for 60% decomposition of the tetrafluoroborate salt produces two mole of monomer for each mole of ruthenium red. For ruthenium red the formulation  $[(\text{NH}_3)_5\text{Ru}^{\text{III}}-\text{O}-\text{Ru}^{\text{IV}}(\text{NH}_3)_4-\text{O}-\text{Ru}^{\text{III}}(\text{NH}_3)_5]^{6+}$  has recently

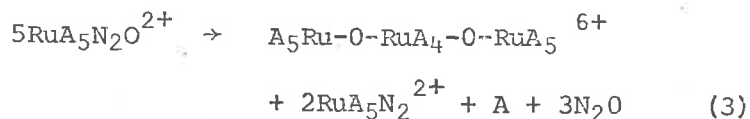
been confirmed by Mossbauer spectroscopy<sup>27</sup> and it is produced from a ruthenium(II) compound therefore with the liberation of four electrons. In the present instance the complex  $[\text{RuA}_5\text{N}_2\text{O}]^{2+}$ , which is itself readily reduced, is the source of the ruthenium red. Now two mole of the nitrous oxide complex require four electrons for reduction. Thus the stoichiometry and products observed are consistent with the known chemistry of the nitrous oxide complex. The reaction can be represented by the equations:



and



summation of equations (1) and (2) leads to equation (3):



Oxide ion and electrons are shown separately in the above reactions; it is possible of course that the disproportionation takes place by transfer of oxygen atoms. The equations represent the stoichiometry of the reaction based on the observed products and do not account for any other ruthenium products which may be present or the side reactions which can lead to their formation.

The mass spectrum of the gases released in the decomposition showed that nitrogen, nitrous oxide and water were present and their volumes were measured manometrically. No ammonia was detected from

the mass spectrum. The amount of nitrogen formed was about two to three times the amount of nitrous oxide. From the stoichiometry obeyed by the solid products equation (3) was derived and it predicts the release of three mole of nitrous oxide and one mole of ammonia for each five mole of complex decomposed, i.e. 0.8 m mole of gas for each m mole of complex, 0.6 m mole of which is nitrous oxide. From Table 3.9(b) the total number of millimole of gas approaches the value expected if the stoichiometry indicated by equation (3) was realised. However, the composition of the gases is not as predicted by the equation as the amount of nitrous oxide determined is far below that required by the equation. The contribution of water to the total volume arises from partial dehydration of the complexes and is small (~10-15% of the condensable gases determined by the decrease in volume using a dry ice-ethanol trap). The nitrogen in the gases may arise from a subsequent reaction of the released nitrous oxide or from the decomposition of the dinitrogen complex produced. Enough nitrogen gas is present to account for the discrepancy between the theoretical and the actual amount of nitrous oxide present, if the missing part was converted to nitrogen.

The tendency of the nitrous oxide complex to decompose by disproportionation by forming the dinitrogen complex and ruthenium ammine in higher oxidation states is evident in the solid state as well as in solution.

### 3.5 Summary

The crystal structure of the salts  $[\text{RuA}_5\text{N}_2\text{O}]\text{X}_2$  has been investigated and the ruthenium nitrous oxide linkage has been shown to be substantially linear. An investigation of the complex  $[\text{RuA}_5\text{N}_2\text{O}](\text{PF}_6)_2 \cdot \text{H}_2\text{O}$  has pointed to evidence for the presence of linkage isomers. The attachment of nitrous oxide was previously shown<sup>1</sup> to occur via the oxygen atom, so the possibility of attachment through the nitrogen atom exists. Finally, the thermal decomposition of  $[\text{RuA}_5\text{N}_2\text{O}](\text{BF}_4)_2 \cdot \text{H}_2\text{O}$  was shown to proceed by a stoichiometry similar to that found<sup>1</sup> for the decomposition in solution.

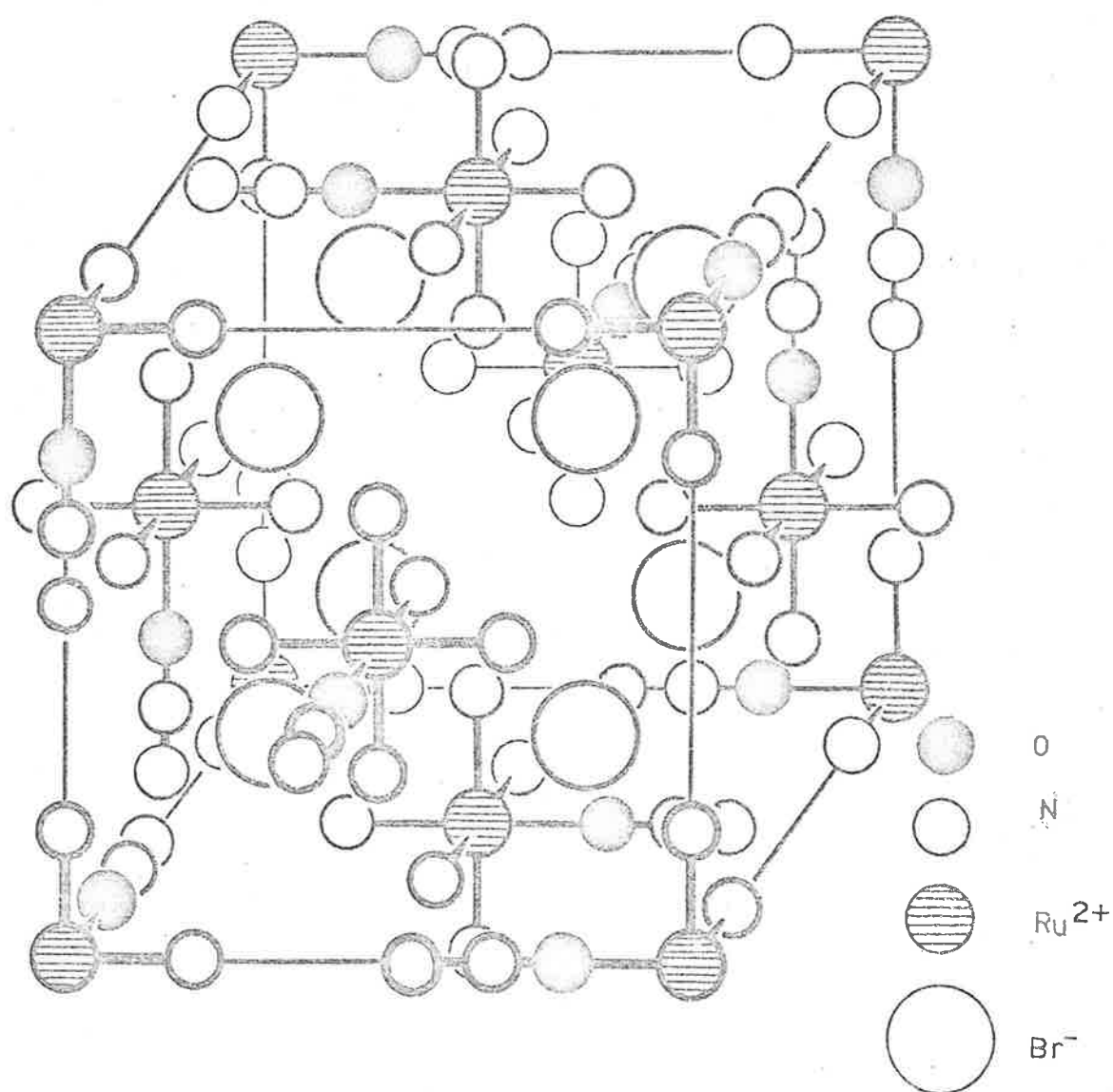


FIGURE 3.1  
STRUCTURE OF THE NITROUS OXIDE COMPLEXES

TABLE 3.1

*Cell Parameters for Dinitrogen and Nitrous Oxide Complexes* $[RuA_5Y]X_2$ ,  $Y = N_2, N_2O$ .

X	Y = N <sub>2</sub> O (Å)	Y = N <sub>2</sub> <sup>1</sup> (Å)
Br <sub>2</sub>	10.16 (5) <sup>2</sup>	10.41
I <sub>2</sub>	10.80 (5)	10.94
(BF <sub>4</sub> ) <sub>2</sub> ·H <sub>2</sub> O	11.25 (5)	
(BF <sub>4</sub> ) <sub>2</sub>	11.25 (5)	11.17
αβ-(PF <sub>6</sub> ) <sub>2</sub> <sup>3</sup>	11.85 (5) }	11.79
α-(PF <sub>6</sub> ) <sub>2</sub> <sup>3</sup>	11.92 (5) }	

<sup>1</sup> Values taken from ref. 2.<sup>2</sup> Standard deviations in parenthesis.<sup>3</sup> The terminology αβ and α is fully described in section 3.3.

The αβ solid has two ν<sub>3</sub> (N<sub>2</sub>O stretching mode) bands at 2280 and 2222 cm<sup>-1</sup>. On heating to 60°C for 2-3 hours the latter (β) peak disappears giving rise to the α solid.

TABLE 3.2

*Observed and Calculated Structure Factors for  $[\text{RuA}_5\text{N}_2\text{O}]\text{Br}_2$ .<sup>1</sup>*

h k l	F <sub>O</sub>	F <sub>C</sub>	h k l	F <sub>O</sub>	F <sub>C</sub>
1 1 1	a	161	6 2 2	b	56
2 0 0	b	3	4 4 4	225	238
2 2 0	325	361	7 1 1 } 5 5 1 }	213	198 <sup>c</sup>
3 1 1	163	122			
2 2 2	143	163	6 4 0	b	0
4 0 0	284	431	6 4 2	351	191
3 3 1	119	98	7 3 1	236	70
4 2 0	b	23	8 0 0	170	203
4 2 2	325	262	8 2 2 } 6 6 0 }	266	325 <sup>c</sup>
5 1 1 } 3 3 3 }	196 <sup>c</sup>	218 <sup>c</sup>	7 5 1 }	233	175 <sup>c</sup>
4 4 0	271	311	5 5 5 }		
5 3 1	218	113	8 4 0	251	165
4 4 2	b	30	9 1 1 } 7 5 3 }	218	151 <sup>c</sup>
6 0 0	b	11			
6 2 0	301	241			
5 3 3	175	98			

a obscured by beam stop.

b unobserved reflection.

c intensity for sum of reflections of same  $h^2 + k^2 + l^2$ .<sup>1</sup> Taken from ref. 1.

TABLE 3.3

*Site Occupancy Factors, Atomic Fractional Coordinates and  
Isotropic Thermal Parameters for  $[\text{RuA}_5\text{N}_2\text{O}]\text{Br}_2$ .*

	Occupancy	x	y	z	B ( $\text{\AA}^2$ )
Ru	0.1666	0.0	0.0	0.0	1.50
Br	0.3333	0.25	0.25	0.25	3.50
NH <sub>3</sub> , N(1)	1.0000	0.214	0.0	0.0	5.00
O	0.1666	0.43	0.0	0.0	3.50
N(2)	0.1666	0.313	0.0	0.0	3.50



TABLE 3.4

*Infrared Spectra of  $[RuA_5N_2O]X_2$  ( $X = Br^-$ ,  $I^-$ ,  $BF_4^-$ ,  $PF_6^-$ ).<sup>1</sup>*

Band positions expressed as  $cm^{-1}$ .

Assignment	Anion: $Br^-$	$I^-$	$BF_4^-$	$PF_6^-$
$\nu_3$ ( $N_2O$ )	2239	2252	2270	2280 ( $\alpha$ ) 2222 ( $\beta$ )
$\nu_1$ ( $N_2O$ )	1161	1180	1209	1222
$2\nu_1$ ( $N_2O$ )	2315 (w)		2415 (w)	
$\nu$ ( $N_2$ )	2110	2128	2144	2165

TABLE 3.5

*Ratio of  $\alpha$  and  $\beta$  Peaks of  $[\text{RuA}_5\text{N}_2\text{O}](\text{PF}_6)_2$  Prepared Under  
Various Conditions.*

Concentration of $[\text{RuA}_5\text{OH}_2]^{2+}$ used	Pressure of Nitrous Oxide	Ratio of $\alpha:\beta$ Areas	Overall Effect
<i>a) Effect of Nitrous Oxide Pressure</i>			
0.085M	14 atmos	0.8	$\alpha < \beta$
0.085M	14 "	0.75	$\alpha < \beta$
0.085M	21 "	2.0	$\alpha > \beta$
0.085M	21 "	2.3	$\alpha > \beta$
0.085M	29 "	1.3	$\alpha > \beta$
0.085M	29 "	1.2	$\alpha > \beta$
0.053M	1 "	0.77	$\alpha < \beta$
0.068M	0.5 "	1.0	$\alpha \approx \beta$
<i>b) Effect of <math>[\text{RuA}_5\text{OH}_2]^{2+}</math> Concentration</i>			
0.023M	21 atmos	1.0	$\alpha \approx \beta$
0.023M	21 "	1.1	$\alpha \approx \beta$
0.085M	21 "	2.0	$\alpha > \beta$
0.085M	21 "	1.5	$\alpha > \beta$
0.103M	21 "	1.3	$\alpha > \beta$
0.171M	21 "	1.4	$\alpha > \beta$

TABLE 3.6

a) Formation of  $[\text{RuA}_5\text{N}_2]^{2+}$  from  $\alpha$  and  $\alpha\beta$  Solids in Solution.<sup>1</sup>

Concentration Monomer from $\alpha\beta$ solid <sup>5</sup>		Concentration of Monomer from corresponding $\alpha$ solid <sup>2</sup>	
Calculated <sup>4</sup>	Found	Calculated	Found
$2.10 \times 10^{-3}$	$2.02 \times 10^{-3} \text{ M}$	$2.10 \times 10^{-3}$	$2.09 \times 10^{-3} \text{ M}$
$2.75 \times 10^{-3}$	$2.66 \times 10^{-3} \text{ M}$	$2.75 \times 10^{-3}$	$2.65 \times 10^{-3} \text{ M}$
$2.10 \times 10^{-3}$	$1.98 \times 10^{-3} \text{ M}$	$2.10 \times 10^{-3}$	$1.84 \times 10^{-3} \text{ M}$
$3.50 \times 10^{-3}$	$3.33 \times 10^{-3} \text{ M}$	$3.50 \times 10^{-3}$	$3.31 \times 10^{-3} \text{ M}$

b) Formation of  $[\text{RuA}_5\text{OH}_2]^{2+}$  from  $\alpha$  and  $\alpha\beta$  Solids in Solution.<sup>3</sup>

Aquo Concentration in $\alpha\beta$ Solid		Aquo Concentration from corresponding $\alpha$ solid <sup>2</sup>	
Calculated	Found	Calculated	Found
$2.40 \times 10^{-3}$	$2.36 \times 10^{-3} \text{ M}$	$2.40 \times 10^{-3}$	$2.22 \times 10^{-3} \text{ M}$
$2.01 \times 10^{-3}$	$1.98 \times 10^{-3} \text{ M}$	$2.01 \times 10^{-3}$	$1.55 \times 10^{-3} \text{ M}$
$1.50 \times 10^{-3}$	$1.47 \times 10^{-3} \text{ M}$	$1.50 \times 10^{-3}$	$1.42 \times 10^{-3} \text{ M}$

<sup>1</sup> Measured at 221 nm using  $1.80 \times 10^4 \text{ M}^{-1} \text{ cm}^{-1}$  as the molar absorptivity (value from ref. 22).

<sup>2</sup> Normalised so that direct comparison can be made, i.e. calculations are based on the same weights of complex in both cases.

<sup>3</sup> Measured at 268 nm using  $570 \text{ M}^{-1} \text{ cm}^{-1}$  as the molar absorptivity (value from ref. 1).

<sup>4</sup> Calculations based on the weight of solid used, and assuming a monomeric nitrous oxide complex,  $[\text{RuA}_5\text{N}_2\text{O}](\text{PF}_6)_2 \cdot \text{H}_2\text{O}$ . Molecular weight 538.2.

<sup>5</sup> The  $\alpha$  solid was prepared from the  $\alpha\beta$  solid by heating until the  $\beta$  peak had disappeared.

TABLE 3.7

*Gas Evolved from Low Temperature Decomposition of  $[\text{RuA}_5\text{N}_2\text{O}](\text{PF}_6)_2$ .<sup>1</sup>*

Volumes in millilitres.

$V_{\text{TOTAL}}$	$V_{\text{CONDENSABLE}}^2$	$V_{\text{NON-CONDEN.}}^3$	$V_{\text{MOLAR}}$	% MOLAR
0.199	0.151	0.048	1.96	10.2
0.075	0.066	0.009	1.72	4.3
0.067	0.061	0.006	1.95	3.4
0.303	0.241	0.062	1.75	17.3
0.255	0.201	0.054	1.75	14.6
0.300	n.d. <sup>4</sup>	-	1.85	16.2
0.140	n.d.	-	2.11	6.6
0.390	n.d.	-	1.95	19.6
0.253	n.d.	-	1.51	16.7

<sup>1</sup> All volumes corrected to S.T.P.

<sup>2</sup> Determined by trapping the gases in liquid nitrogen.

<sup>3</sup> Calculated for one mole of gas release at S.T.P.

<sup>4</sup> n.d. = not determined.

TABLE 3.8

*Infrared Stretching Frequencies of Thiocyanate Linkage Isomers.<sup>a</sup>*

Complex	$\nu_3$ (C-N stretch) $\text{cm}^{-1}$	$\nu_1$ (C-S stretch) $\text{cm}^{-1}$
$\text{Co}(\text{NH}_3)_5\text{NCS}^{2+}$ b	2125	806
$\text{Co}(\text{NH}_3)_5\text{SCN}^{2+}$ b	2100	710
$\text{Rh}(\text{NH}_3)_5\text{NCS}^{2+}$	2145	815
$\text{Rh}(\text{NH}_3)_5\text{SCN}^{2+}$	2115	730
$\text{Ir}(\text{NH}_3)_5\text{NCS}^{2+}$	2140	825
$\text{Ir}(\text{NH}_3)_5\text{SCN}^{2+}$	2110	700

<sup>a</sup> Taken in part from ref. 14.<sup>b</sup> ref. 15.

TABLE 3.9(a)

*Thermal Decomposition of Nitrous Oxide Complexes.**Formation of Monomer and Ruthenium Red.*

All quantities expressed as millimole.

Anion	Monomer	Ruthenium Red	Ratio Monomer:Red
$\text{BF}_4^-$	$4.96 \times 10^{-4}$	$2.48 \times 10^{-4}$	2:1
$\text{BF}_4^-$	$1.70 \times 10^{-3}$	$6.14 \times 10^{-4}$	2.77:1
$\text{BF}_4^-$	$1.63 \times 10^{-2}$	$8.22 \times 10^{-3}$	1.99:1
$\text{PF}_6^-$	$4.06 \times 10^{-4}$	$9.05 \times 10^{-5}$	4.49:1
$\text{PF}_6^-$	$1.32 \times 10^{-3}$	$3.17 \times 10^{-4}$	4.16:1

TABLE 3.9(b)

*Gaseous Products from the Thermal Decomposition of Nitrous Oxide  
Complexes.<sup>1</sup>*

All quantities expressed as millimole.

Anion	mM[RuA <sub>5</sub> N <sub>2</sub> O]X <sub>2</sub> used	Total Gas Evolved	Nitrogen	Water	Nitrous Oxide	% Molar Volume <sup>3</sup>
BF <sub>4</sub>	0.106	0.054	0.041	0.001	0.012	51.0
BF <sub>4</sub>	0.118	0.083	0.056	n.d. <sup>2</sup>	0.027	70.7
BF <sub>4</sub>	0.116	0.075	0.057	0.001	0.017	65.0
PF <sub>6</sub>	0.082	0.055	0.051	0	0.004	69.3
PF <sub>6</sub>	0.079	0.058	0.039	n.d. <sup>2</sup>	0.019	54.7

<sup>1</sup> Corrected to S.T.P.

<sup>2</sup> n.d. = not determined.

<sup>3</sup> Calculated assuming one mole of gaseous product per mole of solid.

## CHAPTER 3

## REFERENCES

1. G.J. Sparrow, Ph.D. Thesis, University of Adelaide, 1972;  
A.A. Diamantis and G.J. Sparrow, J. Chem. Soc. (Dalton Transactions), in the press.
2. F. Bottomley and S.C. Nyburg, Chem. Comm., 1966, 897;  
Acta Crystallogr., 1968, B24, 1289.
3. M.R. Snow and R.F. Boomsma, Acta Crystallogr., 1972, B28, 1908.
4. Using programme FUORFLS (a modification of ORFLS by M.R. Taylor) and the University of Adelaide CDC 6400 Computer. Source of atomic scattering factors:  $\text{Ru}^{2+}$  and  $\text{Br}^-$ , P.A. Doyle and P.S. Turner, Acta Crystallogr. (A), 1968, 24, 390; O, N, C, "International Tables for X-ray Crystallography", Vol. III, p. 202 (Kynoch Press: Birmingham, 1962).
5. J.L. Griggs, K.N. Rao, L.H. Jones and R.M. Potter, J. Mol. Spectroscopy, 1968, 25, 34.
6. P.G. Wilkinson and N.B. Houk, J. Chem. Phys., 1956, 24, 528.
7. F. Bottomley and J.R. Crawford, J. Amer. Chem. Soc., 1972, 94, 9092.
8. B.R. Davis and J.A. Ibers, Inorg. Chem., 1970, 9, 2768.
9. H. Taube and J.N. Armor, Chem. Comm., 1971, 287.
10. J.R. Van Wazer, "Phosphorus and Its Compounds", Vol. I, p. 803, Interscience Publishers Inc., New York, 1958.
11. J.N. Armor and H. Taube, J. Amer. Chem. Soc., 1969, 91, 6874.



12. A.A. Diamantis and G.J. Sparrow, *Chem. Comm.*, 1970, 819.
13. A.H. Norbury and A.I.P. Sinha, *Quart. Rev.*, 1970, 24, 69.
14. J.L. Burmeister, *Coord. Chem. Rev.*, 1966, 1, 205 and references therein.
15. D.A. Buckingham, I.I. Creaser and A.M. Sargeson, *Inorg. Chem.*, 1970, 9, 655.
16. Y. Kozirovsky and M. Folman, *Israel J. Chem.*, 1969, 7, 595; *Trans. Faraday Soc.*, 1969, 65 244.
17. E. Borello, L. Cerrutti, G. Chiotti and F. Guglielminotti, *Inorg. Chim. Acta*, 1972, 6, 45.
18. A. Zecchina, L. Cerrutti and E. Borello, *J. Catal.*, 1972, 25, 55.
19. L. Mandelcorn, *Chem. Rev.*, 1959, 59, 827.
20. F.A. Cotton and G. Wilkinson, "Advanced Inorganic Chemistry", Second Edn., Interscience Publishers, New York, 1966, p. 223 ff.
21. J.L. Burmeister, *Coord. Chem. Rev.*, 1968, 3, 225 and references therein.
22. J.N. Armor and H. Taube, *J. Amer. Chem. Soc.*, 1970, 92, 6170.
23. H. Hartmann and C. Buschbeck, *Z. Phys. Chem. (Frankfurt)*, 1957, 11, 120.
24. Yu. G. Borod'ko, G.I. Kozub and Yu. P. Myagkov, *Russ. J. Phys. Chem.*, 1970, 44, 643.
25. J.M. Fletcher, B.F. Greenwood, C.J. Hardy, D. Scargill and J.L. Woodward, *J. Chem. Soc.*, 1961, 2000.

26. J.N. Armor and H. Taube, J. Amer. Chem. Soc., 1971, 93, 6476.
27. C. Clausen, R. Prados and M. Good, Inorg. and Nucl. Chem. Letts., 1971, 7, 485.
28. K. Nakamoto, "Infrared Spectra of Inorganic and Coordination Compounds", John Wiley and Sons, New York, 1963, p. 80.
29. J.C.D. Brand and J.C. Speakman, "Molecular Structure: The Physical Approach", Edward Arnold (Publishers) Ltd., 1964, p. 155.
30. J. Fergusson, J. Love and W. Robinson, Inorg. Chem., 1972, 11, 1662.

## CHAPTER 4

THE REACTION OF NITROUS OXIDE WITH DIAQUO TETRAAMMINE RUTHENIUM(II)  
SPECIES

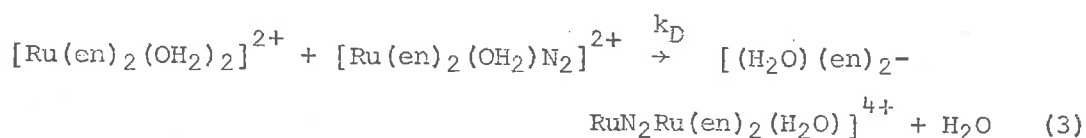
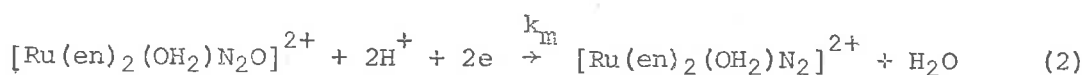
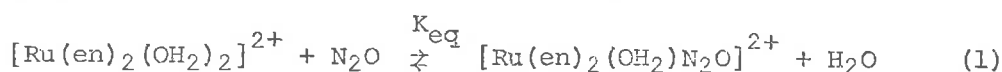
## 4.1 Introduction

Nitrous oxide complexes have been prepared for ruthenium(II) pentaammine.<sup>1</sup> Some recent investigations<sup>2,3</sup> have explored the possibility of preparing nitrous oxide complexes of bis-ethylene-diamine ruthenium(II) species. These later attempts were unsuccessful, but the presence of a nitrous oxide species in solution was demonstrated from an examination of the ultraviolet spectrum. The present study has reinvestigated the preparative attempts and also attempted the preparation of the analogous tetraammine ruthenium(II) species.

4.2 The Reaction of *cis*-[Ru(en)<sub>2</sub>(OH<sub>2</sub>)<sub>2</sub>]<sup>2+</sup> with Nitrous Oxide

In the presence of a reducing agent, the reaction of *cis*-diaquo bis-ethylenediamine ruthenium(II), *cis*-[Ru(en)<sub>2</sub>(OH<sub>2</sub>)<sub>2</sub>]<sup>2+</sup>, with nitrous oxide leads to formation of the corresponding monomer and dimer dinitrogen complexes.<sup>2</sup> Bellen<sup>2</sup> was able to show quantitatively, that the reaction with nitrous oxide gives faster conversion to the dinitrogen complexes than with nitrogen gas, but no measurements of the rate constants were reported. However, the rate of formation of the monomer dinitrogen complex from nitrogen has been measured<sup>4</sup> as  $8.0 \times 10^{-2} \text{ M}^{-1} \text{ sec}^{-1}$ . The reaction with nitrous oxide was

essentially complete within one hour, with mainly (>60%) monomer being produced. The amount of monomer produced depended on the initial concentration of the diaquo species present. Thus, when the initial ruthenium concentration was  $10^{-3}$  M, the amount of monomer present accounted for more than 80% of the ruthenium present after one hour. On the basis of these observations the following mechanism was proposed:<sup>2</sup>



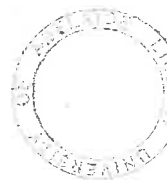
Reaction (1) was regarded as rate determining, the nitrous oxide complex being reduced as soon as it was formed. The effect of temperature on the reaction was not investigated before and Table 4.1 lists the results of such a study. A plot of  $\log k$  against  $1/T$  was a straight line in agreement with the Arrhenius equation. From these results  $\Delta H^\ddagger$  for the reaction at  $25^\circ\text{C}$  was calculated as  $38.6 \text{ kJ mole}^{-1}$  while  $\Delta S^\ddagger$  was  $-16.1 \text{ J K}^{-1} \text{ mole}^{-1}$ . The value of  $\Delta H^\ddagger$  is very low in comparison with the values obtained for the reaction of aquo pentaammine ruthenium(II) with nitrous oxide<sup>5</sup> ( $\Delta H^\ddagger = 73.6 \text{ kJ mole}^{-1}$ ) and azide ( $\Delta H^\ddagger = 74.9 \text{ kJ mole}^{-1}$ ).

By exposing dilute solutions of  $\text{cis}-[\text{Ru}(\text{en})_2(\text{OH}_2)_2]^{2+}$  to high pressures of nitrous oxide for 15 minutes, then examining the

ultraviolet spectrum, a species with an absorption maximum at 236 nm was observed. A molar absorptivity of  $5050 \text{ M}^{-1} \text{ cm}^{-1}$  was calculated.<sup>2</sup> The peak soon decayed to give a new maximum at 222 nm. The peak at 236 nm was assigned<sup>2</sup> to the nitrous oxide intermediate by comparison with the spectrum of  $[\text{RuA}_5\text{N}_2\text{O}]\text{X}_2$  which has a maximum at 238 nm.<sup>1</sup> In solution, the nitrous oxide complexes are reversibly dissociated to form the ruthenium(II) aquo species, which can reduce the nitrous oxide complex to the monomer.<sup>1</sup> Thus the shift in absorption maximum was attributed to formation of the monomer.

The value of the molar absorptivity obtained above appears to be low when it is compared with the value for the pentaammine obtained by Sparrow<sup>1</sup> ( $1.2 \times 10^4 \text{ M}^{-1} \text{ cm}^{-1}$ ) and Taube<sup>5</sup> ( $1.7 \times 10^4 \text{ M}^{-1} \text{ cm}^{-1}$ ). Two independent determinations of the molar absorptivity gave values of  $4.97 \times 10^3 \text{ M}^{-1} \text{ cm}^{-1}$  and  $5.64 \times 10^3 \text{ M}^{-1} \text{ cm}^{-1}$  confirming the value obtained by Bellen. The apparent molar absorptivity calculated on the ruthenium(II) concentration is similar to that obtained for the pentaammine ruthenium(II) species at a pressure of one atmosphere of nitrous oxide ( $\epsilon \approx 3 \times 10^3 \text{ M}^{-1} \text{ cm}^{-1}$ ).<sup>5</sup> By analogy with the pentaammine complex the ethylenediamine complex is also extensively dissociated in solution.

From his observations with the pentaammine, Sparrow<sup>1</sup> was able to design the most favourable conditions for the isolation of the nitrous oxide complex. From the equilibrium in equation (1) above, high pressures of nitrous oxide would favour the formation of the nitrous



oxide complex by increasing the concentration of nitrous oxide in solution. Immediate precipitation of the nitrous oxide complex from solution minimises side reactions to form the dinitrogen complexes. Further it also shifts equilibrium (1) to the right by decreasing the concentration of the nitrous oxide complex in solution. The equilibrium constant for the formation of the pentaammine nitrous oxide complex was found to increase on lowering the temperature.<sup>5</sup> Thus cooling the reaction vessel increases conversion to the product. The same is most probably true for the formation of other nitrous oxide complexes. Moderately high concentrations of the aquo complex were required for isolation of the nitrous oxide complex, but this condition further increases the likelihood of complicating side reactions, viz. the production of the monomer and dimer dinitrogen complexes (see equations (2) and (3)). All attempts to prepare the nitrous oxide complexes were carried out with due regard to the above conditions.

Zotti<sup>3</sup> found that the anions  $\text{Cl}^-$ ,  $\text{Br}^-$ ,  $\text{I}^-$ ,  $\text{BF}_4^-$ ,  $\text{PF}_6^-$  and  $\text{BPh}_4^-$  were all unsuccessful in precipitating the nitrous oxide complex  $[\text{Ru}(\text{en})_2(\text{OH}_2)\text{N}_2\text{O}]\text{X}_2$ . No precipitate was obtained with the first five anions. Tetraphenyl borate gave a precipitate of the aquo complex only. Lithium bromide in ethanol gave a red solid which had an absorption band at  $2090\text{ cm}^{-1}$  in its infrared spectrum. The band was assigned to  $\nu_{\text{N-N}}$  of coordinated dinitrogen in  $[\text{Ru}(\text{en})_2(\text{OH}_2)\text{N}_2]\text{Br}_2$ . An ultraviolet spectrum of the red solid had maxima at 211 nm and 390 nm. No absorption near 240 nm attributable to the nitrous oxide

complex was observed.

The experiments performed by Zotti were repeated. Again only lithium bromide in ethanol and tetraphenyl borate were successful in producing precipitates. Using a solution of tetraphenyl borate, enough of the anion was added to precipitate the aquo complex, which was then redissolved and exposed to thirty atmospheres of nitrous oxide. No precipitate was obtained in this instance. However, a precipitate was obtained when a solution of the aquo and a solution of tetraphenyl borate were placed in separate arms of a reaction vessel, exposed to nitrous oxide then added together. The infrared spectrum of this precipitate had a single absorption band at  $2121.6\text{ cm}^{-1}$ . Also a sharp band was observed at  $1238\text{ cm}^{-1}$ , the  $\nu_1$  region of coordinated nitrous oxide. The band at  $2122\text{ cm}^{-1}$  (lit.<sup>6</sup>  $2130\text{ cm}^{-1}$ ) was assigned to  $\nu_{\text{N-N}}$  of coordinated dinitrogen. No evidence for any band near  $2200\text{ cm}^{-1}$  was found. The band at  $1240\text{ cm}^{-1}$  probably appears due to the absorptions of either the anion or ethylenediamine. When lithium bromide in ethanol was used as a precipitant, a red solid was obtained. It had a single absorption band at  $2080.3\text{ cm}^{-1}$  and no other absorption bands were observed in this region. Also no absorptions in the  $\nu_1$  region of coordinated nitrous oxide were observed. Again this solid appears to be the dinitrogen complex with the band at  $2080\text{ cm}^{-1}$  due to  $\nu_{\text{N-N}}$  of  $[\text{Ru}(\text{en})_2\text{CH}_2\text{N}_2]\text{Br}_2$ . An ultraviolet spectrum of the red compound showed a weak shoulder at  $\sim 225\text{ nm}$ . Three absorptions at  $305\text{ nm}$  (shoulder),  $380\text{ nm}$  and  $440\text{ nm}$ , due to the

presence of  $\text{cis-[Ru(en)}_2\text{Br}_2\text{]Br}$  (lit.<sup>7</sup>  $\lambda_{\text{max}}$  380 nm  $\epsilon$  1510  $\text{M}^{-1} \text{cm}^{-1}$ ; 445 nm  $\epsilon$  1530  $\text{M}^{-1} \text{cm}^{-1}$ ) in the solid, were observed in more concentrated solutions and show that the red solid is highly contaminated with ruthenium(III) species. When the ultraviolet spectrum of the red solid was recorded in nitrous oxide saturated water, no absorptions near 240 nm were observed. This evidence, together with the infrared spectra, showed that no nitrous oxide complex was isolated.

Generally the solubility of the nitrous oxide complex was such that no products could be isolated, this also had the undesirable effect of giving rise to ruthenium(III) species and ruthenium(II) dinitrogen complexes by providing favourable conditions for equation (3). Using higher concentrations of  $[\text{Ru(en)}_2(\text{OH}_2)_2]^{2+}$  is limited by the fact that attempts to concentrate the solution give rise to blue compounds.

#### 4.3 Isolation and Characterisation of Aquo Dinitrogen Oxide

##### *Tetraammine Ruthenium(II) Complexes*

##### 4.3.1 Preparation and Purity of the Complexes

The conditions described in section 4.2 and used in the preparation of the pentaammine nitrous oxide complexes, were also used for preparation of the aquo tetraammine nitrous oxide hexafluorophosphate and tetrafluoroborate salts. No precipitate was obtained with either bromide or iodide, even when the lithium halide in ethanol was used. The halide complexes appear to be too soluble



for isolation under the experimental conditions used.

Both the  $\text{PF}_6^-$  and  $\text{BF}_4^-$  salts were free from substantial amounts of impurities. No dinitrogen complexes were present as adjudged from their infrared spectra. For the  $\text{PF}_6^-$  salt, a possible source of impurity was the diaquo salt, which was sometimes precipitated on addition of the solution of ammonium hexafluorophosphate. In cases where a precipitate was formed, it was redissolved by adding a few drops of water before exposure to nitrous oxide. Even so, some aquo may be precipitated on cooling the reaction mixture in ice, but this will be minimal, as nitrous oxide was admitted to the pressure vessel before the reaction mixture was cooled. It was impossible to recrystallise the complexes as they decompose rapidly in aqueous solution with loss of nitrous oxide.

#### 4.3.2 *Stability of the Complexes*

Both complexes are unstable on exposure to the air losing nitrous oxide to form the dinitrogen complex. The tetrafluoroborate salt was allowed to stand over silica gel under nitrous oxide for one week at  $-5^\circ\text{C}$  with only small formation of the dinitrogen complex. The  $\text{PF}_6^-$  salt, on standing under an atmosphere of nitrous oxide over phosphorus pentoxide at room temperature for two days, showed some formation of the dinitrogen complex. The complexes have a limited stability of about one day at room temperature in a dry atmosphere. At lower temperatures the complexes are stable for longer periods.

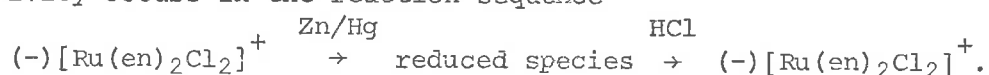
### 4.3.3 Characterisation of the Complexes:

#### (i) Solution Properties.

Loss of nitrous oxide occurred when the complexes were dissolved in 0.1M methane sulphonic acid under argon forming  $[\text{RuA}_4(\text{OH}_2)_2]^{2+}$  quantitatively. The concentration of the diaquo formed was determined by its absorption at 257 nm and by converting it to  $\text{cis-}[\text{RuA}_4\text{Cl}_2]^+$  and determining its concentration spectrophotometrically. The literature value for the diaquo was confirmed by reducing  $\text{cis-}[\text{RuA}_4\text{Cl}_2]^+$  with zinc amalgam in 0.1M methane sulphonic acid. The  $\text{cis-}[\text{RuA}_4\text{Cl}_2]\text{Cl}$  was prepared as described in section 6.1 (p.148). Table 4.2(ii) lists the results obtained for two independent determinations of each of the salts. There is, in some cases, a variance between the molar absorptivity observed and the literature value due, perhaps, to the presence of small amounts of the dinitrogen complexes which have a strong absorption in this region.

When the complexes were oxidised in air in 1M hydrochloric acid conversion to a chloro species, probably  $\text{cis-}[\text{RuA}_4\text{Cl}_2]^+$ , took place. Table 4.2(i) lists the molar absorptivities of the species obtained at its maxima of 262 nm, 314 nm and 352 nm. The maxima are the same as those of  $\text{cis-}[\text{RuA}_4\text{Cl}_2]^+$  and the molar absorptivities of the 262 nm and 314 nm peaks are the same, within experimental error, as the literature values of  $\text{cis-}[\text{RuA}_4\text{Cl}_2]^+$ , but the molar absorptivity of the peak at 352 nm is low in comparison with the literature value. However, the values obtained for the oxidation of the diaquo species,

produced by reduction of  $\text{cis-}[\text{RuA}_4\text{Cl}_2]^+$  in 0.1M methane sulphonic acid, in 1M hydrochloric acid under the same conditions, gave the same values as obtained by oxidation of the nitrous oxide complexes. Thus the results obtained confirm the proposed formulations within experimental error as well as suggest a cis configuration for the complexes. It has been shown<sup>8</sup> that complete retention of optical activity occurs in the reaction sequence



Similar behaviour for the  $\text{cis-}[\text{RuA}_4\text{Cl}_2]^+$  would be anticipated and the results obtained support this proposition. In particular, the results obtained from the oxidation of the nitrous oxide complexes, support a cis stereochemistry of the ion  $[\text{RuA}_4(\text{OH}_2)\text{N}_2\text{O}]^{2+}$ . The trans configuration can be eliminated as  $\text{trans-}[\text{RuA}_4\text{Cl}_2]^+$  has a different spectrum ( $\lambda_{\text{max}}$  333 nm  $\epsilon$   $4.7 \times 10^3 \text{ M}^{-1} \text{ cm}^{-1}$ ).<sup>38</sup>

#### (ii) Microanalysis.

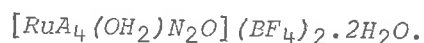
The microanalyses of the compounds were carried out in Melbourne usually within 24 hours of arrival (i.e. three days after preparation). The complexes were sealed in a tube in an atmosphere of dry nitrous oxide. Despite this precaution, the analyses indicated that some loss of nitrous oxide occurred. Samples which were still yellow when analysed gave the best agreement with the calculated values as shown by the results obtained, which are listed in Table 4.3.

Sparrow found<sup>1</sup> that a reaction of the fluoro containing complexes

of ruthenium pentaammine nitrous oxide with the combustion boats during ignition of the sample lead to inconsistent metal analyses. In an attempt to overcome this problem, the  $\text{PF}_6^-$  salt was dissolved in water and passed down an ion exchange column in the chloride form. The resultant solution was evaporated to dryness and the ruthenium content determined by reduction to the metal. Again the results were very inconsistent as shown in Table 4.3. Either the exchange was not complete or hydrolysis of the  $\text{PF}_6^-$  allowed some fluoride to pass through the column. Hence the reaction of the combustion boats with fluoride was not entirely eliminated.

The microanalytical results obtained support the formulation of the complexes as given above and in Table 4.3.

(iii) *Release of Nitrous Oxide from*



The amount of nitrous oxide present in the tetrafluoroborate salt was determined by oxidation with cerium(IV) sulphate and measuring the volume of gas evolved manometrically and determining the composition mass spectrometrically. Cerium(IV) sulphate oxidises the dinitrogen complex with quantitative release of dinitrogen gas.<sup>9,10</sup> It was found for the pentaammine nitrous oxide that only 70-80% of the gas released with cerium(IV) sulphate was nitrous oxide, the rest being nitrogen.<sup>1</sup> Similar results were obtained for the tetraammine complex. Table 4.4 lists the total amount of gas evolved, the

composition of the gas and the amount of gas expected for the complete release of one mole. The absence of any gas evolution approaching two mole eliminates the possibility that the compound is a bis (dinitrogen oxide) species. There is not perfect agreement between the amount of gas released and the amount expected for one mole. Further, all of the gas released is not nitrous oxide. However, the release of gas does approach the value for one mole and falls within the range of experimental error for the determinations.

The decomposition of the pentaamine nitrous oxide complex gave similar results. The method of initiating the oxidation is such that the possibility that some of the nitrous oxide complex is reduced to the dinitrogen complex cannot be excluded and the cerium(IV) sulphate would attack it releasing nitrogen. Hydrolysis of the nitrous oxide complex may occur to form the diaquo species which accomplishes the subsequent reduction of another nitrous oxide molecule to the dinitrogen complex before oxidation by cerium(IV) sulphate.

Although the gas releases do not constitute proof for the purity of the complexes they are entirely consistent with the formulation of the complexes with one mole of coordinated nitrous oxide.

#### 4.3.4 *Infrared Spectra of the Complexes*

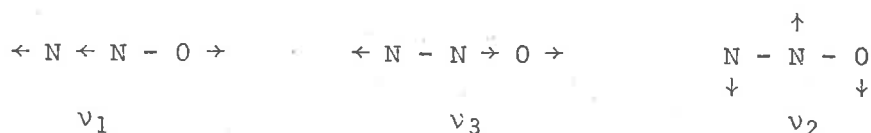
Gaseous nitrous oxide has four fundamental vibrational frequencies.<sup>11a</sup> These are

$\nu_1$ , the pseudosymmetric stretch;

$\nu_3$ , the pseudoasymmetric stretch;

and  $\nu_2$ , the doubly degenerate bend.

The absorptions are observed at 1286, 2224 and 589  $\text{cm}^{-1}$  respectively.



The  $\nu_1$  stretching vibration can be regarded mainly as a stretching of the nitrogen-oxygen bond and the  $\nu_3$  vibration a stretching of the nitrogen-nitrogen bond. This is only an approximation as both bonds are involved in the vibration.

When nitrous oxide is adsorbed onto alkali halide films all three fundamental vibrations are observed<sup>12,13</sup> (Table 4.5). The appearance of multiple absorptions for some fundamentals was explained by assuming that the nitrous oxide molecules are situated on two energetically different adsorption sites, the most energetic sites being occupied first. It was concluded that the nitrous oxide was adsorbed perpendicularly to the surface through its oxygen atom. The shifts in frequency of  $\nu_3$  and  $\nu_1$  compared with the free gas are  $\Delta\nu_3 \approx +10 \text{ cm}^{-1}$  and  $\Delta\nu_1 -10 \text{ to } -60 \text{ cm}^{-1}$ . Thus, qualitatively the N-N bond is strengthened by the interaction and the N-O bond is weakened.

A more detailed investigation of nitrous oxide adsorbed onto  $\alpha$ -chromia has been carried out.<sup>14</sup> All three fundamentals of nitrous oxide were observed. Multiple absorptions were observed in the  $\nu_3$

and  $\nu_1$  regions. By studying the absorptions as a function of gas pressure, it was concluded that there are two sets of absorptions present. These sets of absorptions are  $2238\text{ cm}^{-1}$ - $1237\text{ cm}^{-1}$  and  $2305\text{ cm}^{-1}$ - $1339\text{ cm}^{-1}$ . The shifts observed are  $\Delta\nu_3 +14\text{ cm}^{-1}$ ,  $\Delta\nu_1 -49\text{ cm}^{-1}$  and  $\Delta\nu_3 +81\text{ cm}^{-1}$ ,  $\Delta\nu_1 +53\text{ cm}^{-1}$  respectively. A consideration of the molecular orbitals of nitrous oxide shows that both terminal atoms have a higher electron density associated with them than the central nitrogen atom. It was therefore concluded that both end atoms could act as donor atoms in coordination or surface compounds. As the first pair of absorptions give shifts in the same direction as those observed for absorptions on alkali halides, it was concluded that these arise due to attachment through the oxygen atom. The other pair of absorptions are due to attachment through the nitrogen atom.

In coordinated nitrous oxide two additional vibrations can be expected as well as the above, a metal-donor atom stretch and a metal-donor atom deformation, the last being doubly degenerate in a symmetrical situation. Of these only  $\nu_3$  and  $\nu_1$  have been positively identified.<sup>1</sup> No other bands could be confidently assigned due to the presence of other vibrations in those regions of the spectrum. The shifts observed on coordination of the nitrous oxide are in the same sense as those found for the O-attachment of nitrous oxide to alkali halides and  $\alpha$ -chromia. Based on a normal coordinate analysis of the isotopically substituted nitrous oxide complexes it was

concluded that the attachment to the metal occurred through the oxygen atom.<sup>1</sup>

Table 4.6 lists the absorptions observed for the tetraammine nitrous oxide complexes isolated, together with the assignment of each vibration. Both the  $\nu_3$  and  $\nu_1$  absorptions of nitrous oxide were observed. For the  $\text{BF}_4^-$  a single  $\nu_3$  and  $\nu_1$  absorption was observed, whereas for the  $\text{PF}_6^-$  two absorptions in the  $\nu_3$  region and one  $\nu_1$  absorption were observed. The doublet of  $\nu_3$  absorptions for the  $\text{PF}_6^-$  is the same behaviour as observed for the pentaammine. The reason for the appearance of both peaks in the pentaammine was discussed in section 3.4. For the tetraammine the same reasons can be advanced and thus the presence of N- and O-bonded isomers accounts for the appearance of the two peaks. Again no  $\nu_1$  peak associated with the second  $\nu_3$  peak was observed.

The shifts observed on coordination of the nitrous oxide are  $\Delta\nu_3 = +60 \text{ cm}^{-1}$ ,  $\Delta\nu_1 = -24 \text{ cm}^{-1}$  for the  $\text{PF}_6^-$  salt and  $\Delta\nu_3 = +51 \text{ cm}^{-1}$ ,  $\Delta\nu_1 = -46 \text{ cm}^{-1}$  for the  $\text{BF}_4^-$  salt. Again they parallel those observed for O atom attachment to various surfaces. Furthermore, the shifts observed are similar to those observed for the corresponding pentaammine salts. Thus, the complexes contain oxygen-bonded nitrous oxide. Further the shifts indicate that the nitrogen-nitrogen bond has been strengthened and the nitrogen-oxygen bond weakened.

Chatt<sup>15</sup> has described the bonding in the pentaammine dinitrogen ruthenium(II) complexes as a synergistic process, with  $\sigma$  donation of



electrons from coordinated dinitrogen and back-bonding into an empty  $\pi$  orbital of dinitrogen. Such a process resulted in a marked decrease in the bond order of the dinitrogen ligand as evidenced by the decrease of the dinitrogen stretching frequency ( $\nu_{\text{N-N}} = 2331 \text{ cm}^{-1}$  in the free gas,  $\nu_{\text{N-N}} \approx 2100 \text{ cm}^{-1}$  in the complexes).

The nitrous oxide molecule has energy levels comparable to those of nitrogen (see Table 4.7). The first unfilled molecular orbital is the  $3\pi$  with an energy of  $-7.4 \text{ eV}$ , while the highest filled orbital is the  $2\pi$  with an energy of  $-12.89 \text{ eV}$ .<sup>16</sup> The highest filled  $\sigma$  orbital, the  $7\sigma$ , has an energy of  $-16.38 \text{ eV}$ . The  $7\sigma$  and unfilled  $3\pi$  orbitals are of energies nearly identical to the  $1\pi_g$  antibonding and  $3\sigma_g$  bonding orbitals of dinitrogen. A  $\sigma$  donation of electrons from the  $7\sigma$  orbital to the metal and back-donation into the unfilled  $3\pi$  antibonding orbital of nitrous oxide could explain the bonding in these compounds. The  $2\pi$  orbital is not of the correct symmetry for  $\sigma$  donation to the metal and it cannot accept electrons from the metal  $t_{2g}$  orbitals because it is filled. Such a bonding description implies that a weakening of the bonds could occur similar to that observed in the dinitrogen complexes. However, only the N-O bond is weakened. It has been shown that the  $7\sigma$  orbital is weakly antibonding.<sup>40</sup> Thus  $\sigma$  donation from the  $7\sigma$  orbital to the metal moderately strengthens both the N-O and N-N bonds. But, back-donation into the  $3\pi$  molecular orbital weakens the N-O bond more than the N-N bond. Taken overall, the effect of  $\sigma$  donation and  $\pi$  back-bonding is to weaken the N-O bond and strengthen

the N-N bond relative to the free gas.

The intensities of the two fundamental nitrous oxide vibrations observed in the complexes decrease in the order:

$$\nu_1 > \nu_3$$

whereas in the free gas the order is:

$$\nu_3 > \nu_1 > \nu_2.$$

The position in the above sequence of the  $\nu_2$  absorption of nitrous oxide in the complexes is not known, as it was not observed. However, it is probable that it is even weaker than the  $\nu_3$  vibration. The intensity of the  $\nu_1$  band was found to depend on the anion such that  $\text{BF}_4^- > \text{PF}_6^-$ ; the  $\nu_3$  intensity of both salts was almost the same. The effect of the anion on the intensity changes of  $\nu_1$  can be explained by the effect each anion has on the amount of back-donation of electrons into the  $3\pi$  antibonding orbital of nitrous oxide, by using analogous arguments to those used for the variation of the intensity of the  $\nu_{\text{N-N}}$  vibration of  $[\text{RuA}_5\text{N}_2]\text{X}_2$  and  $[\text{OsA}_5\text{N}_2]\text{X}_2$  with anion. Folkesson<sup>20</sup> argues that a high electron density in the  $\pi$  antibonding orbitals of the N-N group corresponds to an increase in the N-N distance. Further, when the N-N distance increases there is a flow of electrons into the antibonding  $\pi$  orbitals. Thus, the change of N-N distance is associated with a change in electron density over the M-N-N entity. Hence there is a large variation of dipole moment and therefore of intensities of both the N-N stretching vibration and the M-N<sub>2</sub> stretch. An effect which weakens the N-N bond strengthens

the M-N<sub>2</sub> bond. Anions which assist the movement of electrons into the  $\pi$  antibonding orbitals (i.e. the most polarisable anions) will show the highest intensity variations.

Similar arguments apply to the nitrous oxide complexes. It was found that the pentaammine nitrous oxide complexes have a variation of both  $\nu_3$  and  $\nu_1$  in the order:  $\text{PF}_6^- > \text{BF}_4^- > \text{I}^- > \text{Br}^-$  and  $\text{PF}_6^- < \text{BF}_4^- < \text{I}^- < \text{Br}^-$  respectively.<sup>1</sup> The  $\pi$  antibonding orbital is located on the O-N bond mainly, and back-bonding will increase the electron distribution in this orbital. Consequently the O-N bond is weakened and the N-N and Ru-O bonds are strengthened. The increase in charge on this bond increases its dipole moment and so the intensity of the vibration. Further, the N-N bond will be only slightly affected so its intensity will not alter as dramatically. The effect is such that the two intensities are oppositely affected. The smallest anion is more able to approach the central cation and will thus affect the back-bonding process the most. Hence,  $\text{BF}_4^-$  has a larger effect than  $\text{PF}_6^-$  on the intensities of the observed vibrations.

The position of the  $\nu_3$  and  $\nu_1$  absorption maxima are also dependent on the anion. Similar behaviour is observed for  $[\text{RuA}_5\text{N}_2\text{O}]\text{Z}_2$  and  $[\text{RuA}_5\text{XY}]\text{Z}_2$  ( $\text{XY} = \text{N}_2, \text{CO}$ ;  $\text{Z} = \text{monovalent anion}$ ).<sup>1,17,18,19</sup> Thus it was found<sup>17,18</sup> that  $\nu_{\text{XY}}$  moves to higher frequencies with the size of  $\text{Z}$ , i.e.  $\text{PF}_6^- > \text{BF}_4^- > \text{I}^- > \text{Br}^- > \text{Cl}^-$ . The explanation advanced by Chatt<sup>17,18</sup> was, that electrostatic interactions between the anion and the ammine groups polarise the coordinated ammonia with consequent

electron release to the ruthenium atom and then into the  $\pi$  anti-bonding orbitals of XY, so lowering  $\nu_{XY}$ , this lowering being greatest with the smallest anion. Sparrow also considered this effect to be operative in the  $[\text{RuA}_5\text{N}_2\text{O}]\text{Z}_2$  complexes.<sup>1</sup> Such an effect would be present in  $[\text{RuA}_4\text{OH}_2(\text{N}_2\text{O})]\text{X}_2$  complexes, hence the different positions of the absorption maxima.

Positions of ammonia absorptions in the infrared spectra of complexes have been shown to vary with the oxidation state of the metal.<sup>11b,21</sup> The most sensitive vibrations are the symmetric deformation and the rocking frequencies with the higher oxidation state exhibiting higher deformation and rocking frequencies. This relationship has been observed for hexaammine<sup>21</sup> and certain nitrile<sup>22,23</sup> complexes of ruthenium(II) and (III). The dinitrogen complexes  $[\text{RuA}_5\text{N}_2]\text{X}_2$  and the nitrous oxide complexes  $[\text{RuA}_5\text{N}_2\text{O}]\text{X}_2$  show ammonia absorption bands at frequencies similar to those observed for ruthenium(III) ammine complexes.<sup>24,1</sup> In these cases the back-donation of electrons into the  $\pi$  antibonding orbitals of the ligand increases the electronegativity of the metal toward the ammonia ligands. This is reflected in higher metal ammonia stretching frequencies than those complexes where there is no  $\pi$ -acceptor ligand. Table 4.8 lists the ammonia vibrations of some ruthenium complexes, along with those observed for the tetraammine.

The position of the ammonia vibrations in the tetraammine complexes are similar to those observed for ruthenium(III) complexes

indicating substantial back-bonding. Further, the positions of the N-H vibrations, which occur at higher frequencies for ruthenium(II) than ruthenium(III) complexes,<sup>21</sup> are also indicative of a ruthenium(III) complex. Thus, the significant amount of back-bonding from the metal to the nitrous oxide ligand, as indicated by the infrared spectra, probably account for the stability of these types of complexes.

Evidence for the presence of water in the complexes was also observed in the infrared spectra. Two types of water should be present in the complexes, viz. lattice and coordinated water. Absorptions near  $3550\text{ cm}^{-1}$  and  $3620\text{ cm}^{-1}$  as well as a shoulder at  $1700\text{ cm}^{-1}$  have been assigned to lattice water in both complexes. These values are in agreement with the lattice water vibrations found for the pentaammine nitrous oxide salts<sup>1</sup> and for a series of ruthenium(III) ethylenediamine complexes.<sup>7</sup>

Peaks for coordinated water have been observed at  $1030\text{ cm}^{-1}$ ,  $600\text{ cm}^{-1}$  in addition to the peaks observed for lattice water.<sup>1</sup> These vibrations were weak. Some very weak absorptions were found in these regions but due to their intensity and also interference from the anion absorptions, it is difficult to assign them to coordinated water with any certainty. A weak peak at  $1330\text{ cm}^{-1}$  was present in both tetraammine salts but was not present in the pentaammine complexes. This peak may be due to the presence of water in the complexes.

#### 4.3.5 Electronic Absorption Spectrum

Generally, absorptions in the electronic spectra of transition metal complexes arise due to d-d transitions and to charge transfer transitions.<sup>25</sup> The d-d transitions are strictly forbidden by the selection rules for the free ion but often become weakly allowed for the complex. The intensity of such a band is therefore very weak (molar absorptivity  $\sim 100$ ). On the other hand, the charge transfer transitions are fully spin allowed, and result from the transfer of electrons from metal to ligand, ligand to metal or transitions within the ligand molecular orbitals. The intensity of these types of transitions is very high (molar absorptivity  $\sim 10^4$ - $10^5$ ).<sup>25</sup>

The electronic configuration of ruthenium(II), cobalt(III) and rhodium(III) is  $d^6$  and the complexes of these ions are generally octahedral and diamagnetic. In strong ligand fields such complexes have a  $^1A_{1g}$  ground state and two absorption bands corresponding to transitions from the ground state to the  $^1T_{1g}$  and  $^1T_{2g}$  excited states are observed. As the symmetry of the complexes is lowered the degeneracy of the triplet states is removed and more transitions are possible. Table 4.9 lists the observed maxima and the band assignments for some representative  $d^6$  complexes. From the table the band at shorter wavelengths is assigned to the  $^1A_{1g} \rightarrow ^1T_{2g}$  transition and the one at longer wavelengths to the  $^1A_{1g} \rightarrow ^1T_{1g}$  transition. The molar absorptivities are small as anticipated for such d-d transitions.

The complex  $[\text{RuA}_5\text{CO}]^{2+}$  has the two absorptions shown in Table 4.9. The intensity of the second maximum appears to be too weak for a  $d\pi \rightarrow \pi^*$  (CO) charge transfer as previously assigned.<sup>26</sup> This is especially true when compared with the other ruthenium amines which have comparable intensities but have been assigned<sup>27</sup> as  $^1\text{A}_{1g} \rightarrow ^1\text{T}_{2g}$  transition. It is suggested that the strong absorption near 220 nm of the dinitrogen complexes and near 240 nm of the nitrous oxide complexes should also be assigned to metal to ligand ( $\pi^*$ ) transitions.<sup>1,28</sup>

The tetraammine nitrous oxide complex has a strong absorption at 230 nm with a molar absorptivity of  $6.40 \times 10^3 \text{ M}^{-1} \text{ cm}^{-1}$ . This value was calculated by dissolving the hexafluorophosphate salt in 1M hydrochloric acid and the absorbance at 230 nm was measured after 40 and 90 seconds respectively. The solutions were allowed to oxidise to  $[\text{RuA}_4\text{Cl}_2]^+$  and the final absorbance of this ion was used to calculate the initial concentration of the nitrous oxide complex. The half-time for decomposition of the complex is 35 sec (see below) and this value was used to estimate the molar absorptivity. The value obtained is lower than that observed for the pentaammine ( $\lambda_{\text{max}} 238 \text{ nm} \in 1.2 \times 10^4 \text{ M}^{-1} \text{ cm}^{-1}$ )<sup>1</sup> a decrease which is observed for  $[\text{RuA}_5\text{N}_2]^{2+}$  ( $\lambda_{\text{max}} 221 \text{ nm} \in 1.8 \times 10^4 \text{ M}^{-1} \text{ cm}^{-1}$ )<sup>29</sup> and  $[\text{RuA}_4(\text{OH}_2)\text{N}_2]^{2+}$  ( $\lambda_{\text{max}} 220 \text{ nm} \in 1.4 \times 10^4 \text{ M}^{-1} \text{ cm}^{-1}$ ).<sup>4</sup> Clearly, the position and intensity suggests that it is a metal to ligand ( $\pi^*$ ) transition. No bands attributable to the d-d transitions were observed,

probably because the solutions were too weak.

#### 4.3.6 Rate of Decomposition of *cis*-[RuA<sub>4</sub>(OH<sub>2</sub>)N<sub>2</sub>O](BF<sub>4</sub>)<sub>2</sub>·2H<sub>2</sub>O

The rate of decomposition of the complex was studied by following the decrease in absorbance at 230 nm in 0.1M hydrochloric acid as solvent. The temperature was maintained with a water bath. From the rates obtained, a value of the enthalpy and entropy of activation was calculated. Table 4.10 lists the rate constants at various temperatures.

A value of 96.2 kJ mole<sup>-1</sup> was calculated for the enthalpy of activation for [RuA<sub>5</sub>N<sub>2</sub>O]<sup>2+</sup> decomposition.<sup>1</sup> Values for the activation enthalpy for the loss of nitrogen from [RuA<sub>5</sub>N<sub>2</sub>]<sup>2+</sup> and [RuN<sub>2</sub>Cl<sub>2</sub>(H<sub>2</sub>O)(THF)] have been reported as 117 kJ mole<sup>-1</sup><sup>29</sup> and 96 kJ mole<sup>-1</sup><sup>30</sup> respectively. The value calculated for the tetraammine was 76.7 ± 1.5 kJ mole<sup>-1</sup>. The similarity of the values obtained indicates that the metal ligand bond strengths are similar for all four complexes, if it is assumed that breaking of the metal-ligand bond is a determining factor in the substitution reaction. Then as the nitrous oxide bonds through its oxygen atom, the Ru-O- and Ru-N- have about equal bond strengths.

The values of  $\Delta S^\ddagger$  determined for the pentaammine (-45 J K<sup>-1</sup> mole<sup>-1</sup>) and the tetraammine (-21.8 ± 5 J K<sup>-1</sup> mole<sup>-1</sup>) at 298°K are both negative and large. These values, along with the high values of  $\Delta H^\ddagger$ , indicate that a dissociative mechanism is operative. Put another



way, bond breaking is more important than bond making in the transition state. For the tetraammine, retention of the cis configuration is observed as the final product of the reaction is  $\text{cis}[\text{RuA}_4\text{Cl}_2]^+$ . Thus the five-coordinate intermediate retains a tetragonal pyramidal arrangement.<sup>31</sup> The tetraammine complex has a half-time of decomposition in solution only slightly different to that of the pentaammine nitrous oxide complex (35 sec cf 38 sec).

#### 4.3.7 Powder Pattern of $[\text{RuA}_4(\text{OH}_2)\text{N}_2\text{O}](\text{PF}_6)_2 \cdot \text{H}_2\text{O}$

For the salts  $[\text{RuA}_5\text{N}_2\text{O}]\text{X}_2$  ( $\text{X} = \text{Br}^-$ ,  $\text{I}^-$ ,  $\text{BF}_4^-$  and  $\text{PF}_6^-$ ), a study of the powder patterns indicated a face centred cubic structure with the cell constants listed in Table 3.1. These values are similar to those observed for the isostructural salts  $[\text{RuA}_5\text{N}_2]\text{X}_2$ .<sup>32</sup> On this basis it was concluded that the ruthenium to nitrous oxide linkage was substantially linear (see section 3.2).

The powder pattern of the tetraammine hexafluorophosphate salt was obtained in the same way as the pentaammine salts. In this case the pattern could also be indexed for a face centred cubic structure with a cell constant of  $11.9 \text{ \AA}$ . This value is the same (within experimental error) as the value of  $11.85 \text{ \AA}$  and  $11.79 \text{ \AA}$  observed for  $[\text{RuA}_5\text{N}_2\text{O}](\text{PF}_6)_2 \cdot \text{H}_2\text{O}$  and  $[\text{RuA}_5\text{N}_2](\text{PF}_6)_2$ <sup>32</sup> respectively. The structure of all three salts is thus the same, with a substantially linear metal to ligand bond. This result is not entirely unexpected as both water and ammonia occupy nearly the same volume in a molecule

(Van der Waal's volume 13 and 14 cc mole<sup>-1</sup> respectively<sup>33</sup>). Thus the replacement of an ammonia ligand by water would not be expected to cause a major structural rearrangement.

Because of the instability of the complex, single crystals could not be obtained so precluding a detailed X-ray structural examination. However, the similarity of the powder pattern obtained with that of  $[\text{RuA}_5\text{N}_2](\text{PF}_6)_2$  is good evidence that the two species are isostructural.

#### 4.4 Summary

When solutions  $\text{cis-}[\text{Ru}(\text{en})_2(\text{OH}_2)_2]^{2+}$  were exposed to high pressures of nitrous oxide, a species with an absorption maximum at 236 nm was formed. It rapidly decayed and its instability did not allow isolation.

Complexes of the composition  $[\text{RuA}_4(\text{OH}_2)\text{N}_2\text{O}]\text{X}_2$  ( $\text{X} = \text{BF}_4^-$ ,  $\text{PF}_6^-$ ) were formed when solutions of  $\text{cis-}[\text{RuA}_4(\text{OH}_2)_2]^{2+}$  were exposed to 30-40 atmospheres of nitrous oxide. Their infrared spectra were typical of those observed for other ruthenium ammine nitrous oxide complexes. An investigation of the properties of the two complexes led to the formulation given above, and a X-ray powder pattern established a face centred cubic structure with a substantially linear metal to nitrous oxide bond. The rapid decomposition of the complex in solution ( $t_{1/2} \approx 35$  sec) did not allow any single crystals to be grown for detailed structural analysis. A decomposition rate

122.

of  $1.66 \times 10^{-2} \text{ sec}^{-1}$  at  $25^{\circ}\text{C}$ ,  $\Delta H^{\ddagger} = 76.7 \text{ kJ mole}^{-1}$ ,  $\Delta S^{\ddagger} = -21.8$   
 $\text{J K}^{-1} \text{ mole}^{-1}$  indicated a dissociative tetragonal pyramidal transition  
state in the decomposition mechanism.

TABLE 4.1

*The Effect of Temperature on the Reaction Between  
 $\text{cis-}[\text{Ru}(\text{en})_2(\text{OH}_2)_2]^{2+}$  and Nitrous Oxide*

Temperature $^{\circ}\text{C}$	$k_{\text{obs}} \times 10^3 \text{ sec}^{-1}\dagger$	$k \times 10^2 \text{ M}^{-1} \text{ sec}^{-1}$
24.9	$3.39 \pm 0.03$	$11.64 \pm 1.12$
30.0	$3.11 \pm 0.06$	$15.02 \pm 0.72$
35.8	$3.54 \pm 0.07$	$21.10 \pm 1.48$
35.9	$3.16 \pm 0.03$	$18.71 \pm 1.31$
40.4	$2.65 \pm 0.02$	$25.39 \pm 1.47$

$\dagger k_{\text{obs}} = k \times [\text{N}_2\text{O}]$ .

The concentration of nitrous oxide in solution was determined using the value of Henry's Law constant as obtained from ref. 34.

TABLE 4.2

*Solution Properties of cis-[RuA<sub>4</sub>(OH<sub>2</sub>)N<sub>2</sub>O]X<sub>2</sub>*All molar absorptivities expressed as M<sup>-1</sup> cm<sup>-1</sup>.*(i) Conversion to cis-[RuA<sub>4</sub>Cl<sub>2</sub>]<sup>+</sup>.*

The molar absorptivities were measured at the wavelengths (nm) indicated after oxidation in 1M HCl.

	Experimental		Literature <sup>38</sup>		Diagno <sup>a</sup>
X = BF <sub>4</sub> <sup>-</sup> .2H <sub>2</sub> O.					
ε <sub>314</sub>	1.39 ± 0.03 × 10 <sup>3</sup>	} average of two determ'ns	1.38 × 10 <sup>3</sup>		1.30 × 10 <sup>3</sup>
ε <sub>352</sub>	1.34 ± 0.09 × 10 <sup>3</sup>		1.64 × 10 <sup>3</sup>		1.40 × 10 <sup>3</sup>
ε <sub>262</sub>	0.55 ± 0.03 × 10 <sup>3</sup>		0.52 × 10 <sup>3</sup>		0.67 × 10 <sup>3</sup>
X = PF <sub>6</sub> <sup>-</sup> .H <sub>2</sub> O.					
ε <sub>314</sub>	1.42 ± 0.01 × 10 <sup>3</sup>	} average of three determ'ns	1.38 × 10 <sup>3</sup>		1.30 × 10 <sup>3</sup>
ε <sub>352</sub>	1.38 ± 0.04 × 10 <sup>3</sup>		1.64 × 10 <sup>3</sup>		1.40 × 10 <sup>3</sup>
ε <sub>262</sub>	0.50 ± 0.04 × 10 <sup>3</sup>		0.52 × 10 <sup>3</sup>		0.67 × 10 <sup>3</sup>

*(ii) Conversion to [RuA<sub>4</sub>(OH<sub>2</sub>)<sub>2</sub>]<sup>2+</sup>.*

The molar absorptivity was measured at 257 nm in 0.1M methane sulphonic acid which was flushed with argon.

X	Experimental	Literature <sup>39</sup>	Diagno <sup>b</sup>
BF <sub>4</sub> <sup>-</sup> ·2H <sub>2</sub> O	4.80 ± 0.02 × 10 <sup>2c</sup>	4.70 × 10 <sup>2</sup>	5.02 ± 0.10 × 10 <sup>2c</sup>
PF <sub>6</sub> <sup>-</sup> ·H <sub>2</sub> O	5.24 ± 0.14 × 10 <sup>2c</sup>	4.70 × 10 <sup>2</sup>	5.02 ± 0.10 × 10 <sup>2c</sup>

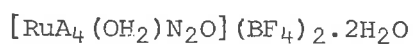
<sup>a</sup> Values observed when [RuA<sub>4</sub>(OH<sub>2</sub>)<sub>2</sub>]<sup>2+</sup> was oxidised in 1M HCl for 30 min

<sup>b</sup> Determined by reduction of cis-[RuA<sub>4</sub>Cl<sub>2</sub>]<sup>+</sup> with zinc amalgam in 0.1M methane sulphonic acid.

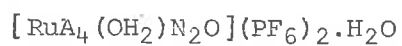
<sup>c</sup> Average of two determinations.

TABLE 4.3

*Microanalytical Results Obtained for the Nitrous Oxide  
Complexes*



	% N	% H	% F
Calculated:	19.06	4.12	34.48
Found:	18.63	4.09	35.20



	% N	% H	% F	% Ru
Calculated:	15.59	2.99	42.28	18.75
Found:	16.56	2.89	37.6	- brown sample
	14.9	2.57	39.6	- yellow sample
	-	-	-	21.5
	-	-	-	23.6

TABLE 4.4

Release of Gases from *cis*-[RuA<sub>4</sub>(OH<sub>2</sub>)N<sub>2</sub>O](BF<sub>4</sub>)<sub>2</sub>·2H<sub>2</sub>O<sup>†</sup>

Wt. of Solid Used (mgm)	Total Vol. N <sub>2</sub> + N <sub>2</sub> O		Volume of N <sub>2</sub> O		Volume of N <sub>2</sub>		Calculated* Volume ml
	ml	%	ml	%	ml	%	
4.29	0.20 <sub>0</sub>	91.7	0.16	76.6	0.03	15.1	0.21 <sub>8</sub>
7.72	0.33 <sub>5</sub>	85.5	0.29 <sub>2</sub>	74.5	0.04 <sub>3</sub>	10.9	0.39 <sub>2</sub>
11.93	0.58 <sub>4</sub>	96.4	0.50 <sub>2</sub>	82.8	0.08 <sub>2</sub>	13.5	0.60 <sub>6</sub>
14.21	0.66 <sub>4</sub>	92.0	0.56 <sub>5</sub>	78.3	0.09 <sub>9</sub>	13.7	0.72 <sub>2</sub>

<sup>†</sup> Oxidising agent used was 0.01M cerium(IV) sulphate.

\* Based on one mole of gas evolved for each mole of complex.

TABLE 4.5

*Infrared Absorptions of Nitrous Oxide Adsorbed onto Surfaces*All absorptions expressed as  $\text{cm}^{-1}$ .

Surface	$\nu_3$	$\nu_1$	$\nu_2$	Reference
NaCl	2240	1252	582	12
	2225	1265	571	
	2193 ( $\text{N}^{14}\text{N}^{15}\text{O}$ )			
NaBr	2235	1247	579	12
	2222	1261	567	
		1274		
NaI	2250	1248	582	12
	2232	1257	578	
		1272	568	
CsCl	2235	1288	582	13
		1272	575	
CsBr	2241	1284	580	13
	2233	1263		
CsI	2238	1287	576	13
	2227	1275	570	
		1260		
$\alpha$ -Chromia	2238	1237		I <sup>a</sup>
	2305	1339		14 II <sup>a</sup>

- <sup>a</sup> I: Postulated oxygen bonding.  
 II: Postulated nitrogen bonding.



TABLE 4.6

*Infrared Spectra of cis-[RuA<sub>4</sub>(OH<sub>2</sub>)N<sub>2</sub>O]X<sub>2</sub>.nH<sub>2</sub>O*All absorptions expressed as cm<sup>-1</sup>.

X = BF <sub>4</sub> <sup>-</sup> , n = 2	X = PF <sub>6</sub> <sup>-</sup> , n = 1	Assignment
3610 s	3620 s	ν <sub>OH</sub>
3540 s	3560 s	
3375 s	3380 s	ν <sub>NH</sub>
3300 s	3300 s	
2275 m	2284 m	ν <sub>3</sub> N <sub>2</sub> O
	2224 m	
1700 sh	1700 sh	δOH <sub>2</sub>
1630 m	1635 m	δNH <sub>3</sub> asym.
1300 m	1300 m	δNH <sub>3</sub> sym.
1220 s	1235 s	ν <sub>1</sub> N <sub>2</sub> O
1050 s,br	850 s	ν <sub>3</sub> BF <sub>4</sub> <sup>-</sup> PF <sub>6</sub> <sup>-</sup>
530 w	570 w,sh	ν <sub>4</sub> BF <sub>4</sub> <sup>-</sup> , PF <sub>6</sub> <sup>-</sup>
780 <sup>a</sup> m	765 <sup>a</sup> w,sh	ρNH <sub>3</sub>
1335 w	1330 w	
840 w	1090 w	
	515 w,br	

<sup>a</sup> Identified as shoulders partly obscured by the anion.

TABLE 4.7

*Energy Levels of Molecular Orbitals of Some Molecules*<sup>16,37</sup>

N <sub>2</sub>		N <sub>2</sub> O		CO	
Orbital	Energy	Orbital	Energy	Orbital	Energy
1 $\pi_g$	-7.0	3 $\pi$	-7.4	2 $\pi$	-6
3 $\sigma_g$	-15.6	2 $\pi$	-12.89	5 $\sigma$	-14.0
1 $\pi_u$	-17.1	7 $\sigma$	-16.38	1 $\pi$	-16.6
2 $\sigma_u$	-18.7	6 $\sigma$	-17.65	4 $\sigma$	-19.7
2 $\sigma_g$	-35.5	1 $\pi$	-20.11	3 $\sigma$	-43.4

All energies in electron volts.

TABLE 4.8

*Ammonia Vibrations of Selected Ruthenium Ammines*All absorptions expressed as  $\text{cm}^{-1}$ .

Complex	$\delta\text{NH}_3$ asym.	$\delta\text{NH}_3$ sym.	$\rho\text{NH}_3$
$[\text{RuA}_5\text{N}_2\text{O}](\text{BF}_4)_2$ <sup>1</sup>	1630	1295	760
$[\text{RuA}_5\text{N}_2](\text{BF}_4)_2$ <sup>24</sup>	1630	1297	768
$[\text{RuA}_4(\text{OH}_2)\text{N}_2\text{O}](\text{BF}_4)_2$	1630	1300	780
$[\text{RuA}_6](\text{BF}_4)_3$ <sup>21</sup>	1629	1353, 1293	774
$[\text{RuA}_6](\text{BF}_4)_2$ <sup>21</sup>	1628	1273	741
$[\text{RuA}_5\text{N}_2\text{O}](\text{PF}_6)_2$ <sup>1</sup>	1627	1296	770
$[\text{RuA}_5\text{N}_2](\text{PF}_6)_2$ <sup>24</sup>	1634	1298	770
$[\text{RuA}_4(\text{OH}_2)\text{N}_2\text{O}](\text{PF}_6)_2$	1635	1300	765

TABLE 4.9

*Electronic Spectra of Low Spin  $d^6$  Octahedral Metal Complexes*

Complex	$\lambda_{\text{max}}$ nm	$\epsilon_{\text{max}}$ $\text{M}^{-1} \text{cm}^{-1}$	Assignment	Ref.
$[\text{CoA}_6]^{3+}$	476	55.3	$^1\text{A}_{1g} \rightarrow ^1\text{T}_{1g}$	35
	339	46.2	$^1\text{A}_{1g} \rightarrow ^1\text{T}_{2g}$	
$[\text{CoA}_5(\text{OH}_2)]^{3+}$	485	48.3	$^1\text{A}_{1g} \rightarrow ^1\text{T}_{1g}$	35
	340	46.2	$^1\text{A}_{1g} \rightarrow ^1\text{T}_{2g}$	
$[\text{RhA}_6]^{3+}$	305	134	$^1\text{A}_{1g} \rightarrow ^1\text{T}_{1g}$	35, 36
	255	101	$^1\text{A}_{1g} \rightarrow ^1\text{T}_{2g}$	
$[\text{RuA}_6]^{2+}$	320	100	$^1\text{A}_{1g} \rightarrow ^1\text{T}_{1g}$	27
	275	475	$^1\text{A}_{1g} \rightarrow ^1\text{T}_{2g}$	
$[\text{Ru}(\text{en})_3]^{2+}$	310	360	$^1\text{A}_{1g} \rightarrow ^1\text{T}_{1g}$	27
$[\text{RuA}_5\text{CO}]^{2+}$	360	17.0	$^1\text{A}_{1g} \rightarrow ^1\text{T}_{1g}$	26
	277	258	$d\pi \rightarrow \pi^* (\text{CO})$	
$[\text{RuA}_5\text{N}_2]^{2+}$	221	$1.8 \times 10^4$	$\text{metal} \rightarrow \pi^*$	28
$[\text{RuA}_5\text{N}_2\text{O}]^{2+}$	238	$1.2 \times 10^4$	$\text{metal} \rightarrow \pi^*$	1

TABLE 4.10

*Rate Data for the Decomposition of  $[\text{RuA}_4(\text{OH}_2)\text{N}_2\text{O}](\text{BF}_4)_2 \cdot 2\text{H}_2\text{O}$*

Temperature °C	$k_{\text{obs}}$ ( $\text{sec}^{-1}$ )
20.5	$(0.85 \pm 0.04) \times 10^{-2}$
24.4	$(1.66 \pm 0.06) \times 10^{-2}$
24.3	$(1.60 \pm 0.07) \times 10^{-2}$
29.3	$(2.43 \pm 0.11) \times 10^{-2}$
29.4	$(2.54 \pm 0.11) \times 10^{-2}$

## CHAPTER 4

## REFERENCES

1. G.J. Sparrow, Ph.D. Thesis, University of Adelaide, 1972;  
A.A. Diamantis and G.J. Sparrow, J. Chem. Soc. (Dalton),  
in the press.
  2. J.C. Bellen, Honours Report, University of Adelaide, 1970.
  3. E. Zotti, Honours Report, University of Adelaide, 1971.
  4. L.A.P. Kane-Maguire, J. Inorg. Nucl. Chem., 1971, 33, 3963.
  5. J.N. Armor and H. Taube, J. Amer. Chem. Soc., 1969, 91, 6874.
  6. L.A.P. Kane-Maguire, P.S. Sheridan, F. Basolo and R.G. Pearson,  
J. Amer. Chem. Soc., 1968, 90, 5295.
  7. J.A. Broomhead and L.A.P. Kane-Maguire, J. Chem. Soc. (A),  
1967, 546.
  8. J.A. Broomhead, private communication to L. Kane-Maguire  
quoted in ref. 4.
  9. D.E. Harrison and H. Taube, J. Amer. Chem. Soc., 1967, 89, 5706.
  10. D.E. Harrison, E. Weissberger and H. Taube, Science, 1968,  
159, 320.
  11. K. Nakamoto, "Infrared Spectra of Inorganic and Coordination  
Compounds", Wiley, New York, 1963, (a) p. 79, (b) p. 149.
  12. Y. Kozirovski and M. Folman, Trans. Farad. Soc., 1969, 65, 244.
  13. Y. Kozirovski and M. Folman, Israel J. Chem., 1969, 7, 595.
  14. E. Borello, L. Cerruti, G. Ghiotti and E. Guglielminotti,  
Inorg. Chim. Acta, 1972, 6, 45.
-

15. J. Chatt, Proc. Roy. Soc. B., 1969, 172, 327.
  16. J.W. Rabalias, J.M. McDonald, V. Scherr and S.P. McGlynn, Chem. Rev., 1971, 71, 73.
  17. J. Chatt, G.J. Leigh and N. Thankarajan, J. Organometal. Chem., 1970, 25, C77.
  18. J. Chatt, G.J. Leigh and N. Thankarajan, J. Chem. Soc. (A), 1971, 3168.
  19. Yu. G. Borod'ko, S.M. Vinogradova, Yu. P. Myagkov and D.D. Mozzhukin, Zhur. strukt. Khim., 1970, 11, 269.
  20. B. Folkesson, Acta Chem. Scand., 1972, 26, 4008.
  21. A.D. Allen and C.V. Senoff, Can. J. Chem., 1967, 45, 1337.
  22. R.E. Clarke and P.C. Ford, Inorg. Chem., 1970, 9, 227.
  23. R.E. Clarke, R.D. Foust and P.C. Ford, Inorg. Chem., 1970, 9, 1933.
  24. A.D. Allen, F. Bottomley, R.O. Harris, V.P. Reinslau and C.V. Senoff, J. Amer. Chem. Soc., 1967, 89, 5595.
  25. L.E. Orgel, "An Introduction to Transition Metal Chemistry: Ligand Field Theory", Methuen, London, 1966, Chapter 6.
  26. J.A. Stanko and T.W. Starinshak, Inorg. Chem., 1969, 8, 2156.
  27. H.H. Schmidtke and D. Garthoff, Helv. Chim. Acta, 1966, 49, 2039.
  28. J.E. Fergusson and J.L. Love, Rev. Pure and Appl. Chem. (Aust.), 1970, 20, 33.
  29. J.N. Armor and H. Taube, J. Amer. Chem. Soc., 1970, 92, 6170.
  30. A.E. Shilova and A.E. Shilov, Kinetika i. Kataliz, 1969, 10, 267.
-

31. M.L. Tobe, "Inorganic Reaction Mechanisms", Nelson, London, 1972, p. 103.
32. F. Bottomley and S.C. Nyburg, *Acta Crystallogr.*, 1968, B24, 1289.
33. A. Bondi, *J. Phys. Chem.*, (1964), 68, 441.
34. "International Critical Tables", Vol. III, McGraw-Hill Book Co. Inc., New York, 1928, p. 269.
35. C.K. Jørgensen, "Absorption Spectra and Chemical Bonding in Complexes", Pergamon Press Ltd., London, 1962, p. 293.
36. H.H. Schmidtke, *Z. Phys. Chem. (Frankfurt)*, 1964, 40, 96.
37. R.S. Mulliken, *Can. J. Chem.*, 1958, 36, 10.
38. H. Hartmann and C. Buschbeck, *Z. Phys. Chem. (Frankfurt)*, 1957, 11, 120.
39. C.M. Elson, J. Gulens and J.A. Page, *Can. J. Chem.*, 1971, 49, 207.
40. C.R. Brundle and D.W. Turner, *Internat. J. Mass Spectrometry Ion Phys.*, 1969, 2, 195.



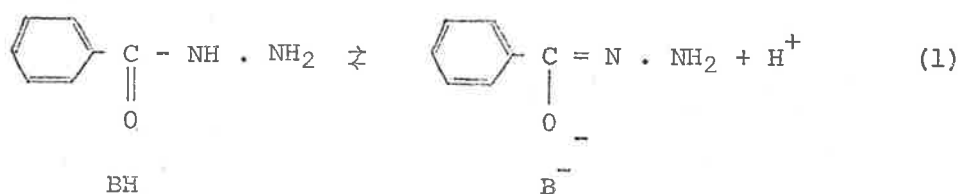
## CHAPTER 5

## REACTION OF BENZOYLHYDRAZINE AND CHLOROPENTAAMMINE RUTHENIUM(III)

## CHLORIDE

## 5.1 Introduction

The ligand N-benzoylhydrazine (BH), is well known for its ability to coordinate to transition metals.<sup>1,3,13</sup> The possibility of keto-enol tautomerism exists for the ligand and is represented in equation (1).



Some evidence for this process has been obtained by a study of the ultraviolet spectrum of the ligand at various pH's.<sup>2</sup> Thus both cationic and neutral complexes of transition metals should be formed, given the correct conditions. In fact complexes of the type  $\text{CoB}_3$  and  $\text{Co}(\text{BH})_3\text{SO}_4 \cdot 2\text{H}_2\text{O}$  have been isolated.<sup>3</sup>

Hydrazine,<sup>4</sup> monoarylhydrazine<sup>5</sup> and benzoylhydrazine<sup>6,7</sup> have been used in the preparation of dinitrogen complexes. The dinitrogen complex  $[\text{RuA}_5\text{N}_2]^{2+}$  was formed from ruthenium trichloride and hydrazine,<sup>4,14</sup> via an intermediate hydrazino complex,  $[\text{RuA}_5(\text{N}_2\text{H}_4)]^{3+}$ . Phenylhydrazine, benzylhydrazine and  $\beta$ -naphthylhydrazine are known<sup>5</sup> to react with chloropentaammine ruthenium(III) in aqueous solution to form  $[\text{RuA}_5\text{N}_2]^{2+}$ . With phenylhydrazine, the other products of the reaction were identified as benzene, phenol and biphenyl.<sup>5</sup>

The rhenium(I) complex,  $\text{Re}(\text{PPh}_3)_2(\text{CO})_2\cdot\text{Cl}(\text{N}_2)$ , was formed<sup>6,7</sup> by the reaction of carbon monoxide in a methanol-benzene solvent, with the benzoylazo complex in figure 5.1. The oxidation state of the metal is formally (III) and so the metal is reduced when the benzoyl group is cleaved from the intermediate.

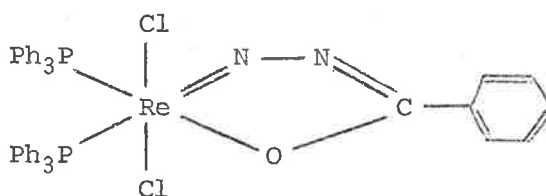


Figure 5.1: Benzoylazo complex of rhenium(III).

A similar benzoylazo complex or the monomer dinitrogen complex may be formed when chloropentaammine ruthenium(III) reacts with benzoylhydrazine in aqueous solution. As benzoylhydrazine is a chelating agent a tetraammine intermediate may be expected with  $\text{cis-}[\text{RuA}_4(\text{OH}_2)\text{N}_2]^{2+}$  produced on cleavage of the benzoyl group. Alternatively the benzoylhydrazine may act as a monodentate ligand producing  $[\text{RuA}_5\text{N}_2]^{2+}$  on cleavage of the benzoyl group.

## 5.2 The Reaction of Chloropentaammine Ruthenium(III) with

### *N*-benzoylhydrazine

Benzoylhydrazine reacted with the chloropentaammine in water to give an orange solution from which cationic complexes could be isolated by the addition of the appropriate anion. The complexes contained the correct amount of halide ion for the formula

$[\text{RuA}_5\text{BH}]\text{X}_3$  ( $\text{X} = \text{Br}^-, \text{I}^-$ ) (see section 6.6). Analyses for carbon and hydrogen were always low and nitrogen somewhat high, and this can be attributed to the instability of the complexes forming the monomer dinitrogen complex in the solid state. Boiling the complexes in concentrated hydrochloric acid gave a yellow precipitate identified from its ultraviolet spectrum as chloropentaammine ruthenium(III),  $[\text{RuA}_5\text{Cl}]^{2+}$  ( $\lambda_{\text{max}} 330 \text{ nm } \epsilon 1.81 \times 10^3 \text{ M}^{-1} \text{ cm}^{-1}$ ; lit.<sup>8</sup>  $\lambda_{\text{max}} 328 \text{ nm } \epsilon 2.00 \times 10^3 \text{ M}^{-1} \text{ cm}^{-1}$ ). On this basis the complexes were formulated with benzoylhydrazine as a monodentate neutral ligand  $[\text{RuA}_5\text{BH}]\text{X}_3$ .

The magnetic moment of the complex was determined at  $35^\circ\text{C}$  as 1.84 BM and this value is in the range observed for other ruthenium(III)  $d^5$  complexes,<sup>9</sup> and confirms the oxidation state of the metal.

### 5.3 Infrared Spectra of the Complexes

Benzoylhydrazine has two potential donor atoms in the terminal nitrogen atom or the carbonyl oxygen atom. Coordination through the N atom in the keto form should be detectable by the strong carbonyl stretching frequency in the infrared spectrum. Coordination through the O atom in the enol form gives rise to a C=N stretching frequency. Thus the infrared spectra of the complexes were examined in nujol mulls and are listed in Table 5.1.

Assignments of bands in the infrared spectrum of N-benzoylhydrazine have been reported<sup>10</sup> and are given in Table 5.2. Keto complexes of benzoylhydrazine show the amide I, II and III bands, displaced to lower

frequency because of coordination in their infrared spectra.<sup>11</sup> No amide bands are observed in the enol complexes but strong absorptions at  $\sim 1350 \text{ cm}^{-1}$  ( $\nu_{\text{C-O}}$ ) and  $\sim 1600 \text{ cm}^{-1}$  ( $\nu_{\text{C=N}}$ ) are observed.<sup>11</sup> In coordinated benzoylhydrazine Baker<sup>13</sup> has shown that bands occur in the range  $1620$  to  $1655 \text{ cm}^{-1}$  and are probably due to the amide I band. Because of the intensity of the absorption observed in the infrared spectra of the complexes near  $1630 \text{ cm}^{-1}$  and the splitting (see Table 5.1) it was apparent that the complexes contained the amide I band and therefore the keto form of the ligand. Moreover, it is not possible to decide from infrared spectra alone whether the keto ligand acts as a monodentate or bidentate group. Baker<sup>13</sup> points out that the range of absorptions overlap and the difficulty is compounded by the presence of the asymmetric ammonia vibrations, which are known<sup>12</sup> to occur at  $\sim 1630 \text{ cm}^{-1}$  for ruthenium(III) amines. However the evidence presented above and the isolation of the pentaammine dinitrogen salts from solutions of the complexes leaves no doubt that the benzoylhydrazine ligand acts as a monodentate.

Other bands in the infrared spectrum were assigned to the ligand vibrations, as given in Table 5.1, by comparison with the infrared spectrum of the free ligand and the infrared spectra of other ruthenium(III) ammine complexes.

#### 5.4 Electronic Absorption Spectrum

The electronic spectrum of  $[\text{RuA}_5(\text{BH})]^{3+}$  was recorded in water and

acid and the molar absorptivities calculated. A single absorption maximum was observed at 420 nm, which decreased in intensity on standing. A shoulder at 225 nm increased in intensity and a single isosbestic point was observed at 246 nm. The disappearance of the maximum at 420 nm was relatively slow in acid ( $t_{1/2} = 2-3$  hrs), and spectra were recorded as soon as possible after preparation of the solutions. In 0.01M sulphuric acid (pH ~2) the molar absorptivity was  $1.85 \times 10^4 \text{ M}^{-1} \text{ cm}^{-1}$ , and in water (pH ~4) the molar absorptivity was  $1.78 \times 10^4 \text{ M}^{-1} \text{ cm}^{-1}$ . The molar absorptivity of a preparation standing for two days at room temperature decreased to  $3.30 \times 10^3 \text{ M}^{-1} \text{ cm}^{-1}$ .

The absorption at 420 nm is of such an intensity that it is most likely associated with a charge transfer transition rather than a d-d transition. Benzoylhydrazine has a single absorption maximum at 230 nm ( $\epsilon > 10^4 \text{ M}^{-1} \text{ cm}^{-1}$ ) which probably arises due to  $\pi \rightarrow \pi^*$  transitions. An intense absorption is apparently present in the complexes beyond 200 nm, the limit of the instrument used. It is reasonable to suggest that this is largely ligand in character with the position and intensity perturbed by coordination. The other absorption (at 420 nm) arises due to a metal to ligand charge transfer.

### 5.5 Decomposition of $[\text{RuA}_5\text{BH}]\text{Br}_3$

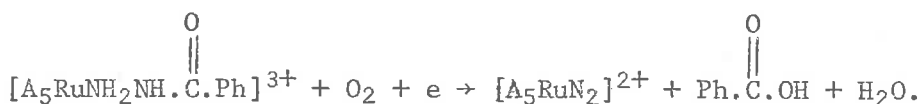
The decomposition of the complex was monitored by following the decrease in absorption of the peak at 420 nm. The product of the reaction was monomer dinitrogen complex identified by the appearance

of its absorption maximum in the ultraviolet (lit.<sup>14</sup>  $\lambda_{\text{max}}$  221 nm found 225 nm), and by the infrared spectrum of the product precipitated from solution with lithium bromide in ethanol (found  $\nu_{\text{N-N}}$  2120  $\text{cm}^{-1}$  lit.<sup>14</sup> 2114  $\text{cm}^{-1}$ ) and with tetrafluoroborate (found 2145  $\text{cm}^{-1}$  lit.<sup>14</sup> 2144  $\text{cm}^{-1}$ ).

The stoichiometry of the reaction was determined from the ultraviolet spectrum by determining the concentration of the benzoylhydrazine complex and the monomer from their absorbances at 420 nm and 221 nm respectively. A 1:1 relationship was obeyed over the first sixty to ninety minutes of reaction, for which the stoichiometry was investigated.

The decomposition reaction was investigated over the hydrogen ion concentration range 0.001-0.1M using a hydrochloric acid-lithium chloride medium to maintain ionic strength. The data in Table 5.3 show that the observed first order rate constant is independent of hydrogen ion concentration. Further, from the data the enthalpy of activation at 26°C was calculated as  $44.3 \pm 6.1 \text{ kJ mole}^{-1}$  and the entropy as  $-180 \pm 40 \text{ J mole}^{-1} \text{ deg}^{-1}$ . The value of  $\Delta H^\ddagger$  is similar to those observed for the hydrolysis of N-bonded cyanate coordinated to ruthenium ( $\Delta H^\ddagger \approx 48 \text{ kJ mole}^{-1}$ ).<sup>15</sup> It is also known that hydrazides are hydrolysed to hydrazine and the corresponding carboxylic acid.<sup>16</sup> In both hydrolyses the reaction involves the breaking of a nitrogen carbon bond.

The decomposition can be represented by the equation:



Oxygen is present in the system as no precautions were made to exclude it, and its concentration<sup>18</sup> at 25°C is  $\sim 1 \times 10^{-3}$  M, i.e. an excess of oxygen is present. The decomposition is comparable to the hydrolysis of amides under similar conditions, but with some alteration due to coordination. Thus, in  $10^{-3}$  M acid the rates of hydrolysis<sup>17</sup> of trifluoro- and trichloro-acetanilide are  $1.0 \times 10^{-8} \text{ sec}^{-1}$  and  $1.3 \times 10^{-9} \text{ sec}^{-1}$  compared with  $5.23 \times 10^{-5} \text{ sec}^{-1}$  for the complexed benzoylhydrazine. No definite proposals as to the mechanism of the reaction can be made as the effect of oxygen was not fully investigated, but the breaking of the carbon nitrogen bond would appear to be the rate determining step.

### 5.6 Summary

The reaction of benzoylhydrazine and chloropentaammine ruthenium(II) produces the monomer dinitrogen complex proceeding through a relatively stable intermediate which was isolated. The rate of decomposition of the intermediate measured in an acidic medium was  $5.23 \times 10^{-5} \text{ sec}^{-1}$  and the stoichiometry of the reaction indicated a one to one relationship of monomer dinitrogen complex and benzoylhydrazine complex.

TABLE 5.1

*Infrared Spectra of the Complexes  $[RuA_5(BH)]X_3$  ( $X = Br^-$ ,  $I^-$ ,  $BF_4^-$ ,  $PF_6^-$ )*

All frequencies expressed as  $cm^{-1}$ .

Assignment	$X = Br^-$	$I^-$	$BF_4^-$	$PF_6^-$
$\nu_{N-H}$	3280 } br 3140 }	3280 } 3200 } br 3180 }	3340 s 3280 s 3220 sh,w	3300 br
$\nu_{C=O}$ ?	1635 m }	1640 m }	1630-1645 br	1640 s
$\delta NH_3$ asym	1600 m }	1610 m }	-	-
$\delta NH_3$ sym	1300 s	1300 s	1360 m } 1305 s }	1340 m } 1300 s }
Amide III	1235 s	1250 s	1255 s	1250 s
$\delta C-H$	1170 m	1170 m	a	1170 m
	1040 s	1040 s	a	1045 s
$\delta C-H$	1020 s	1025 s	a	1025 s
$\nu_3 BF_4^-$			1060 br,s	
$\nu_3 PF_6^-$				850
$\rho NH_3$	770 w	780 s	780 s a	780 sh a
	725 s	730 sh	725 m	725 sh
$\pi C-H$	705 sh	705 m	705 m	705 w
$\pi C-H$	640 s	640 s	630 s	640 w
$\nu_4 BF_4^-$ , $PF_6^-$			530 s	565 s

br: broad

s: strong

w: weak

sh: shoulder

m: medium

a: area covered by anion



TABLE 5.2

*Infrared Spectrum of N-Benzoylhydrazine*<sup>10</sup>All frequencies expressed as  $\text{cm}^{-1}$ .

Assignment	Frequency	Assignment	Frequency
$\nu_{\text{NH}_2}$ or	3280 s	$\delta\text{C-H}$	1298 w
$\nu_{\text{N-H}}$	3180 s	Amide III	1250 w
	3010 s	$\delta\text{C-H}$	1183 w
	2070 w		1154 vw
Amide I	1664 s	$\omega\text{NH}_2$	1118 m
$\beta\text{NH}_2$	1618 s	$\delta\text{C-H}$	1024 vw
$\nu_{\text{C-C}}$	1608 sh	$\gamma\text{NH}_2$	990 m
$\nu_{\text{C-C}}$	1582 s		984 m
Amide II	1527 sh	$\pi\text{C-H}$	966 vw
			917 w
$\nu_{\text{C-C}}$	1492 w		863 m
$\nu_{\text{C-C}}$	1450 w		801 m
$\tau\text{NH}_2$	1349 s		747 w
	1320 w		690 s

 $\nu$ : stretch $\pi$ : out of plane deformation $\beta$ : bend $\tau$ : twist $\delta$ : in plane deformation $\omega$ : wag $\gamma$ : rocking

TABLE 5.3

*Observed First Order Rate Constants for Decomposition of  $[\text{RuA}_5\text{BH}]\text{Br}_3$*

$T^\circ \text{ K}$	$k_{\text{obs}} \times 10^5 \text{ sec}^{-1}$	$[\text{H}^+] \text{ M}$	$[\text{LiCl}] \text{ M}$
299	$5.23 \pm 0.58$	0.001	0.099
303	$7.56 \pm 0.75$	0.001	0.099
309	$9.55 \pm 0.81$	0.001	0.099
299	$4.96 \pm 0.41$	0.010	0.090
299	$5.03 \pm 0.50$	0.100	0

## CHAPTER 5

## REFERENCES

1. J.S. Aggarwal, N.L. Darbari and J.N. Ray, *J. Chem. Soc.*, 1929, 1941.
2. K. Nagano, H. Tsukahara, H. Konoshita and Z. Tamara, *Chem. Pharm. Bull.*, 1963, 11, 797.
3. J.F. Alcock, R.J. Baker and A.A. Diamantis, *Aust. J. Chem.*, 1972, 25, 289.
4. F. Bottomley, *Can. J. Chem.*, 1970, 48, 351.
5. V.B. Shur, I.A. Tikhonova, E.F. Isaeva and M.E. Vol'pin, *Isv. Akad. Nauk. S.S.S.R. Ser. Khimii*, 1971, 10, 2357.
6. J. Chatt, J.R. Dilworth and G.J. Leigh, *J. Organometal. Chem.*, 1970, 21, 49.
7. J. Chatt, J.R. Dilworth, G.J. Leigh and V.D. Gupta, *J. Chem. Soc.*, 1971, 2631.
8. H. Hartmann and C.K. Buschbeck, *Z. Phys. Chem. (Frankfurt)*, 1957, 11, 120.
9. F.A. Cotton and G. Wilkinson, "Advanced Inorganic Chemistry", Wiley and Sons, New York, Second Edition, 1966, p. 1000.
10. M. Mashima, *Bull. Chem. Soc. Japan*, 1963, 36, 210.
11. P.V. Gogorishvili, Yu. Ya. Kharitonov, M.V. Karkarashvili and R.I. Machkhoshvili, *Zh. Neorg. Khimii*, 1969, 14, 2891.
12. A.D. Allen and C.V. Senoff, *Can. J. Chem.*, 1967, 45, 1337.
13. R.J. Baker, Ph.D. Thesis, Univ. of Adel., October, 1966.

14. A.D. Allen, F. Bottomley, R.O. Harris, V.P. Reinslau and C.V. Senoff, J. Amer. Chem. Soc., 1967, 89, 5595.
15. P.C. Ford, Inorg. Chem., 1971, 10, 2153.
16. I.L. Finar, "Organic Chemistry, Volume I, The Fundamental Principles", Longmans, Green and Co., London, 1960, p. 195.
17. S.O. Eriksson and C. Holst, Acta Chem. Scand., 1966, 20, 1892.
18. "Handbook of Chemistry and Physics", Chemical Rubber Company, R.C. Weast, Editor, Cleveland, Ohio, 1969, pB-136.

## CHAPTER 6

## EXPERIMENTAL

## 6.1 Preparation of Compounds

6.1.1 Hexaammine ruthenium(III) trichloride was purchased from Johnson Matthey Company Limited and used as received.

## 6.1.2 Chloropentaammine Ruthenium(III) Chloride

[RuA<sub>5</sub>Cl]Cl<sub>2</sub> was prepared by the literature methods from RuCl<sub>3</sub><sup>1</sup> or ruthenium hexaammine.<sup>2</sup> It was recrystallised from 0.1M hydrochloric acid.

Found: Cl, 36.2<sub>1</sub>. H<sub>15</sub>Cl<sub>3</sub>N<sub>5</sub>Ru requires Cl, 36.3<sub>9</sub>.

Molar absorptivities of the preparations ranged from 1.82-1.92 × 10<sup>3</sup> M<sup>-1</sup> cm<sup>-1</sup> (lit.<sup>2</sup> 1.93 × 10<sup>3</sup> M<sup>-1</sup> cm<sup>-1</sup>).

## 6.1.3 Chlorohydroxotetraammine Ruthenium(III) Chloride

[RuA<sub>4</sub>(OH)Cl]Cl was purchased from Alfa Inorganics and used as received.

Found: Cl, 34.6<sub>0</sub>; H, 5.16; N, 22.6<sub>6</sub>; Ru, 34.5.

H<sub>13</sub>Cl<sub>2</sub>N<sub>4</sub>ORu requires Cl, 27.6<sub>0</sub>; H, 5.10; N, 21.8<sub>0</sub>; Ru, 39.31.

Following this unexpected result the complex obtained was examined in more detail. The electronic spectrum of the solid in water exhibited two peaks, 335 nm and 538 nm, as well as a shoulder at 226 nm. A solution of the compound in water was added to a Sephadex cation exchange resin and 0.1M HCl used to elute the complex. Initially,

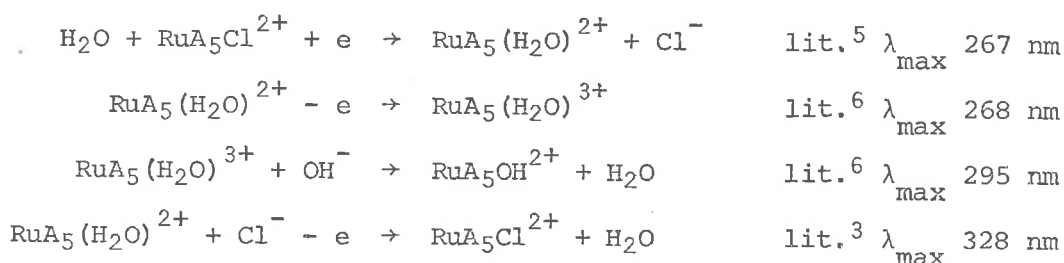
two bands were observed: a yellow band which moved first, and a red band which remained at the top of the column. The ultraviolet spectrum of the eluted yellow species had maxima at 273 nm and 332 nm. When the yellow species was completely eluted 1M HCl was used as eluant. With this eluant the red band began to move down the column revealing a third brown band at the top, which did not move when 5M HCl was used as eluant. The spectrum of the red species had a maximum at 345 nm and one at 540 nm.

The original compound was reducible using Pt black/H<sub>2</sub>, the pink colour changed to yellow when the reduction was complete. This procedure is expected to replace any chloro groups in the ruthenium(III) compound by aquo groups in the resulting ruthenium(II) ammine. Oxidation of the yellow species in air in the presence of chloride ion should regenerate the chloro complex, while in the absence of chloride the aquo complex of the next highest stable oxidation state would be obtained (e.g.  $\text{RuA}_5(\text{H}_2\text{O})^{2+} \rightarrow \text{RuA}_5\text{H}_2\text{O}^{3+}$ ). The spectra of the species obtained by the treatment described above were recorded. The spectrum of the yellow reduced species was recorded under argon and had a maximum at 264 nm. On standing in the air the maximum intensified and shifted to 267 nm. The same behaviour was observed when oxygen was bubbled through the reduced solution. Addition of one drop of caustic soda caused a shift of the maximum from 267 nm to 295 nm with an intensification of the absorbance. On standing in the air in 1M HCl, the maximum of the reduced species was shifted from 265 nm to

330 nm.

The infrared spectrum of the original complex was recorded in nujol and as a potassium bromide disc and the absorptions are listed in Table 6.1 along with those of  $[\text{Ru}(\text{NH}_3)_5\text{Cl}]\text{Cl}_2$  for comparison. For both compounds the absorptions are the same, except around  $3500\text{ cm}^{-1}$  where the chloropentaammine has only a very weak absorption, but the original compound has a strong absorption. This absorption persisted even when the compound was dried in vacuo over phosphorus pentoxide at room temperature for two days. The absorption probably arises from  $\nu_{\text{O-H}}$  of lattice water. Another absorption for lattice water should be observed between  $1630\text{--}1600\text{ cm}^{-1}$  (H-O-H bending mode)<sup>3</sup> but this is obscured by the ammonia vibrations in that region. For hydroxo complexes of ruthenium, Scargill<sup>4</sup> observed M-O-H bending modes at  $1000\text{--}970\text{ cm}^{-1}$  in addition to the absorptions at  $3500\text{ cm}^{-1}$ . No absorptions for the original complex were observed in this region.

On the basis of the analytical, infrared and ultraviolet spectra the complex is formulated as  $[\text{Ru}(\text{NH}_3)_5\text{Cl}]\text{Cl}_2$  containing a small amount of an impurity. The absence of any M-O-H bands in the infrared, while not definitive, is strong evidence that this is not a hydroxo compound. Thus, the spectral observations described above can be explained if the red compound is mainly the chloropentaammine, by the following series of equations:



The molar absorptivities for each of the above species, calculated assuming the compound was the chloropentaammine, are listed in Table 6.2. These observations are consistent with a formulation of the complex as ~80-85% chloropentaammine.

#### 6.1.4 *cis*-Dichlorotetraammine Ruthenium(III) Chloride

*cis*-[RuA<sub>4</sub>Cl<sub>2</sub>]Cl was prepared by the method of Gleu and Breuel<sup>8</sup> from [RuA<sub>5</sub>OH]S<sub>2</sub>O<sub>6</sub>. Molar absorptivities of the recrystallised compound were:  $\lambda_{\text{max}}$  352 nm  $\epsilon$  1620 M<sup>-1</sup> cm<sup>-1</sup> (lit.<sup>7</sup> 1640 M<sup>-1</sup> cm<sup>-1</sup>); 314 nm  $\epsilon$  1370 M<sup>-1</sup> cm<sup>-1</sup> (lit.<sup>7</sup> 1380 M<sup>-1</sup> cm<sup>-1</sup>); 262 nm  $\epsilon$  495 M<sup>-1</sup> cm<sup>-1</sup> (lit.<sup>7</sup> 520 M<sup>-1</sup> cm<sup>-1</sup>).

#### 6.1.5 *cis*-Dichloro bis(ethylenediamine) Ruthenium(III) Chloride

*cis*-[Ru(en)<sub>2</sub>Cl<sub>2</sub>]Cl was prepared by Beattie's<sup>9</sup> modification of Broomhead's<sup>10</sup> method.

#### 6.1.6 Sodium Azide

Technical NaN<sub>3</sub> was recrystallised twice from deionised water and dried in vacuo over P<sub>2</sub>O<sub>5</sub> at room temperature. Titration with standard 0.103M silver nitrate showed the compound to be greater than 99.9% pure.



### 6.1.7 *Precipitating Agents*

Analar chemicals were used wherever possible for the precipitating agents used in the precipitation of the azido, dinitrogen and dinitrogen oxide complexes.

## 6.2 *Analyses*

Carbon, hydrogen, nitrogen, fluorine were determined by the Australian Microanalytical Service, Melbourne, two to three days after the preparation of the complexes. Chlorine, bromine and iodine were determined in Adelaide by potentiometric titration with silver nitrate.

Ruthenium was determined by heating the sample in a platinum boat to 600°C in the air for one hour. It was then heated in a stream of hydrogen at 600°C for a further hour and then cooled under hydrogen. The residue was weighed as ruthenium metal. For tetrafluoroborate and hexafluorophosphate salts this method was unsatisfactory, because of a reaction with the boats. They were converted to a chloride salt by ion exchange and then determined as described.

## 6.3 *Production of Ruthenium(II) Solutions*

Solutions of ruthenium(III) compounds are very readily reduced to the corresponding ruthenium(II) compound by a variety of reducing agents. Typically the  $E_0$  for the reduction of the pentaammine ruthenium(III) is of the order of 0.2 V.<sup>11</sup> Four methods of reduction

were used:

- (1) zinc amalgam;
- (2) amalgamated zinc;
- (3) hydrogen on platinum black, and
- (4) electrolytic reduction.

#### 6.3.1 Zinc Amalgam

Zn(Hg) was prepared by the method of Vogel.<sup>12a</sup> The aquo ammine ruthenium(II) solution was then prepared from the corresponding chloro species by stirring with the amalgam under argon.

#### 6.3.2 Amalgamated Zinc

Zn/Hg was prepared by the method of Vogel,<sup>12b</sup> and the aquo ammine was prepared as for zinc amalgam.

#### 6.3.3 Hydrogen on Platinum Black

Pt(H<sub>2</sub>) reductions were carried out in a Schlenk<sup>13</sup> tube. The solution was degassed by bubbling with argon. The gas stream was switched to hydrogen and this was bubbled into the solution with a tube, around which the platinum black was wrapped. The reduced solution could then be removed under argon when the reduction was complete. Pt(H<sub>2</sub>) reductions were used for the preparation of solutions used in the preparation of dinitrogen oxide complexes.

#### 6.3.4 *Electrolytic Reductions*

Electrolytic reductions were carried out in a glass vessel using a mercury pool as the cathode. The vessel was a Schlenk tube with a piece of platinum wire sealed near the bottom of the tube, and a side-arm with a B10 joint attached about half-way up the tube. The anode compartment was a glass tube with a B24 joint, a sintered glass disc at the bottom and a small hole below the B24 joint to act as a gas outlet. Platinum foil inside the tube near the sintered glass disc acted as the anode. During the electrolysis the system was sealed and a gas passed over the solution. The electrolyte containing the ruthenium solution was added onto the mercury pool and deoxygenated by bubbling with argon via the side-arm. Electrical contact was made by allowing some of the electrolyte solution to diffuse into the anode through the sintered glass disc. The reduction proceeded under argon at  $-0.6$  V relative to a saturated calomel electrode. Reduction was complete when the current remained constant around 50-100  $\mu$ A for ten minutes. The ruthenium(II) solution was removed through the side-arm in a stream of argon.

Electrolytic reduction was used to follow the variation of the rate of the reaction between  $[\text{RuA}_5\text{H}_2\text{O}]^{2+}$  and azide ion with varying pH. The pH of solution remained reasonably constant (within 0.2-0.5 units) if care was taken to minimise hydrogen production during electrolysis. The reaction was initiated when a known volume of freshly prepared, deoxygenated, standard azide solution, at the pH of the reduced solution,

was added through the side-arm in a counter stream of argon. The voltage was maintained to ensure no hydrogen production for the duration of the reaction (~ one hour). This method was also used to produce solutions of  $\text{RuA}_5\text{H}_2\text{O}^{2+}$  for the reactions between it and sodium azide in the absence of a reducing agent.

### 6.3.5 Estimate of Ruthenium(II) Content of Reduced Solutions

Amalgamated zinc and the electrolytic means of reduction of  $[\text{RuA}_5\text{Cl}]^{2+}$  were both checked for completeness. To achieve this a known volume of the reduced solution was added to an excess of a ferric sulphate solution and the resultant ferrous ion determined with o-phenanthroline. Estimation of the ferrous ion was based on determining the absorbance at 510 nm where the molar absorptivity of  $\text{Fe(o-phen)}_3^{2+}$  was determined as  $1.10 \times 10^4 \text{ M}^{-1} \text{ cm}^{-1}$  (lit.<sup>14</sup>  $1.11 \times 10^4 \text{ M}^{-1} \text{ cm}^{-1}$ ). The molar absorptivity was determined using known volumes of standard ferrous ammonium sulphate solution ( $1.54 \times 10^{-3} \text{ M}$ ) made up to 50 ml with 5 ml of sodium acetate-sulphuric acid buffer, 4 ml of 0.25% solution of o-phenanthroline in water and water. For the test solutions 1 ml aliquots of the reduced solution were added to 5 ml of ferric sulphate in 0.1M sulphuric acid under argon and then made up to 50 ml with buffer, water and o-phenanthroline as described above. Also 1 ml of the reduced solution was added to 10 ml of 1M HCl and allowed to oxidise in air, thus regenerating  $[\text{RuA}_5\text{Cl}]^{2+}$  and providing a check on its concentration. From these

experiments it was concluded that both methods lead to 100% reduction. The results for some of the runs are shown in Table 6.3.

#### 6.4 Preparation of Nitrous Oxide Complexes

The dinitrogen oxide complexes of the ruthenium amines were prepared in the presence of an excess of precipitating agent from the corresponding aquo species and 30-40 atmospheres of nitrous oxide. The reaction vessel was a glass test tube with a B24 stopper, and the pressure vessel in figure 6.1 was used.

While a solution of the chloro complex (either  $[\text{RuA}_5\text{Cl}]^{2+}$ ,  $\text{cis-}[\text{RuA}_4\text{Cl}_2]^+$  or  $\text{cis-}[\text{Ru en}_2\text{Cl}_2]^+$ ) was being reduced, the pressure vessel and reaction tube were evacuated then filled with argon using a vacuum line and the cycle repeated several times. Several drops of a saturated solution of the precipitating agent were added to the aquo ruthenium (reduced species) solution, but not enough to cause precipitation. Any solid which did happen to precipitate was redissolved by adding water. The reduction was then continued for a further 5 minutes to ensure that no oxidised species were present. The reduced solution was then transferred under argon to the reaction tube in the pressure vessel. The top of the pressure vessel was flushed with argon and sealed to the bottom, a constant stream of argon being maintained over the reduced solution. Nitrous oxide was admitted to the pressure vessel through tap A, making sure that all

connections were flushed with the gas to the exclusion of air. The pressure was maintained for 30 minutes while the apparatus was cooled in ice. The pressure was released slowly, and the reaction vessel quickly stoppered in a stream of nitrous oxide from the cylinder. It was transferred to a nitrogen glove box and any solids precipitated were isolated, washed with deoxygenated water, and then ethanol, and dried over phosphorus pentoxide in vacuo, in the absence of light.

For the pentaammine complexes no analysis was performed because these compounds are well known from Sparrow's work;<sup>5,15</sup> for the ethylenediamine no complexes were isolated. The analyses for the tetraammine complexes are listed in Table 4.3.

The compounds are stable at  $-5^{\circ}\text{C}$  in the absence of moisture for about a week. They decomposed at higher temperatures to the dinitrogen complex.

$[\text{RuA}_4(\text{OH}_2)\text{N}_2\text{O}](\text{BF}_4)_2 \cdot 2\text{H}_2\text{O}$  was obtained as a pale yellow solid (yield 31-42 mg; 20-25%), using sodium tetrafluoroborate (1 g in 5 ml of water) as the precipitating agent.

$[\text{RuA}_4(\text{OH}_2)\text{N}_2\text{O}](\text{PF}_6)_2 \cdot \text{H}_2\text{O}$  was obtained as a pale yellow solid (yield 40-50 mgm; 25-30%) using ammonium hexafluorophosphate (1 g in 3 ml of water) as the precipitating agent. Some aquo complex was also precipitated but this was redissolved with water before transferring to the pressure vessel.

Sodium iodide (1 g in 5 ml of water), sodium bromide (1 g in 3 ml

of water) and lithium iodide (0.5 g in 3 ml of ethanol) were used as precipitants. No solids were obtained with the sodium halides. A dark solid was obtained with LiI but its infrared spectrum revealed that no nitrous oxide or nitrogen complexes were present.

#### 6.5 Preparation of Azido Pentaammine Ruthenium(II) Complexes

The apparatus used is shown in figure 6.1. It is an inverted Y tube with a B19 joint and a tap for gas inlet. In one arm of the tube a saturated solution of the precipitant was placed and deoxygenated by bubbling with argon. Sodium azide was placed in the other arm of the tube and the apparatus stoppered under argon. A solution of  $\text{RuA}_5\text{OH}_2^{2+}$  in water was prepared by reducing  $[\text{RuA}_5\text{Cl}]^{2+}$  electrolytically. This was transferred under argon to the arm containing sodium azide. Immediately an intense orange coloured solution was formed which faded on standing. By pouring the precipitating agent onto the orange solution, as soon as practicable, a red precipitate was obtained. This was isolated in a nitrogen glove bag and washed with ethanol. The compounds proved to be very unstable, rapidly losing their red colour to become the pale yellow colour of the corresponding dinitrogen complex.

The halide ion was determined by titration with silver nitrate on a freshly prepared sample of the complex. No interference by precipitation of azide ion as  $\text{AgN}_3$  occurred as the solubility products of  $\text{AgN}_3$  and  $\text{AgBr}$  are  $3.16 \times 10^{-9}$  and  $3.16 \times 10^{-13}$  respectively.<sup>21</sup>

The values obtained for five independent determinations were 37.3, 41.4, 39.9, 39.3 and 39.7 expected for  $[\text{RuA}_5\text{N}_3]\text{Br}$  25.9% and for  $[\text{RuA}_5\text{N}_3]\text{Br}_2$  42.7%.

#### 6.6 Preparation of Benzoylhydrazine Complexes

Ruthenium pentaammine trichloride (59 mgm 0.20 m mole) and N-benzoylhydrazine (30.4 mg 0.22 m mole) were added to 5 ml of water in a test tube and dissolved by warming. The solution turned orange and 2 ml of a saturated solution of the appropriate precipitating agent was added and the mixture was cooled in ice. Within five minutes a precipitate was formed, which was recrystallised from hot water. The recrystallised solid was washed with cold water and ether and dried over  $\text{P}_2\text{O}_5$  in vacuo.

Using lithium bromide an orange solid (98.7 mg 63.7% yield) was obtained and analysed for bromide ion by titration with silver nitrate, after it was decomposed with hydrogen peroxide.

Found: % Br, 43.7, 42.5, 42.9.

Calculated for  $\text{C}_7\text{H}_{23}\text{N}_7\text{OBr}_3\text{Ru}$ : % Br, 43.5.

Using lithium iodide a green solid (141.9 mg 60.0%) was obtained and analysed for iodide ion as before.

Found: % I, 56.5, 56.5.

Calculated for  $\text{C}_7\text{H}_{23}\text{N}_7\text{OI}_3\text{Ru}$ : % I, 54.2%.

Using sodium tetrafluoroborate and ammonium hexafluorophosphate yellow solids were obtained in 28% and 45% yields respectively. No



analyses were performed on these salts.

## 6.7 *Spectral Measurements*

### 6.7.1 *Infrared Spectra*

These were recorded in the range  $4000\text{--}250\text{ cm}^{-1}$  on a Perkin Elmer 457 grating infrared spectrophotometer. Spectra were recorded as Nujol mulls between potassium bromide plates ( $4000\text{--}400\text{ cm}^{-1}$ ) or between polyethylene plates ( $600\text{--}250\text{ cm}^{-1}$ ). Some spectra were also recorded as potassium bromide discs.

The absorption positions of coordinated dinitrogen oxide were measured relative to carbon monoxide<sup>16</sup> ( $2300\text{--}2000\text{ cm}^{-1}$ ), ammonia vapour<sup>16</sup> ( $1250\text{--}1100\text{ cm}^{-1}$ ) and water vapour<sup>17</sup> ( $400\text{--}250\text{ cm}^{-1}$ ) as calibrants in the ranges indicated. The accuracy of the frequencies is better than  $\pm 0.5\text{ cm}^{-1}$ .

### 6.7.2 *Electronic Absorption Spectra*

Spectra were recorded using a Unicam SP700 recording spectrophotometer or a Perkin-Elmer model 402 recording spectrophotometer. Molar absorptivities were recorded using a Shimadzu model QR-50 spectrophotometer. The decomposition of  $\text{RuA}_4(\text{H}_2\text{O})\text{N}_2\text{O}(\text{BF}_4)_2 \cdot 2\text{H}_2\text{O}$  was followed using the 402 instrument on a fixed wavelength time drive with a scan speed of  $\frac{1}{2}\text{ cm}$  per minute. This instrument and a Unicam SP800 recording spectrophotometer were used for repetitive scanning.

The spectra of air-sensitive solutions were recorded under an inert

atmosphere (usually argon). The spectrophotometer cell was flushed with argon and then the solution was added against a counterstream of argon, through a T-piece attached to the top of the cell by a B10 joint. The cell was then sealed with a lightly greased stopper in a stream of gas from the T-piece and the spectrum recorded.

### 6.7.3 Mass Spectra

Gas samples were analysed for dinitrogen, argon, dinitrogen oxide and water vapour using an Associated Electrical Industries MS10 mass spectrometer fitted with a gas inlet apparatus and a Hitachi Perkin-Elmer model RMU-6D mass spectrometer.

Argon and water vapour were detected at  $m/e$  values of 40 and 18 respectively.

Nitrous oxide was observed to have fragments at  $m/e$  values of 14 ( $N^+$ ), 16 ( $O^+$ ), 28 ( $N_2^+$ ), 30 ( $NO^+$ ) and 44 ( $N_2O^+$ ). Nitrogen has fragments at  $m/e$  values of 14 ( $N^+$ ) and 28 ( $N_2^+$ ). Mixtures of the two gases could be determined by comparing the intensity of the peaks at 14, 28, 30, and 44. In this way the presence of nitrogen in a sample of nitrous oxide could be detected.

### 6.8 Powder Photographs

X-ray powder patterns were recorded with a Nonius general purpose camera (radius, 28.86 mm; effective radius, 28.20 mm) with nickel filtered  $CuK\alpha$  radiation ( $\lambda = 1.542 \text{ \AA}$ ). Samples were mounted in 0.3 mm

glass capillaries. The position and intensities of the lines were measured with a Nonius II densitometer.

### 6.9 Manometric Measurements

Manometric measurements were performed on the apparatus in figure 6.2 which was thermostatted to room temperature before each reading. During measurements the tap H was open to the atmosphere and the two arms of the manometer were levelled with the screw levelling device. The two arms were adjudged as level with a cathetometer using black shading on the mercury meniscus. Measurements against vacuum were made by opening tap H to the pumps. The head of mercury was measured with the cathetometer. Using a vernier scale the meniscus positions could be read to 0.001 cm.

The volume change at S.T.P. during a reaction was calculated using the expression

$$V = \left\{ \frac{P_f}{T_f} (V_0 + B_f) - \frac{P_i}{T_i} (V_0 + B_i) \right\} \frac{T_{273.16}}{P_{760}}$$

where  $B_f$ ,  $T_f$ ,  $P_f$  are final readings and  $B_i$ ,  $T_i$ ,  $P_i$  are initial readings of the left-hand side burette, temperature and pressure respectively. The values of  $P_i$  and  $P_f$  were corrected for the vapour pressure of the solvent. Thus,

$$P_i \text{ or } P_f = P_{\text{measured}} - \text{solvent vapour pressure.}$$

$V_0$  is the volume of the apparatus to the zero line of the burette.

This was calibrated by trapping a small volume of air in the apparatus

and measuring the volume and pressure changes produced on it by changing the position of the mercury reservoir. As

$$P(V_0 + B) = \text{constant}$$

the volume of the apparatus  $V_0$ , was obtained from a plot of the burette reading  $B$ , versus the reciprocal of the pressure,  $1/P$ .

Gas samples for mass spectral analyses were collected in the sample tube through taps E and F, or via the trap T if this was required, using a Toepler pump.

#### 6.10 Balances

Solids for analyses or for the determination of molar absorptivities were weighed on a Cahn Model G2 Electrobalance. All other weighings were made on a Mettler H16 balance weighing to 0.01 mg. The latter weighings were made in a glass weighing tube whose capacity was approximately 100 mg. It was sealed with a ground glass stopper. A thin glass rod was attached to the base of the weighing tube in order to facilitate manipulations.

#### 6.11 Gases

All gases were obtained from Commercial Industrial Gases (Australia) Limited. Dinitrogen (oxygen free), hydrogen and argon were used as received. Nitrous oxide was passed through a chromous chloride bubbler to remove oxygen, and then through phosphorus pentoxide drying towers before being used.

Deoxygenated nitrous oxide at forty atmospheres was obtained by collecting the dried, deoxygenated nitrous oxide in a meteorological balloon (volume ~45 litres) and then condensing the filled balloon into a small gas cylinder (volume ~100 cc) which was immersed in liquid nitrogen. Two to three cycles were necessary to fill the small cylinder and a pressure of 40 atmospheres (the vapour pressure of nitrous oxide at room temperature) was maintained for three to five preparations of the nitrous oxide complexes.

## 6.12 Characterisation of the Tetraammine Nitrous Oxide Complexes

### 6.12.1 Solution Properties

Conversion to  $[\text{RuA}_4(\text{OH}_2)_2]^{2+}$  was achieved by pipetting 5 ml of degassed 0.1M methane sulphonic acid onto weighed amounts of the solid in a Schlenk tube under argon. The molar absorptivity was recorded by transferring the solution under argon to a spectrophotometer cell and measuring the absorbance at the appropriate wavelength.

Conversion to  $\text{cis-}[\text{RuA}_4\text{Cl}_2]^+$  was achieved by dissolving the weighed solids in 10 ml of 1M hydrochloric acid and stirring in the air for 30-60 minutes.

### 6.12.2 Release of Nitrous Oxide from $[\text{RuA}_4(\text{OH}_2)\text{N}_2\text{O}](\text{BF}_4)_2 \cdot 2\text{H}_2\text{O}$

The nitrous oxide content of the complex was determined using the vacuum line in figure 6.2. The oxidising agent, cerium(IV) sulphate ( $10^{-2}$  M 5 ml), was degassed by the freeze-pump-thaw method

in a two-neck flask, the volume of which was known. The nitrous oxide complex was added from a weighing tube, through the second neck, onto the frozen solution in the air. The flask was evacuated and the solution thawed as quickly as possible. It was stirred for one hour.

When the oxidation was complete (after one hour) the pressure and volume of the system were recorded. The solution was frozen in liquid nitrogen and the non-condensable gas (nitrogen) was pumped off. The nitrous oxide was then distilled over to the trap T. This was achieved by cooling the trap in liquid nitrogen, and cooling the reaction vessel to  $-30^{\circ}\text{C}$  to  $-40^{\circ}\text{C}$ . The solution was allowed to thaw and the dissolved nitrous oxide was collected using the same temperatures. Several blank runs showed that two more cycles ensured that all the nitrous oxide had been collected. Distillation of the nitrous oxide from the trap, at  $-40^{\circ}\text{C}$ , to another vessel which was cooled in liquid nitrogen (two cycles), gave dry nitrous oxide.

After the nitrous oxide had been removed, the vapour pressure of the solution was determined by degassing the solution until a constant pressure was obtained. The reaction flask was then removed and the nitrous oxide was distilled from trap T, at  $-30^{\circ}$  to  $-40^{\circ}\text{C}$ , into a calibrated cap, cooled in liquid nitrogen, at joint J. The pressure and the burette reading were recorded.

From the initial readings and the vapour pressure of the solution, the total gas evolved (nitrogen and nitrous oxide) was calculated.

The volume of nitrous oxide was calculated from the final set of readings. The results are given in Table 4.4.

### 6.13 The Reaction Between $[\text{RuA}_5(\text{OH}_2)]^{2+}$ and Azide

#### 6.13.1 Kinetic Studies

During the reactions 0.10 or 0.25 ml samples were withdrawn under argon and added to argon saturated 0.1M sulphuric acid in a Schlenk tube.

Zinc amalgam reductions were carried out in a two-necked flask attached to the vacuum line in figure 6.2 at joint J. A solution of  $[\text{RuA}_5\text{Cl}]\text{Cl}_2$  was added to the flask and degassed by the freeze-pump-thaw method. When the degassing was complete argon was admitted to the vessel and a known volume of standard amalgam was added to the solution through the second neck in a counterstream of argon. The amalgam was stirred for 30-40 minutes which was sufficient to ensure complete reduction of the chloropentaammine to the aquo species. The reaction was commenced when a known weight of sodium azide was added through the second neck of the flask in a counterstream of argon. The solution was stirred for a further hour during which time samples were removed under argon, appropriately diluted and their ultraviolet spectra examined. Usually the reactions were carried out at room temperature. In other cases the temperature was maintained by circulating water around the flask from a thermostatted ( $\pm 0.1^\circ\text{C}$ ) water bath.

Reactions in the absence of a reducing agent were also performed

on the vacuum line in a two-necked flask. In these cases a weighed amount of azide was added to the flask, which was evacuated then filled with argon (three cycles). The aquo species was produced by one of the methods described in section 6.3, usually zinc amalgam reduction. It was then transferred under argon to the flask containing the azide and stirred for one to two hours, samples being withdrawn in the meantime.

Some measurements of the gas evolved from these reactions were also carried out. In such cases a different procedure was adopted. The aquo was produced in the same way as before. The azide was weighed into a two-necked flask. Attached to the second neck was another two-necked flask. This apparatus was joined to the vacuum line at joint J, evacuated then filled with argon (three cycles). The aquo solution was transferred under argon to the second two-necked flask and frozen-pumped-thawed until a constant pressure was obtained. The solution was poured onto the azide and stirred for one hour, after which time the readings of the burette and pressure were recorded. The solution was frozen in liquid nitrogen and all the non-condensable gases pumped off. The vapour pressure of the solution was determined by degassing the solution until a constant pressure was obtained. Thus the amount of gas evolved was determined and the results are tabulated in Table 2.5.

Reactions at constant pH were performed using electrolytic reduction and the procedure described in section 6.3.4 was adopted.



In some other runs solid sodium azide was added in a counterstream of argon, otherwise the same conditions were maintained.

Hydrogen on platinum black reductions were performed using a Schlenk tube with a second joint fitted near the bottom of the tube. The chloro pentaammine was reduced with hydrogen for 30 minutes and then weighed amounts of azide were added. This method was not used for the reasons outlined in section 2.3, i.e. volatilization of the hydrazoic acid.

#### 6.13.2 Stoichiometry

The products of the reaction between  $[\text{RuA}_5\text{OH}_2]^{2+}$  and azide ion were the dinitrogen complexes  $[\text{RuA}_5\text{N}_2]^{2+}$  and  $[\text{A}_5\text{RuN}_2\text{RuA}_5]^{4+}$  identified from their absorption maxima in the ultraviolet and estimated from the published molar absorptivities (see Table 2.2). The likely other products are ammonia, hydroxylamine or hydrazine.

For the identification of products a solution which was  $10^{-2}$  M in  $\text{RuA}_5\text{Cl}_3$  was reduced under argon with zinc amalgam. Sodium azide was added and the reaction allowed to proceed until the ultraviolet spectrum indicated 100% conversion to the dinitrogen complexes. The solution was applied to an ion exchange column (Amberlite IRL20  $\text{H}^+$  form) and washed with water. Tests of the eluant with ferric ions gave a red colouration, which arose because of the formation of  $[\text{Fe}(\text{H}_2\text{O})_5\text{N}_3]^{2+}$ . Potassium chloride (0.2M) was passed down the column and the eluants tested with Nessler's reagent.<sup>12c</sup> With ammonium

ion this reagent gives an orange-brown colloidal suspension; while with hydrazine or hydroxylamine thick grey precipitates are obtained. The eluant gave an orange-brown precipitate. Further, tests of the eluant for hydrazine with para-dimethyl aminobenzaldehyde were negative. Thus the other product of the reaction was ammonium ion. It was found that 200 ml of potassium chloride solution were required to elute the ammonium ion completely, the bulk of the material being eluted in the first 75-80 ml, as adjudged by spot testing with the Nessler's reagent solution.

Nessler reagent was used at first to determine the amount of ammonium ion produced in the reaction. However, impurities eluted from the resin together with the ammonium ion, caused the precipitation of a brownish solid from solution, and the absorbances recorded were not reproducible. The method was then abandoned.

Another method of ammonia determination is offered by the Kjeldahl determination.<sup>12d</sup> The accuracy of the method was checked using a solution of 0.107M ammonium chloride standardised against silver nitrate. The quantitative recovery of ammonium ion from the resin was tested by first absorbing the ion onto the ion exchange column and eluting it with potassium chloride solution. The solution collected by this procedure was evaporated on a steam bath to 10-20 ml and the ammonia steam distilled from concentrated caustic soda solution into a saturated solution of boric acid. The boric acid was titrated potentiometrically with  $2.9 \times 10^{-2}$  M hydrochloric acid, prepared from

standardised 0.116M stock acid, and hence the ammonium ion was determined. Values of ammonium ion determined with and without the pre-treatment described above are compared in Table 6.4, and untreated and pre-treated determinations gave the same ammonium ion concentrations, within experimental error. The results also show good agreement of experimentally determined and theoretical amounts of ammonium ion present. Thus the method was acceptable as a means of ammonium ion determination and the method of pre-treatment as outlined above showed the validity of ammonia determination by this means.

The ammonia present in the reaction mixtures may arise from sources other than as a product of the reaction. Loss of ammonia from the monomer dinitrogen complex product, the reactant aquo species, ammonia arising from the column or from sodium azide reduction, were each investigated.

Ammonia loss from the monomer and aquo species were checked by stirring 0.01M solutions of each in 0.1M sulphuric acid under nitrogen and argon respectively, applying 10 ml of each solution to an ion-exchange column and eluting the ammonia with 0.2M potassium chloride. The ammonia was determined as before and the results, listed in Table 6.5, show the loss of one mole of ammonia for each mole of complex initially present. Other experiments (see section 2.4) showed that chloride ion catalysed the ammonia dissociation.

The correction for ammonia arising from the columns was

determined by washing the column with 200 ml of 0.2M potassium chloride, evaporating the elutions to 10-20 ml on a steam bath and determining the ammonia as before. It was found that three washings of a column reduced the number of mole of ammonia to  $9.30 \times 10^{-6}$  from  $20.9 \times 10^{-6}$  and the former value was applied as a correction for column ammonia, each column being appropriately treated before use.

Ammonia production from azide reduction was checked by stirring a 0.06M solution of sodium azide in 0.1M sulphuric acid with zinc amalgam and determining the ammonia as before. The amount of ammonia detected was less than  $10^{-7}$  mole, low enough for this source to be ignored relative to the other corrections which were applied.

For determination of the stoichiometry a solution of chloropentaammine ruthenium(III) (0.01M) was reduced under argon with zinc amalgam and when the reduction was complete sodium azide (0.03-0.05M) was added. When the reaction was complete (as adjudged by 100% formation of the dinitrogen complexes) a 10 ml sample was applied to the ion exchange column and the ammonium ion eluted with either 0.2M potassium chloride or 0.2M potassium nitrate. The total ammonia in solution was determined by the procedure outlined above, and the ammonium ion resulting as a direct consequence of the reaction was calculated by applying the appropriate corrections as given below. The stoichiometry was then determined from four individual runs and five independent determinations.

When potassium chloride was used as eluant two corrections for ammonia were made: the correction for column ammonia ( $9.30 \times 10^{-6}$  mole) plus the correction for loss of one mole of ammonia arising from the dinitrogen monomer ( $1.11 \times 10^{-5}$  mole), i.e.  $1.12 \times 10^{-5}$  mole for a typical run was deducted from the total ammonia determined.

When potassium nitrate was used as eluant two corrections for ammonia were applied. Column ammonia was  $2.09 \times 10^{-5}$  mole as unwashed columns were used in these experiments. A further  $2.15 \times 10^{-5}$  mole arose from some ammonia loss from the monomer in the absence of chloride ion (see Table 6.5). Thus a total of  $4.24 \times 10^{-5}$  mole was deducted from the total ammonia determined, and this correction applied for the last three values of Table 2.7.

The values in Table 2.7 confirm the stoichiometry of the reaction between  $[\text{RuA}_5\text{OH}_2]^{2+}$  and azide as was discussed in section 2.4.

#### 6.14 Thermal Decomposition of $[\text{RuA}_5\text{N}_2\text{O}]\text{X}_2$ ( $\text{X} = \text{BF}_4, \text{PF}_6$ )

The thermal decomposition of the nitrous oxide complexes was carried out using a flask of known volume attached to the vacuum line, in figure 6.2, at joint J. The temperature of the decomposition was controlled using an oil bath. Measurements of volume and pressure were taken at room temperature as described previously. Both the low temperature decomposition of the  $\alpha\beta$ - $[\text{RuA}_5\text{N}_2\text{O}](\text{PF}_6)_2$  and the high temperature decompositions were performed using this apparatus.

Measurements of the amount of dinitrogen monomer and ruthenium red produced, with high temperature decomposition, were made by using an ion-exchange technique. A weighed amount of the decomposed solid was dissolved in water and applied to a column of Bio-Rad Sephadex AG 50W-X2 cation exchange resin. The monomer was found to elute with 200 ml of 0.1M sulphuric acid, while the ruthenium red remained at the top of the column as a brown band (in acidic conditions ruthenium red is oxidised to ruthenium brown<sup>18</sup>). The monomer was made up to 250 ml in a volumetric flask with 0.1M acid and estimated from its absorbance at 221 nm.<sup>19</sup> Ruthenium red was estimated from its absorbance at 532 nm by dissolving a known weight in 5 ml of water.<sup>18</sup>

#### 6.15 pH and Millivolt Measurements

These were performed using a Horiba Type F-5 pH meter. For pH measurements the instrument was standardised with a solution of 0.050M potassium hydrogen phthalate, pH 4.00 at 20°C.

#### 6.16 Computer Calculations

Solution of the simultaneous equations, for estimation of monomer and dimer complexes, and least square calculations were performed on the University of Adelaide's CDC6400 computer.

### 6.17 *Magnetic Measurements*

The magnetic moment of the benzoylhydrazine complex was determined by the method of Evans<sup>20</sup> using water as a solvent and tertiary butanol as a reference compound. The measurements were made on a Varian model T60 nuclear magnetic resonance spectrometer.

TABLE 6.1

*Infrared Spectra of  $[\text{RuA}_5\text{Cl}]\text{Cl}_2$  and Red Compound*All band positions recorded as  $\text{cm}^{-1}$ .

Assignment	$[\text{RuA}_5\text{Cl}]\text{Cl}_2$	Red Compound
$\nu_{\text{O-H}}$	-	3500 m, sh
$\nu_{\text{N-H}}$	3300-3140 br, s	3300-3140 br, s
$\delta\text{NH}_3$ asym	1620 s	1620 s
	-	1400 m
$\delta\text{NH}_3$ sym	1305 s	1305 s
$\rho\text{NH}_3$	810 s	810 s
$\nu_{\text{Ru-N}}$	495 w	495 w
	471 w, sh	471 w, sh
	461 m	461 m



TABLE 6.2

*Molar Absorptivities of Ruthenium Species*

Species	$\lambda_{\text{max}}$ nm	$\epsilon_{\text{max}}$ M <sup>-1</sup> cm <sup>-1</sup>	Reference	Observed <sup>a</sup>
[RuA <sub>5</sub> Cl] <sup>2+</sup>	328	$1.93 \times 10^3$	2	$1.58 \times 10^3$
[RuA <sub>5</sub> OH] <sup>2+</sup>	295	$2.1 \times 10^3$	6	$2.2 \times 10^3$
[RuA <sub>5</sub> OH <sub>2</sub> ] <sup>2+</sup>	267	570	5	540
[RuA <sub>5</sub> OH <sub>2</sub> ] <sup>3+</sup>	268	770	6	715

<sup>a</sup> Observed for the red compound previously formulated as  
 cis-[RuA<sub>4</sub>(OH)Cl]Cl.

TABLE 6.3

*Percent Reduction of Chloropentaammine Ruthenium(III) Chloride*

Method of Reduction	[RuA <sub>5</sub> Cl] <sup>2+</sup> Determined	[RuA <sub>5</sub> H <sub>2</sub> O] <sup>2+</sup> estimated from Fe(o-phen) <sub>3</sub> <sup>2+</sup>	% Reduction
Amalgamated zinc	7.52 × 10 <sup>-3</sup> M	7.61 × 10 <sup>-3</sup> M	101.2
" "	7.52 × 10 <sup>-3</sup> M	8.11 × 10 <sup>-3</sup> M	107.8 <sup>1</sup>
Electrolysis	4.90 × 10 <sup>-3</sup> M	4.87 × 10 <sup>-3</sup> M	99.4
"	4.68 × 10 <sup>-3</sup> M	4.73 × 10 <sup>-3</sup> M	101.1
"	4.68 × 10 <sup>-3</sup> M	4.64 × 10 <sup>-3</sup> M	99.2

<sup>1</sup> A small amount of the amalgamated zinc was transferred and thereby increased the Fe<sup>2+</sup> concentration.

TABLE 6.4  
Kjeldahl Determination of Ammonium Ion

Titre Value (ml)	Number mole of ammonium ion	
	Found Experimentally	True Value
1.61	$4.67 \times 10^{-5}$	$5.05 \times 10^{-5}$
1.76	$5.10 \times 10^{-5}$	"
1.75	$5.08 \times 10^{-5}$	"
1.38	$4.00 \times 10^{-5}$	"
1.68	$4.87 \times 10^{-5}$	"
2.12	$6.15 \times 10^{-5}$	"
3.35	$9.71 \times 10^{-5}$	$10.10 \times 10^{-5}$
3.22	$9.34 \times 10^{-5}$	"
5.25	$15.22 \times 10^{-5}$	$15.15 \times 10^{-5}$

Ammonium Ion Recovered After Ion-Exchange

1.93	$5.59 \times 10^{-5}$	$5.05 \times 10^{-5}$
1.96	$5.68 \times 10^{-5}$	"
3.17	$9.19 \times 10^{-5}$	$10.10 \times 10^{-5}$
3.58	$10.40 \times 10^{-5}$	"
5.15	$14.94 \times 10^{-5}$	$15.15 \times 10^{-5}$

All titrations performed with standardised  $2.90 \times 10^{-2}$  M HCl.

TABLE 6.5

*Ammonia Loss from Pentaammine Ruthenium(II) Species**(i) Aquo Pentaammine Ruthenium(II)<sup>a</sup>*

[RuA <sub>5</sub> Cl <sub>3</sub> ]	Titre Value (ml) <sup>c</sup>	Mole NH <sub>4</sub> <sup>+</sup>	Concentration NH <sub>4</sub> <sup>+</sup>
$1.10 \times 10^{-2}$ M	1.73	$5.02 \times 10^{-5}$	$1.00 \times 10^{-2}$ M
$2.20 \times 10^{-2}$ M	3.55	$10.31 \times 10^{-5}$	$2.06 \times 10^{-2}$ M
$1.10 \times 10^{-2}$ M	3.62	$10.51 \times 10^{-5}$	$1.05 \times 10^{-2}$ M
$1.12 \times 10^{-2}$ M	3.66	$10.61 \times 10^{-5}$	$1.06 \times 10^{-2}$ M
$2.18 \times 10^{-2}$ M	3.83	$11.09 \times 10^{-5}$	$2.22 \times 10^{-2}$ M

*(ii) Dinitrogen Pentaammine Ruthenium(II)<sup>b</sup>*

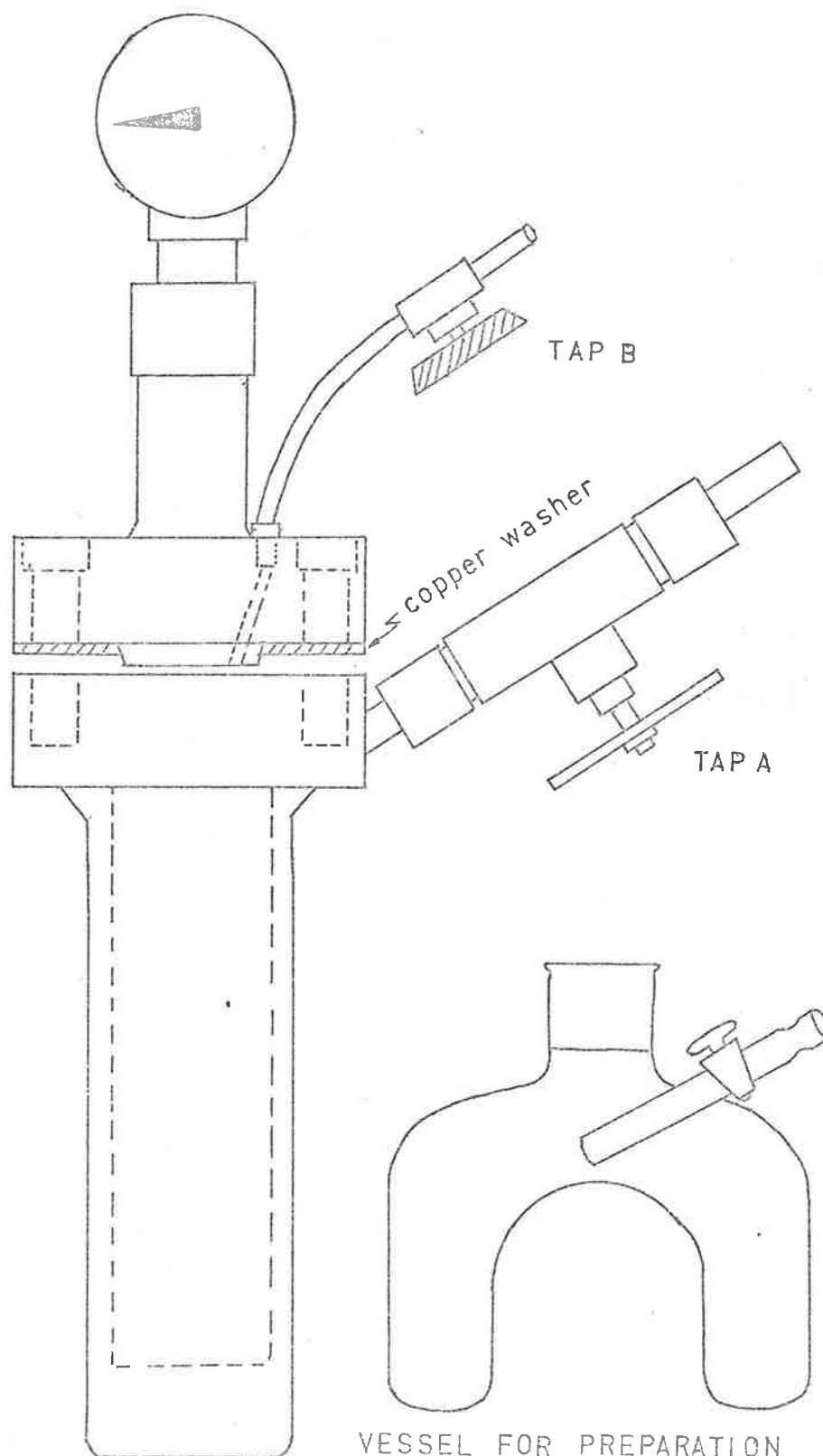
[Monomer]	Titre Value (ml) <sup>c</sup>	Mole NH <sub>4</sub> <sup>+</sup>	Concentration NH <sub>4</sub> <sup>+</sup>
$0.99 \times 10^{-2}$	0.75	$2.15 \times 10^{-5}$	$0.22 \times 10^{-2}$
$1.01 \times 10^{-2}$	0.78	$2.26 \times 10^{-5}$	$0.23 \times 10^{-2}$
$1.12 \times 10^{-2}$ a	1.89	$5.50 \times 10^{-5}$	$1.10 \times 10^{-2}$

<sup>a</sup> In the presence of excess chloride ion.

<sup>b</sup> In the absence of chloride ion.

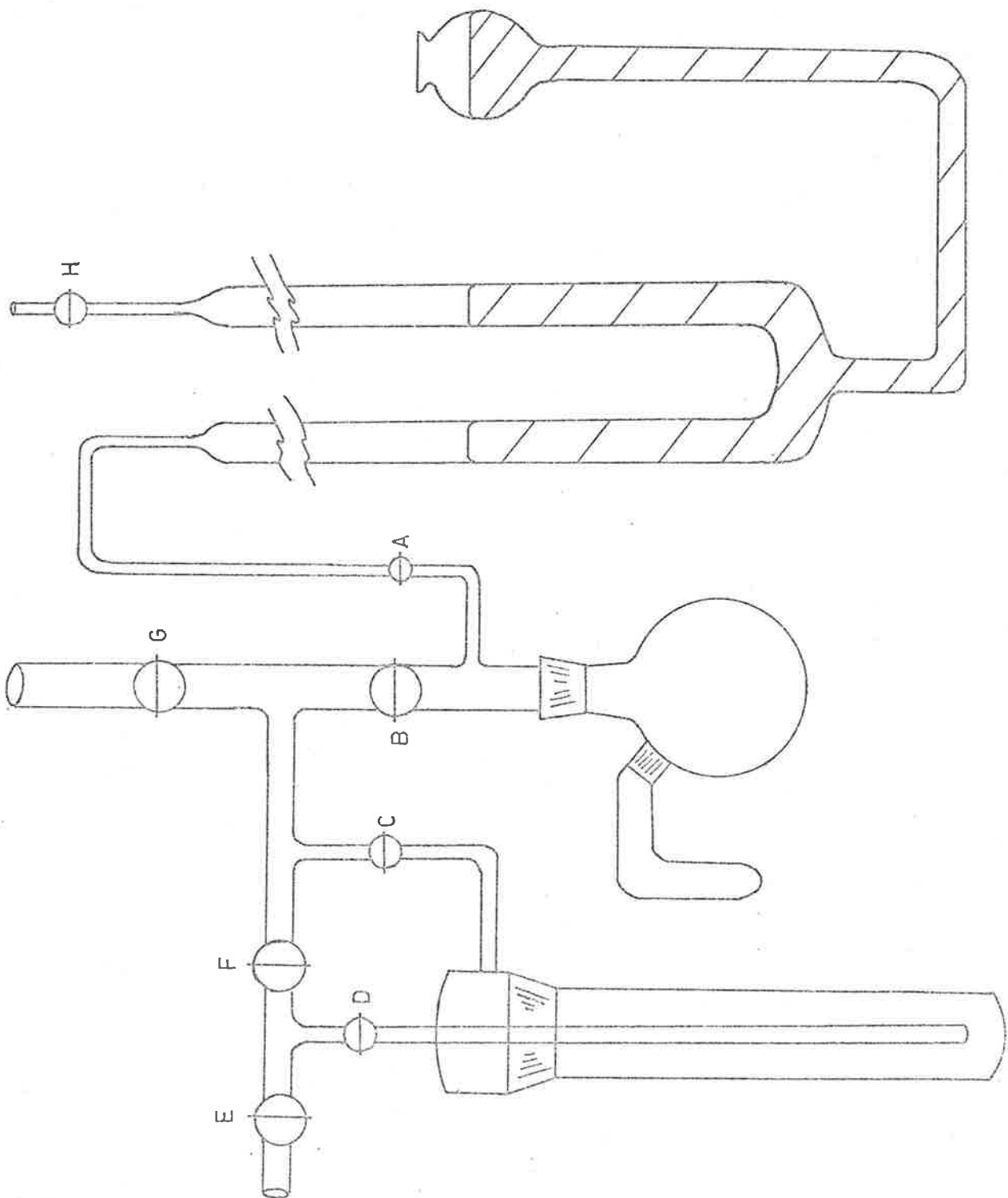
<sup>c</sup> All titrations performed with standardised  $2.90 \times 10^{-2}$  M HCl.

FIGURE 6.1 PRESSURE VESSEL



VESSEL FOR PREPARATION  
OF AZIDO COMPLEXES

FIGURE 6.2 VACUUM LINE



## CHAPTER 6

## REFERENCES

1. A.D. Allen, F. Bottomley, R.O. Harris, V.P. Reinslau and C.V. Senoff, *J. Amer. Chem. Soc.*, 1967, 89, 5595.
2. L.H. Vogt, J.L. Katz and S.E. Wiberley, *Inorg. Chem.*, 1965, 4, 1157.
3. K. Nakamoto, "Infrared Spectra of Inorganic and Coordination Compounds", Wiley, New York, 1963, p. 156.
4. D. Scargill, *J. Chem. Soc.*, 1961, 4444.
5. G.J. Sparrow, Ph.D. Thesis, University of Adelaide, March, 1972; P.C. Ford, J.R. Kuempel and H. Taube, *Inorg. Chem.*, 1968, 7, 1976.
6. T. Elaides, R.O. Harris and P. Reinslau, *Can. J. Chem.*, 1969, 47, 3823.
7. H. Hartmann and C. Buschbeck, *Z. Phys. Chem. (Frankfurt)*, 1957, 11, 120.
8. K. Gleu and W. Breuef, *Z. Anorg. Allg. Chem.*, 1938, 237, 335.
9. J.K. Witschy and J.K. Beattie, *Inorg. Nucl. Chem. Letters*, 1969, 5, 969.
10. J.A. Broomhead and L.A.P. Kane-Maguire, *J. Chem. Soc. (A)*, 1967, 546.
11. J.F. Endicott and H. Taube, *Inorg. Chem.*, 1965, 4, 437.
12. A.I. Vogel, "A Textbook of Quantitative Inorganic Analysis", Third Edition, Longmans, London, 1961, (a) p. 335, (b) p. 338, (c) p. 783, (d) p. 256 ff.

13. S. Herzog, J. Dehnert and K. Lühder in "Technique of Inorganic Chemistry", H.B. Jonassen and A. Weissberger, Editors, Wiley, New York, 1968, Vol. VI, p. 119.
14. W.B. Fortune and M.G. Mellor, Ind. Eng. Chem., Anal. Ed., 1938, 10, 60.
15. A.A. Diamantis and G.J. Sparrow, Chem. Comm., 1970, 819; J. Chem. Soc. (Dalton), to be published.
16. I.U.P.A.C., "Table of Wavenumbers for the Calibration of Infrared Spectrometers", Butterworths, London, 1961.
17. K.N. Rao, Pure and Appl. Chem., 1973, 33, 621.
18. J.M. Fletcher, B.F. Greenwood, C.J. Hardy, D. Scargill and J.L. Woodhead, J. Chem. Soc., 1961, 2000.
19. J.N. Armor and H. Taube, J. Amer. Chem. Soc., 1970, 92, 6170.
20. D.F. Evans, J. Chem. Soc., 1959, 2003.
21. "Stability Constants Part II: Inorganic Ligands", Chemical Society Special Publication No. 7, London, 1958. Compiled by J. Bjerrum, G. Schwarzenbach and L.G. Sillen, p. 112 and 52.